

UNIVERSITY OF CALIFORNIA

Los Angeles

Volatilization of Organic Compounds  
in an Aerated Stirred Tank Reactor

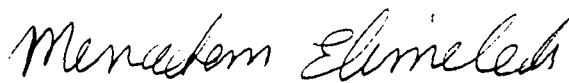
A dissertation submitted in partial satisfaction of  
the requirements for the degree Doctor of Philosophy  
in Civil Engineering

by

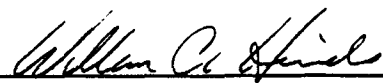
Judy Ann Libra

1991

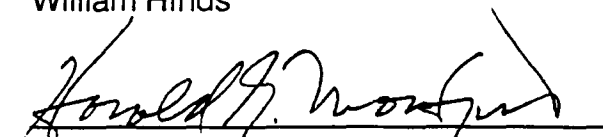
The dissertation of Judy Ann Libra is approved.



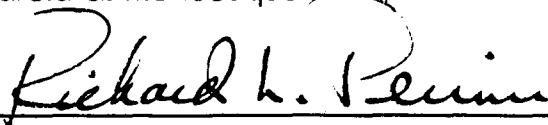
Menachem Elimelech




William Hinds



Harold G. Monbouquette



Richard L. Perrine



Michael K. Stenstrom, Committee Chair

University of California, Los Angeles

1991

## Table of Contents

LIST OF SYMBOLS .....	xi
ACKNOWLEDGEMENTS .....	xv
VITA .....	xvii
ABSTRACT OF THE DISSERTATION .....	xviii
1 Introduction .....	1
2 Theory and literature review .....	6
2.1 Mass transfer coefficients .....	6
2.1.1 Over-all mass transfer coefficients .....	10
2.1.2 Dimensional analysis of mass transfer in a stirred tank .....	13
2.1.3 Empirical correction factors for $k_L a$ .....	17
2.1.4 Two component transfer .....	21
2.1.5 Volatilization in engineered systems .....	25
2.2 Driving force .....	27
2.2.1 Equilibrium concentration - $c^*$ .....	28
2.3 Surface tension .....	32
2.3.1 Effect on mass transfer .....	34
2.4 Coalescence .....	40
2.4.1 Increased coalescence .....	43
2.5 Determination of mass transfer coefficients .....	45
2.5.1 Nonsteady state methods .....	47
Batch model .....	47

Continuous model .....	48
Gas phase oxygen concentration .....	48
Reactor hold-up .....	50
Oxygen probe dynamics .....	51
Nonsteady State Model .....	52
2.5.2 Steady state methods .....	53
2.5.3 Method chosen for volatilization studies .....	55
3 Experimental methods .....	57
3.1 Equipment .....	57
3.2 Batch experiments .....	60
3.3 Continuous flow experiments .....	61
3.3.1 Residence time distribution .....	61
3.3.2 Water/ Air system .....	64
Steady state .....	65
Nonsteady state .....	67
3.3.3 Water/VOC/ Air system .....	68
3.3.4 Water/DSS/ Air and Water/VOC/DSS/ Air system .....	71
3.3.5 Water/Biomass/ Air system .....	72
3.4 VOC analysis .....	73
3.5 Henry's constants .....	74
3.6 Surface tension measurements .....	76
3.7 Experimental design .....	78

4 Results and discussion .....	83
4.1 Oxygen transfer .....	83
4.1.1 Water/Air system .....	83
Batch nonsteady state experiments .....	83
Continuous flow experiments .....	86
4.1.2 Water/VOC/Air system .....	96
4.1.3 Water/DSS/Air system .....	98
4.1.4 Water/Biomass/Air system .....	104
4.2 Volatile organic compound transfer .....	106
4.2.1 Water/VOC/Air system .....	106
4.2.2 Water/DSS/VOC/Air system .....	125
4.2.3 Application of results .....	129
5 Conclusions .....	130
6 References .....	134
7 Appendix .....	142

## List of Figures

Figure 1. Concentration gradient at the interface: oxygen absorption	8
Figure 2. Two film theory with linear concentration gradients	8
Figure 3. Over-all and interfacial concentration differences	11
Figure 4. Geometry of standard stirred tanks with Rushton turbines	16
Figure 5. Correlation developed by Judat (1982) for $k_L a_{O_2}$	16
Figure 6. Approach to equilibrium as a function of liquid depth for benzene absorbed during bubble rise in water	28
Figure 7. Change in bubble surfactant layer in the two hydrodynamic regimes	36
Figure 8. Mass balance on the reactor	46
Figure 9. Typical ranges for mass transfer coefficients and energy input	47
Figure 10. Reactor details	59
Figure 11. Residence time distribution for typical experimental conditions	63
Figure 12. Reactor set-up and sampling points for VOC experiments	66
Figure 13. Surface tension of dodecyl sodium sulfate solutions; compared to other authors	77
Figure 14. Comparison of the three methods used to calculate $K_L a$	82
Figure 15. Comparison of $k_L a_{O_2}$ values calculated with and without adjustment of gas phase concentration	82
Figure 16. Comparison of nonsteady state $k_L a_{O_2}$ values (this work) to the correlation from Judat (1982)	85

Figure 17. Comparison of nonsteady state $k_L a_{O_2}$ values (this work) to the correlation from Linek et al.(1987)	85
Figure 18. Comparison of steady state $k_L a_{O_2}$ values (this work) to the correlation from Judat (1982)	87
Figure 19. Comparison of steady state $k_L a_{O_2}$ values (this work) to the correlation from Linek et al.(1987)	87
Figure 20. Analysis of $k_L a^*$ versus $(P/V)^*$ as a function of $v_s^*$	88
Figure 21. Plot of $k_L a^*/v_s^*$ versus $(P/V)^*$	88
Figure 22. Results from the three experimental methods: nonsteady state with $N_2$ , and with $Na_2SO_3$ deoxygenation, and steady state (this work)	89
Figure 23. Comparison of Judat's correlation to experimental $k_L a_{O_2}$ values from various modified methods	92
Figure 24. Comparison of $k_L a_{O_2}$ values calculated from the two steady state methods: gas phase and liquid phase balances (this work)	92
Figure 25. Comparison of the steady state method with the continuous nonsteady state method	96
Figure 26. Comparison of $k_L a_{O_2}$ measured in tap water to those measured in the presence of VOC's and m-cresol	97
Figure 27. The effect of DSS on the oxygen mass transfer coefficient	99
Figure 28. Dependence of the effect of DSS on reactor hydrodynamics	99

Figure 29. Change in alpha factor with increasing power density for the DSS solutions	101
Figure 30. Comparison of data to the correlation developed by Hwang (1983)	103
Figure 31. Comparison of data to the correlation developed by Osorio (1985)	103
Figure 32. Comparison of $kLa_{O_2}$ values measured in the presence of biomass to those measured in tap water and a DSS solution	105
Figure 33. Dependence of the oxygen and VOC's mass transfer coefficients on power density	108
Figure 34. $\Psi_m$ as a function of the dimensionless power density	108
Figure 35. Comparison of the three methods of calculating $k_{Ga}$ , $k_{Ga}/k_{La}$ , and $\%R_L/R_T$	114
Figure 36. The film mass transfer coefficients and their ratio as a function of power input	114
Figure 37. Relationship between $K_{La_{VOC}}$ , $\Psi_m$ , and $H_c$	118
Figure 38. Dependence of $\Psi_m$ on $H_c$ for various power densities	118
Figure 39. Gas phase saturation as a function of power density	120
Figure 40. Stripping loss as a function of $kLa_{O_2}$ for $\Psi_m = 0.01 \rightarrow 1.0$	122
Figure 41. Stripping loss as a function of liquid flow rate (or hydraulic retention time) for two power densities and the corresponding $\Psi_m$ values	124



Figure 42. Stripping loss as a function of liquid flow rate (or hydraulic retention time) for one power densities and varying $\Psi_m$ values	124
Figure 43. Comparison of $KLa_{VOC}$ values measured in tap water and in a DSS solution ( $\sigma = 55 \text{ mN/m}$ )	126
Figure 44. Alpha factors for oxygen and VOC's as a function of power density for the DSS solution ( $\sigma = 55 \text{ mN/m}$ )	126
Figure 45. Comparison of the vales of $k_{Ca}$ , $k_{Ca}/k_{La}$ , and $\%R_L/R_T$ measured in tap water and the DSS solution	128
Figure 46. Comparison of $\Psi_m$ in tap water and in the DSS solution	128

## List of Tables

Table 1. Removal mechanisms in the activated sludge system	2
Table 2. Variation in $\Psi$ according to mass transfer theories	25
Table 3. Historical development of the theory of surface tension	33
Table 4. Henry's constants and solubilities for the compounds investigated	73
Table 5. GC operating conditions	73
Table 6. Comparison of experimental and published values of $H_c$	76
Table 7. Sensitivity of $K_{La_{Tot}}$ to concentration variations	80
Table 8. Correlations developed from methods modified to account for error sources.	91
Table 9. Characteristics of the biomass suspension	104
Table 10. Experimental results: $k_{La_{O_2}}$ , $K_{La_{VOC}}$ , and $K_{La_{VOC}}/k_{La_{O_2}}$ ( $\Psi_m$ ) for three power ranges	107
Table 11. Comparison of $k_{Ga}/k_{La}$ , $k_{Ga}$ , and $k_{La}$ calculated from the three methods	113
Table 12. Correlations for the various types of mass transfer contactors	116
Table 13. Experimental stripping loss and gas phase saturation	119

## LIST OF SYMBOLS

a	specific interfacial area [ $\text{m}^2/\text{m}^3$ ]
$B_w$	width of baffle [m]
c	conductivity [siemens]
c	mass concentration [mg/L]
$c^*$	equilibrium concentration corresponding to bulk concentration
D	diffusion coefficient [ $\text{m}^2/\text{s}$ ]
d	stirrer diameter [m]
D	reactor diameter [m]
g	gravitational constant [ $\text{m}/\text{s}^2$ ]
h	height of stirrer from reactor bottom [m]
H	height of liquid in reactor [m]
$H_c$	Henry's constant [dimensionless]
k	film mass transfer coefficient [m/s]
K	over-all mass transfer coefficient [1/s]
$\dot{m}$	specific mass transfer rate
N	mass transfer flux
n	stirrer speed [1/s]
P	power [W]
Q	volumetric flow rate [ $\text{m}^3/\text{s}$ ] or [L/h]
R	resistance to mass transfer [s]
$R_{\text{bio}}$	biological reaction rate
T	temperature [K]
V	reactor volume [ $\text{m}^3$ ]
$v_s$	superficial gas velocity [m/s]

### Subscripts

20	measured at 20 C
A	compound A
B	compound B
bio	biological
DSS	dodecyl sodium sulfate
e	effluent
G	gas
i	interfacial
L	liquid
o	influent
O <sub>2</sub>	oxygen
S	superficial gas velocity
T	operating temperature
TP	tap water
VOC	volatile organic compound
WW	wastewater

### Dimensionless Numbers

$k_L a^*$	$k_L a (v_L / g^2)^{1/3}$
$K_{ow}$	octanol/water partition coefficient
Ne	Newton Number (= Power Number) = $P / (\rho n^3 d^5)$
$(P/V)^*$	$P / (V \rho_L (g^4 v_L)^{1/3})$
Re	Reynolds Number = $Q / (d v)$
Sc	Schmidt Number = $v / D_L$
Sh	Sherwood Number = $k_L d / D_L$

$Si^*$	Coalescence Number (not yet defined)
$\sigma^*$	$\sigma/(\rho(v^4g)^{1/2})$
$v_s^*$	$v_s/(gv_L)^{1/3}$
We	Weber Number = $(\rho n^2 d^3)/\sigma$

### Greek Letters

$\alpha$	$K_{La_{ww}}/K_{La_{TP}}$
$\beta$	$C^*_{ww}/C^*_{TP}$
$\nu$	kinematic viscosity [ $m^2/s$ ]
$\rho$	density [ $kg/m^3$ ]
$\sigma$	surface tension [ $mN/m$ ] [=dyne/cm]
$\tau$	oxygen probe time constant
$\theta_H$	hydraulic retention time
$\theta$	temperature correction factor: 1.024
$\Psi$	ratio of the liquid film coefficients = $k_{La_{VOC}}/k_{La_{O_2}}$
$\Psi_m$	ratio of the over-all coefficients = $K_{La_{VOC}}/K_{La_{O_2}}$

### Abbreviations

BOD	biological oxygen demand
CFSTR	continuous flow stirred tank reactor
CMC	critical micelle concentration
COD	chemical oxygen demand
1,2-DCB	1,2-dichlorobenzene
DCM	dichloromethane
DO	dissolved oxygen
DSS	dodecyl sodium sulfate
EPICS	equilibrium partitioning in closed systems

IC	inorganic carbon
OUR	oxygen uptake rate
POTW	publicly owned treatment works
SS	suspended solids
STR	stirred tank reactor
TCE	trichloroethylene
TOC	total organic carbon
TOL	toluene
VOC	volatile organic compound

## ACKNOWLEDGEMENTS

Theories  
are usually the hasty results of  
an impatient intellect,  
that wants to be rid of the phenomena  
and, therefore, puts in their place  
pictures, concepts,  
often just words.

J.W. von Goethe

I would like to express my gratitude to my advisors on both sides of the ocean, Professor Michael K. Stenstrom and Professor Udo Wiesmann, for their help, encouragement, and support throughout my project. I especially appreciate their willingness to start a cooperation between UCLA and TU-Berlin, and their continued enthusiasm until the end. I would also like to thank the other members of my doctoral committee, Professors Menachem Elimelech, William Hinds, Harold Monbouquette, and Richard Perrine for their help and time.

My thanks to Kyoung Sin Ro, whose help and encouragement made it possible for me to carry out my experimental work in Berlin and still graduate. Special thanks to Miriam and Debby for taking care of all the difficulties involved in working off campus, and to Nikos for his help with the experimental work. My friends and former colleagues at UCLA, Sami, Hamid, Lew and Jennifer, Gero and Christel, Rich and Kathy, Lynne and Steve, Gail, Chung, Marisa, Chu, to name but a few, made my years at UCLA enjoyable and enriching. I would like to thank all my colleagues at the TU Berlin for their help and advice. Of course where would I be without the love and support of my parents, my family, and Rolf.

This research was supported by the BP America graduate fellowship program, the German Academic Exchange Service scholarship program, and grants from the NSF-funded Hazardous Substance Control Engineering Research Center, and the Center for the Engineering and Systems Analysis for the Control of Toxics (ESACT).



## VITA

- October 6, 1956    Born, St. Paul, Minnesota
- 1978              Bachelor of Chemical Engineering  
University of Minnesota, Minneapolis
- 1978-1980        Process Engineer  
Celanese Chemical Co., Bay City, Texas
- 1983-1986        Research Assistant  
Institute for Thermodynamics, Technical University Berlin,  
Federal Republic of Germany
- 1986-1988        Research Assistant  
Department of Civil Engineering  
University of California, Los Angeles
- 1987              Master of Science in Civil Engineering  
University of California, Los Angeles
- 1988-1991        BP America Fellowship  
University of California, Los Angeles  
Scholarship from the German Academic Exchange Service.  
Technical University Berlin,  
Institute for Chemical Engineering,  
Federal Republic of Germany

## PUBLICATIONS AND PRESENTATIONS

Cardinal, L.J., J.A. Libra, and M.K. Stenstrom (1987). "Treatment of hazardous substances in conventional biological treatment plants," Poster presented at the First Annual Research Symposium, University of California, Davis.

Stenstrom, M.K., L.J. Cardinal, and J.A. Libra (1989). "Treatment of hazardous substances in wastewater treatment plants," *Environmental Progress*, Vol.8, No.2, 107-112.

## ABSTRACT OF THE DISSERTATION

Volatilization of Organic Compounds  
in an Aerated Stirred Tank Reactor

by

Judy Ann Libra

Doctor of Philosophy in Civil Engineering

University of California, Los Angeles, 1991

Professor Michael K. Stenstrom, Chair

Volatilization must be considered as a removal mechanism when treating wastewaters containing volatile organic compounds (VOC's). This study investigated the simultaneous mass transfer of oxygen and three organic compounds in an aerated stirred tank reactor to determine if the ratio of the two mass transfer coefficients,  $K_{LaVOC}/k_{LaO_2}$  can be used to predict volatilization rates for semi-volatile compounds. This work expands the range of compound volatility and the types of waters investigated to semi-volatile organic compounds in water containing an anionic surfactant over a larger power range than previously studied.

The mass transfer coefficients of oxygen and three VOC's: toluene, dichloromethane, and 1,2-dichlorobenzene, were determined in three water systems: tap water, tap water with an anionic surfactant, dodecyl sodium sulfate (DSS), and tap water with biomass ( $k_{LaO_2}$  only). A steady state method was used. Experiments were made to span the range of mass transfer coefficients found in both

municipal and industrial wastewater treatment processes. The results were analyzed using dimensional analysis.

As power density increased, the liquid film mass transfer coefficient ( $k_L a$ ) increased, while the gas film mass transfer coefficient ( $k_G a$ ) remained constant. Thus, the gas side resistance became important for compounds with lower volatility, and  $K_L a_{VOC}$  approached a constant. The ratio of the two mass transfer coefficients,  $K_L a_{VOC}/k_L a_{O_2}$  ( $\Psi_m$ ), therefore, decreased over the range of power studied. Because  $K_L a_{VOC}$  approached a constant as power increased, the volatilization rates became independent of power. Using the two resistance theory,  $\Psi_m$  can be calculated for a VOC for the reactor operating conditions from its Henry's constant, the ratio of the VOC and oxygen liquid diffusion coefficients and the ratio of the gas and liquid film coefficients ( $k_G a/k_L a$ ). The rate can be predicted using  $\Psi_m$  and  $k_L a_{O_2}$ .

The effect of an anionic surfactant (DSS) on mass transfer varied according to the hydrodynamic conditions in the reactor. In the moderately turbulent region both mass transfer coefficients were reduced in the presence of DSS, recovering to the values found in tap water as power increased. In the highly turbulent region,  $k_L a_{O_2}$  increased significantly. The VOC mass transfer coefficients recovered only to the values found in tap water. Therefore,  $\Psi_{mDSS} = \Psi_{mTP}$ , in the moderately turbulent region and  $\Psi_{mDSS} < \Psi_{mTP}$  in the highly turbulent region.

The effect of biomass on  $k_L a_{O_2}$  was not correlatable with the surface tension of the mixed liquor.

## 1 Introduction

The activated sludge process is a popular method to treat wastewaters. It is used extensively for both municipal and industrial wastewater treatment and is being investigated for the treatment of contaminated groundwaters, landfill leachates, and soils. The process theoretically relies on aerobic microbial degradation (conversion to  $\text{CO}_2$  and  $\text{H}_2\text{O}$ ) to remove toxic compounds and other dissolved organic matter. Therefore, the activated sludge process is preferred over physical processes that concentrate the contaminant in one phase, which must then be disposed of properly.

However, there are other possible removal mechanisms besides biotransformation or biodegradation in the process, so that the ultimate fate of the compound is important to consider when evaluating the effectiveness of the activated sludge process in removing organic contaminants. Often pollutant removal from wastewater is the result of transferring the problem from one of water pollution to one of air pollution, or indirectly, through sludge disposal, transferring the pollutant from water to solids and back again by leaching of the pollutant from the sludge at a landfill or to the air by volatilization when drying the sludge. Which mechanisms are involved and the magnitude of their contribution is important to know when trying to decrease pollution effects from a wastewater.

Removal of toxic compounds in an activated sludge system can be accomplished in three ways:

1. transfer to the solid phase
2. biotransformation/degradation
3. transfer to the air

This study focuses on the transfer of organic compounds from water to air, often called volatilization or stripping. The more volatile the compound, the larger the probability that the compound will be transferred to the air before it can be biodegraded. However, not only the type of compound, but also the type of process determines which removal mechanism dominates. A summary of the unit processes that make up the activated sludge treatment train and the major removal mechanisms of each unit is found in Table 1.

Table 1. Removal mechanisms in the activated sludge system.

UNIT	EXITING STREAM	REMOVAL MECHANISM
Preliminary screening, grit removal	Gas Solids	Volatilization Adsorption
Primary sedimentation	Gas Solids	Volatilization Adsorption
Aeration Basin	Gas	Volatilization Biotransformation/ degradation
Secondary sedimentation	Solid	Adsorption
Chlorination	Gas	Chemical reaction
Effluent discharge	Liquid	Pass Through

Adsorption to solids and subsequent sedimentation as a removal mechanism for volatile organic compounds (VOC's) has been found to be of little importance in the aeration basin (Kincannon and Stover, 1983; Dixon and Bremen, 1984). Although adsorption to primary sludge as a removal mechanism was found to be significant for some VOC's, e.g. up to 33% of the ethylbenzene found in the primary clarifier was removed by adsorption to the sludge (Dixon and Bremen,

1984), a study of 50 publicly owned treatment works (POTW's) (USEPA, 1982) found the total removal due to sludge streams was generally <5% for most of the VOC's investigated. Biological transformation of the VOC can be the major removal mechanism depending on whether the bacteria are acclimated, or have time to produce the enzymes necessary to degrade the compound, i.e. the residence time of the VOC's in the water is long enough. The fate, then, of a VOC can be viewed as being a competition between volatilization and biotransformation.

Chang et al. (1987) provide a good review of the work published on the fate of volatile organic compounds (VOC's). In their study of POTW's in southern California, they found that VOC emissions from POTW's can potentially be a major point source of air pollution. In discussing the results, Corsi et al. (1989) pointed out that the exposure to the emissions of people working around the plant and in the immediate vicinity could be a potential health hazard. The study used a worst case scenario where all the VOC's entering the POTW were removed due to volatilization. This may possibly be the case in POTW's where the biomass in the aeration basin has little chance to acclimate to the varying influent concentrations. VOC losses from the units other than aeration have been reported to be as high as 50% (Berglund et al., 1985). The following conclusions can be drawn from their study: 1) All unit processes in the treatment train have to be evaluated for VOC losses and 2) VOC losses from POTW's can be substantial air pollution point sources.

In order to measure the VOC losses exactly, the gas emissions from the various units must be trapped and analyzed for VOC's. Taking representative samples of gas streams with changing concentrations is a problem that has to be solved in

order to evaluate the volatilization from gas concentrations. The other possibility would be to determine the VOC over-all mass transfer coefficient,  $K_L a_{VOC}$ , for the units and this in conjunction with the liquid concentration can be used to calculate the VOC losses. Since determining the  $K_L a_{VOC}$  for each unit can be very work and time intensive, requiring much analytical chemistry, a simpler method relating easily measured parameters to VOC loss is needed.

The relationship between the mass transfer coefficients for VOC's and oxygen,  $K_L a_{VOC}$  and  $K_L a_{O_2}$ , has been shown to be very useful in natural bodies of water (Smith et al., 1983). Work on relating  $K_L a_{VOC}$  to  $K_L a_{O_2}$  for engineered systems has produced good results for clean water (Roberts and Daendiliker, 1983). In work done with a surface aerator, they showed that the ratio  $K_L a_{VOC}:K_L a_{O_2}$  is constant for highly volatile organic compound over a range of turbulence ( $0.8-320 \text{ W/m}^3$ ) in distilled water and filtered secondary effluent.

The relationship between  $K_L a_{VOC}$  and  $K_L a_{O_2}$  is desirable as a method of calculating the volatilization losses, because  $K_L a_{O_2}$  is usually known. If this relationship is valid for all types of water, and its magnitude and the liquid concentration of the organic compound were known, we would be able to calculate the maximum volatilization losses possible for a certain engineering process. To calculate the real losses, the biotransformation and adsorption of the compounds by the bacteria must also be quantified. In order to use the ratio of the mass transfer coefficients to quantify volatilization in real wastewater situations, this relationship must be validated for contaminated waters.

In order to do this, the effect of wastewater contaminants on mass transfer must be known, qualitatively and quantitatively. Mass transfer of oxygen in clean wa-

ter/air systems has been extensively investigated and correlated with success. However, many parameters change in real wastewaters. Three of the important parameters are 1) the coalescence behavior of the bubbles, 2) the presence of surfactants in the water, and 3) the presence of a solid phase (biomass). In the treatment of municipal wastewater, an increase in mass transfer over the length of the aeration basin is found corresponding to degree of treatment (Stenstrom, 1990). Typical changes in the surface tension of the wastewater are from ~40 mN/m of the basin influent to ~65 mN/m of the effluent. The organic concentration decreases from ~200 to 20 mg BOD/L.

The purpose of this study was to investigate the effect of these parameters on the mass transfer coefficients. By using model wastewaters, the effect of changes in bubble coalescence, and the presence of surfactants and biomass on mass transfer was studied. The mass transfer coefficients of three volatile organic compounds and oxygen were measured with a steady state method in a continuous flow stirred tank reactor (CFSTR) with a sparged turbine aerator. The three compounds were chosen to span the range of volatility to include both liquid and gas side resistance. The compounds investigated were: toluene, dichloromethane, and 1,2-dichlorobenzene. They have dimensionless Henry's constants ranging from 0.240 to 0.095. The surface tension was changed through the addition of an anionic surfactant, dodecyl sodium sulfate (DSS); the bubble coalescence was affected by m-cresol, as well as DSS; and waste sludge from a municipal wastewater treatment plant was used to study the effect of biomass. The experimental work was performed at the Technical University of Berlin, Federal Republic of Germany.



## **2 Theory and literature review**

Bird, Stewart, and Lightfoot in their 1960 edition of Transport Phenomena said: "Two-fluid mass-transfer systems offer many challenging problems: the flow behavior is complicated, the moving interface is virtually inaccessible to sampling, the interfacial area is usually unknown, and many of the practically important systems involve liquid-phase chemical reactions. A better basic understanding of these systems is needed." Thirty years later, the statement is still valid.

The transfer of mass between two phases depends on the properties of each of the two phases and the interface between them, on the properties of the material to be transferred, and on the fluid dynamics of the apparatus used to carry out the transfer. These influences are generally divided into two groups: a mass transfer coefficient and driving force. The driving force is the concentration gradient between the phases and the mass transfer coefficient represents the rest of the influences.

The following section discusses the mass transfer theory, the parameters that influence the mass transfer coefficient and the driving force, and the methods used to measure the mass transfer coefficient.

### **2.1 Mass transfer coefficients**

When material is transferred from one phase to another across a separating interface, resistance to mass transfer causes a concentration gradient to develop in each phase (Figure 1). The resistance in each phase is made up of two parts: the diffusional resistance in the laminar film and the resistance in the bulk fluid.

There is also another resistance to transfer; the interface itself. This resistance is thought to be negligible in most cases, however, exceptions do occur, e.g. when

surface active species concentrate at the interface, or when the mass transfer rate is very high (Treybal, 1968). All current theories on mass transfer, i.e. film, surface renewal, and penetration theory, assume that the resistance in the bulk fluid is negligible and the major resistance occurs in the laminar films on either side of the interface.

Fick's law of diffusion forms the basis for these theories and leads to various relationships between the mass transfer coefficient and the diffusion coefficient,  $D$ , depending on the assumptions and boundary conditions used to integrate Fick's law. In the film theory, the concentration gradient is assumed to be at steady state and linear, (Figure 2) (Lewis and Whitman, 1924). However, the time of exposure of a fluid to mass transfer may be so short that the steady state gradient of the film theory does not have time to develop. The penetration theory was proposed to account for a limited, but constant time that the fluid eddies are exposed to mass transfer at the surface (Higbie, 1935). The surface renewal theory brings in a modification to allow the time of exposure to vary (Danckwerts, 1951). The three theories then predict the film mass transfer coefficient is a function of  $D^n$ , with  $n$  varying from 0.5 to 1.

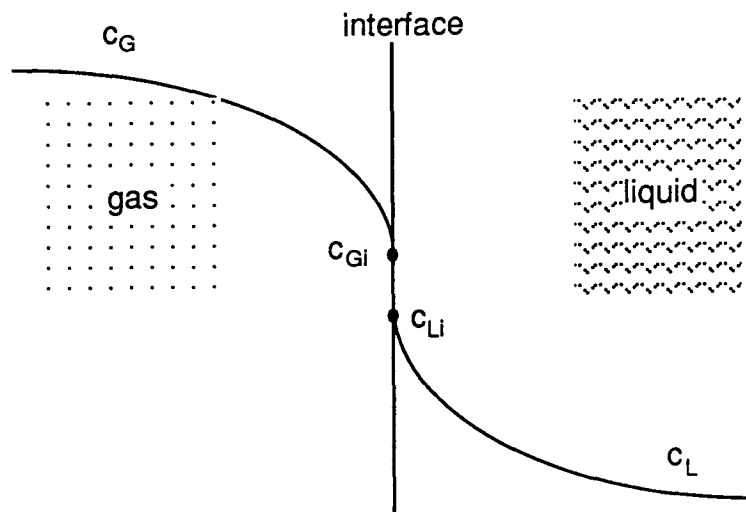


Figure 1. Concentration gradient at the interface: oxygen absorption

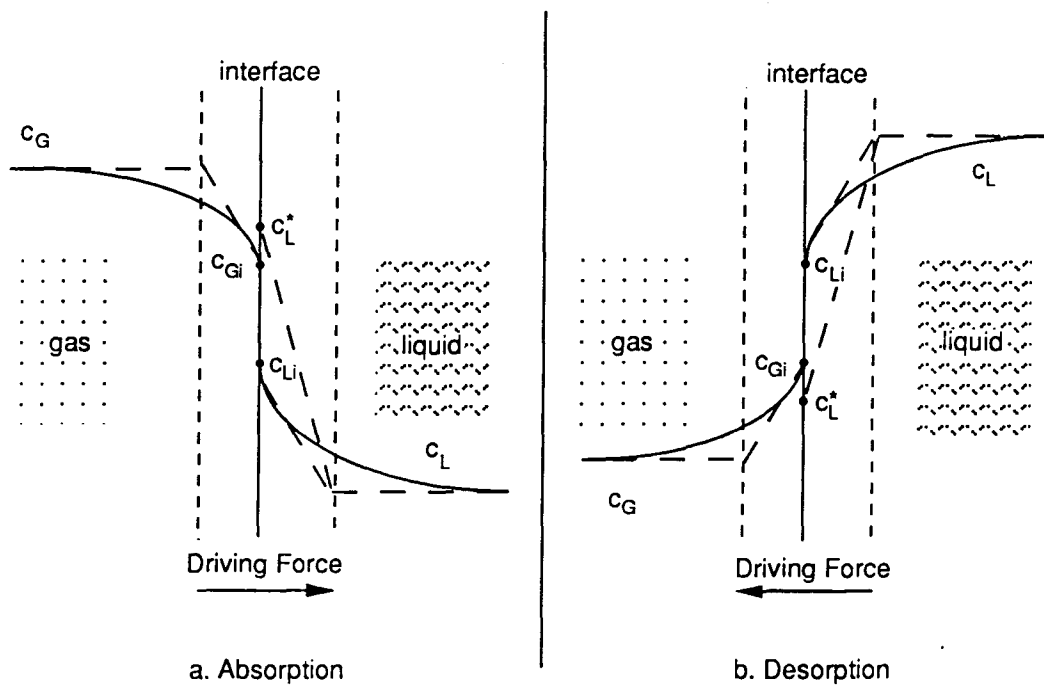


Figure 2. Two film theory with linear concentration gradients.

The mass transfer flux is defined as:

$$N = k_G(c_G - c_{G_i}) = k_L(c_{L_i} - c_L) \quad (1)$$

where:  $N$  = mass transfer flux

$k_L$  = liquid film mass transfer coefficient

$k_G$  = gas film mass transfer coefficient

$c_{L_i}$  = liquid interfacial concentration

$c_{G_i}$  = gas interfacial concentration

$c_{L,G}$  = bulk phase concentration

The concentrations of the diffusing material in the two phases immediately adjacent to the interface are generally unequal, but are usually assumed to be related to each other by the laws of thermodynamic equilibrium.

In order to calculate the specific mass transfer rate, mass per unit time and unit volume, the specific surface area,  $a$ , defined as transfer surface area/volume of liquid, is needed in addition to  $k_L$ .

$$\dot{m} = k_L a (c_{L_i} - c_L) \quad (2)$$

where:  $\dot{m}$  = specific mass transfer rate

$$a = \frac{A}{V} = \text{volumetric interfacial area}$$

The transfer interface produced by most of the mass transfer apparatus we will be considering is in the form of bubbles. Measuring the surface area of swarms

of irregular bubbles is very difficult. This difficulty in determining the interfacial area is overcome by not measuring it separately, but rather lumping it together with the mass transfer coefficient and measuring  $k_L a$  as one parameter.

The concentration of the transferred material in each phase, i.e. the driving force, should theoretically be included in the list of parameters on which the mass transfer coefficient depends (Spalding, 1963). The relation between mass transfer rate and driving force in certain cases, e.g. high mass transfer rates, is non-linear; therefore, the mass transfer coefficient itself depends on the mass transfer rate. This effect arises from the distortion of the velocity and concentration profiles by the flow of the material through the interface (Bird, Stewart, and Lightfoot, 1960). In the limit of small mass transfer rates, which is the case for all of the mass transfer encountered in aeration applications, the distortion may be neglected. This distortion is negligible especially in the direction from the gas phase into the liquid phase, because a much higher transfer rate is required to distort the liquid concentration profile.

### **2.1.1 Over-all mass transfer coefficients**

The experimental determination of the coefficients  $k_L a$  and  $k_G a$  is very difficult. When the Henry's absorption isotherm is linear, over-all coefficients, which are more easily determined by experiment, can be used. Over-all coefficients can be defined from the standpoint of either the liquid phase or gas phase. Each coefficient is based on a calculated over-all driving force, defined as the difference between the bulk concentration of one phase and the equilibrium concentration corresponding to the bulk concentration of the other phase. When the controlling resistance is in the liquid phase, the over-all mass transfer coefficient  $K_L a$  is generally used.

$$N = k_L a (c_{L_i} - c_L) = K_L a (c_L^* - c_L) \quad (3)$$

where:  $c_L^*$  = liquid concentration in equilibrium with the bulk gas concentration

For dilute non-reacting solutions, Henry's law is used to describe the equilibrium distribution between the bulk liquid and gas phase (Figure 3):

$$H_c = \frac{c_G - c_{G_i}}{c_L^* - c_{L_i}} = \frac{c_{G_i} - c_G^*}{c_{L_i} - c_L} \quad (4)$$

and since the function passes through the origin:

$$H_c = \frac{c_{G_i}}{c_{L_i}} = \frac{c_G^*}{c_L} = \frac{c_G}{c_L^*}$$

where:  $H_c$  = dimensionless Henry's constant

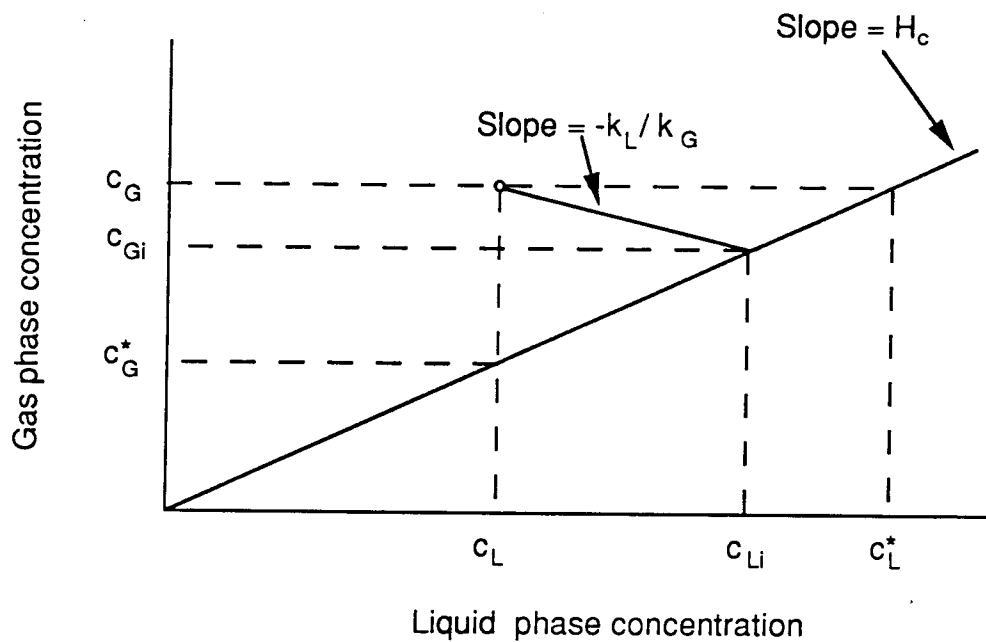


Figure 3. Over-all and interfacial concentration differences (after Sherwood et al., 1975).

Rearranging equation 3 and substituting in the Henry's constant:

$$R_T = R_L + R_G = \frac{1}{K_L a} = \frac{1}{k_L a} + \frac{1}{H_c \cdot k_G a} \quad (5)$$

or:

$$K_L a = \frac{k_L a}{1 + \frac{k_L a}{k_G a \cdot H_c}} \quad (6)$$

where:  $R_T$  = total resistance

$R_L$  = liquid phase resistance

$R_G$  = gas phase resistance

The ratio of  $k_L a / k_G a$  to  $H_c$  is important in deciding where the major controlling resistance lies. When  $k_L a \ll k_G a \cdot H_c$ , the liquid side resistance dominates and  $K_L a = k_L a$ . This is usually true for oxygen transfer, but may not be true for volatilization of organic compounds.  $K_L a$  is defined and valid for systems where  $k_L a \cong k_G a \cdot H_c$ ; however, the over-all mass transfer coefficient is no longer a function of only the liquid phase parameters, but also of the gas phase parameters.

Since the film coefficients are functions of the system fluid dynamics, it is clear that the controlling resistance can be influenced by conditions other than the Henry's constant.

### 2.1.2 Dimensional analysis of mass transfer in a stirred tank

Listing the variables that affect the mass transfer between two phases in a stirred tank, considering the liquid phase resistance, the complexity of the problem becomes clearer:

$$\text{mass transfer rate} = \dot{m} = k_L a \cdot (\text{driving force}) \quad (7)$$

and

$$k_L a = f\left(\frac{P}{V}, v_s; g; \nu_L, \rho_L, \nu_G, \rho_G, D_L, \sigma_L, Si; \text{Reactor geometry}\right) \quad (8)$$

*process parameters*      *physical properties*

where:  $P = \text{power} \left( \frac{M \cdot L^2}{T^2} \right)$

$$V = \text{reactor volume} (L^3)$$

$$v_s = \text{superficial gas velocity} \left( \frac{L}{T} \right)$$

$$g = \text{gravitational constant} \left( \frac{L}{T^2} \right)$$

$$\nu = \text{kinematic viscosity} \left( \frac{L^2}{T} \right)$$

$$\rho = \text{density} \left( \frac{M}{L^3} \right)$$

$$\sigma = \text{surface tension} \left( \frac{M}{T^2} \right)$$

$$D = \text{diffusion coefficient} \left( \frac{L^2}{T} \right)$$

$Si = \text{coalescence behavior of the bubbles}$



Carrying out a dimensional analysis of the above parameters, we find the following relationship for a certain reactor geometry (Zlokarnik, 1978):

$$k_L a \left( \frac{v_L}{g^2} \right)^{1/3} = f \left( \frac{P}{V \rho_L (g^4 v_L)^{1/3}}, \frac{v_s}{(g v_L)^{1/3}}; \frac{\rho_G}{\rho_L}, \frac{v_G}{v_L}, S_{cL}, \sigma^*, Si^* \right) \quad (9)$$

where:  $S_c$  = Schmidt number,  $\frac{v}{D}$

$\sigma^*$  = dimensionless surface tension,  $\frac{\sigma}{\rho(v^4 g)^{1/2}}$

$Si^*$  = Coalescence number, not yet defined

If we want to compare the simultaneous mass transfer of oxygen and a dissolved organic compound in the same liquid/gas system, realizing that the physical properties (except diffusivity) of the phases are the same for both mass transfer coefficients, the above relationship reduces to:

$$k_L a \left( \frac{v_L}{g^2} \right)^{1/3} = f \left( \left[ \frac{P}{V \rho_L (g^4 v_L)^{1/3}} \right], \left[ \frac{v_s}{(g v_L)^{1/3}} \right], S_{cL} \right) \quad (10)$$

A similar analysis could be made for  $k_{cA}$ . The dependence of the over-all mass transfer coefficient on these parameters can then be calculated from the two film coefficients, and  $H_c$  using equation 5.

Dimensional analysis has been applied to the results of oxygen transfer experiments to develop scale-up factors. In oxygen transfer the liquid-side resistance dominates and  $K_L a = k_L a$ . Therefore, no information about  $k_{cA}$  is needed. In clean water/air systems equation 10 reduces to:

$$k_L a \left( \frac{v_L}{g^2} \right)^{\frac{1}{3}} = A \left[ \frac{P}{V \rho_L (g^4 v_L)^{\frac{1}{3}}} \right]^a \cdot \left[ \frac{v_s}{(g v_L)^{\frac{1}{3}}} \right]^b \quad (11)$$

The factor A and the exponents a and b depend on the system geometry.

Figure 4 shows the typical geometry of standard stirred tanks. For Rushton turbines, the assumption:  $b \cong 1-a$ , is often made for the water/air system, then equation 11 can be rearranged:

$$\frac{k_L a}{v_s} \left( \frac{v_L^2}{g} \right)^{\frac{1}{3}} = A \left[ \frac{P}{V \rho_L g v_s} \right]^a \quad (12)$$

where:

$$\frac{k_L a^*}{v_s^*} = \frac{k_L a}{v_s} \left( \frac{v_L^2}{g} \right)^{\frac{1}{3}} = \text{Sorpton number}$$

$$\left( \frac{P}{v} \right)^* = \frac{P}{V \rho_L g v_s} = \text{Dispersion number}$$

In analyzing the  $k_{L\text{O}_2}$ 's reported in 12 publications found by nonsteady state reaeration tests in geometrically similar stirred tanks using water/N<sub>2</sub>/air systems, Judat (1982) used this equation to correlate the data within  $\pm 30\%$  (Figure 5).

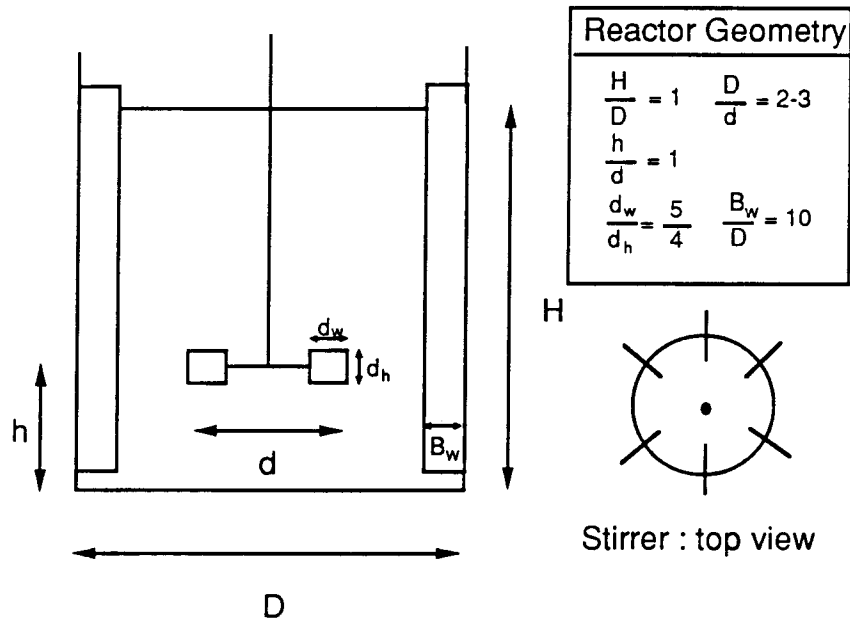


Figure 4. Geometry of standard stirred tanks with Rushton turbines.

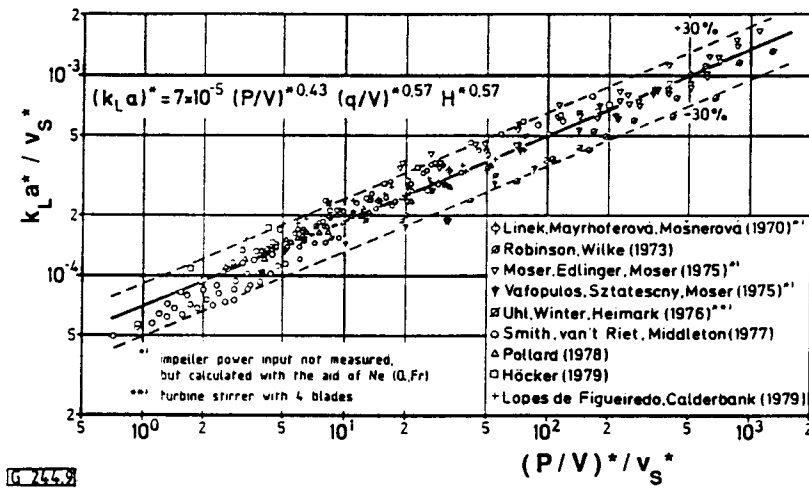


Figure 5. Correlation developed by Judat (1982) for  $k_L a_{O_2}$ .

### 2.1.3 Empirical correction factors for $k_L a$

When evaluating the oxygen mass transfer rate in geometrically similar reactors for various gas/liquid systems, the correlations based on dimensional analysis presented above can be used to predict the mass transfer coefficient for each system. However, in the treatment of wastewater, the constituents of the liquid phase are highly variable depending on the source of the wastewater. The differences between wastewater and tap water may not effect a noticeable change in the density or viscosity, but may drastically change the mass transfer coefficient. This change may be due to changes in surface tension or bubble coalescence behavior; unfortunately, no reliable correlations exist for the dependence of  $k_L a$  on surface tension and a method of quantifying the coalescence behavior of bubbles has yet to be developed.

Another correction necessary for the comparison of  $k_L a$ 's measured under various conditions is the temperature correction to 20°C. Viscosity, density, surface tension, and diffusivity are all affected by temperature. The dependence of these physical properties on temperature is well-known and correlations exist. The influence of temperature on the mass transfer rate should be described by relationships similar to equation 9, however, the influence of the dimensionless groups of physical properties are normally unknown.

In order to aid in the design of wastewater treatment facilities, empirical factors,  $\alpha$  and  $\theta$ , have been developed to quantify the change in the mass transfer coefficient due to contaminants and temperature variations in the wastewater.

The alpha factor,  $\alpha$ , has been defined to quantify the effect of contaminants on the mass transfer coefficient. It is the ratio of the mass transfer coefficient measured in the wastewater to the mass transfer coefficient measured in tap water.

$$\alpha = \frac{k_L a_{WW}}{k_L a_{TP}} \quad (13)$$

The mass transfer rate in full scale reactors used in treating wastewater is often measured in tests using tap water. The  $\alpha$  factor can be used to adjust this mass transfer rate to the mass transfer rate expected for the wastewater. Stenstrom and Gilbert (1981) present a comprehensive review of the literature on  $\alpha$  for aeration. The disadvantages of using a lumped empirical correction factor becomes clear when one considers that  $\alpha$  has been found to change depending on:

- 1) intensity of mixing or turbulence.
- 2) concentration of contaminants
- 3) method of aeration:  
fine bubble < coarse bubble < surface aerators

Obviously the hydrodynamic conditions of the system affects mass transfer differently in wastewater than in tap water. Especially difficult to quantify with the  $\alpha$  value is the effect of wastewater on the interfacial area. Clearly, a better understanding of the relationship between physical properties and  $k_L a_{O_2}$  and the quantification of these physical properties in wastewater is necessary, so that correlations based on dimensional analysis can be made.

Correct determination of  $k_L a$  is, of course, always essential. Brown and Bailod (1982) point out that the  $\alpha$  value from the ratio of two incorrectly measured mass transfer coefficients, apparent mass transfer coefficients, is different from the  $\alpha$  of true mass transfer coefficients. However, for  $k_L a_{O_2}$  values typically found in municipal aeration basins, they find the error introduced is about 6%

and within the accuracy of the  $\alpha$  measurement (10%).

Temperature affects all the physical properties: viscosity, density, surface tension, and diffusivity. The empirical factor most often used to account for the temperature changes in all these parameters is the theta factor,  $\theta$ :

$$k_L a_{20} = k_L a_T \cdot \theta^{(20-T)} \quad (14)$$

where:

$$k_L a_{20} = k_L a \text{ at } 20^\circ\text{C}$$

$$k_L a_T = k_L a \text{ at temperature } T$$

$\theta$  = temperature correction coefficient

In reviewing the literature on temperature corrections, Stenstrom and Gilbert (1981) found values for  $\theta$  range from 1.008 to 1.047, and suggested  $\theta = 1.024$  should be used. Various researchers have proposed that the temperature dependence of  $k_L a$  is not only a function of the physical properties, but also of turbulence. This would suggest that each type of mass transfer apparatus, i.e. surface, diffused, and turbine aerators, has a different correction factor.

Khudenko and Garcia-Pastrana (1987) investigated a temperature correction factor for mass transfer coefficients based on the critical energy required for molecules to penetrate the gas-liquid interface. Although this is still an oversimplified approach considering all the variables dependent on temperature, they made an interesting analysis of the reasons why the temperature correction factor  $\theta$  has often been found to be dependent on hydrodynamic conditions.

They postulate that the main reason for the substantial variations in the temperature correction factor found in the literature is that the temperature correc-

tion factors were developed from apparent mass transfer coefficients, not true mass transfer coefficients. Using computer simulation, they show that the observed temperature correction factor depends on the mass transfer coefficient itself when the apparent mass transfer coefficient is used. Thus explaining the reported dependence of the temperature correction factor on turbulence. In order to examine the effect of surface tension on the temperature correction factor, they added surfactant to the water; the temperature correction factor was not affected. For the temperature range normally found in wastewater treatment plants, 5-30° C, Khudenko and Garcia-Pastrana found their correction factor and the temperature correction factor used in equation 13 (with  $\theta=1.024$ ) to be comparable ( $\pm 5\%$ ).

### 2.1.4 Two component transfer

Now we can consider the transfer of two compounds in opposite directions in the same mass transfer apparatus, compound A in the gas phase and compound B in the liquid phase. Examining the factors influencing mass transfer with liquid-side resistance only:

$$k_L a = f\left(\frac{P}{V}, v_s; g; v_L, \rho_L, v_G, \rho_G, D_L, \sigma_L, Si; \text{ Reactor geometry}\right) \quad (15)$$

It is easy to see that the reactor geometry and the fluid flow rates, therefore, the fluid dynamics of the total system, are the same for both compounds; the interfacial area, along with the bubble coalescence and physical properties of the phases are the same for each compound; and the presence of a solid phase should also have the same effect on both compounds, unless there is mass transfer enhancement due to simultaneous depletion in one of the phases, i.e. fast chemical reactions.

Therefore, the ratio of two liquid film mass transfer coefficients (often called  $\Psi$  for the ratio between VOC's and  $O_2$  mass transfer coefficients) reduces to:

$$\Psi = \frac{k_{LA}}{k_{LB}} = f\left(\frac{D_{LA}}{D_{LB}}\right) \quad (16)$$

When the liquid film resistance dominates ( $K_L a = k_L a$ ), then only the ratio of the liquid diffusion coefficients affects the ratio of the overall mass transfer coefficients for the simultaneous transfer of two compounds in one system.

As discussed in Section 2.1.1, the assumption that the liquid side dominates depends on the ratio of the film coefficients  $k_G a / k_L a$ . In work on volatilization from natural bodies of water, Mackay and Leinonen (1975) report typical



$k_{Ca}/k_{La}$  ratios range from 50-300. Assuming  $k_{Ca}/k_{La} = 200$ , the resistances become approximately equal when  $H_c = 0.005$  and the liquid side resistance dominates ( $k_{La}/K_{La} = 0.95$ ) for  $H_c > 0.10$ . This is valid for natural bodies of water, the system for which the film coefficients were determined. For engineered systems with much more turbulence, i.e. surface and bubble aeration, Munz and Roberts (1984) found  $k_{Ca}/k_{La}$  to be closer to 20 and Hsieh (1990) found a ratio of 6. In such systems, the compounds must be more volatile ( $H_c > 0.95$ , or 3.17 respectively) in order to assume the liquid side resistance dominates. Only very volatile compounds fulfill this requirement.

If we consider an example for toluene:

Given:	$K_{La_{VOC}} = 0.00025 \text{ s}^{-1}$
	$k_{Ca}/k_{La} = 6$
	$H_c = 0.24$
subst.in eqn 5:	$1/0.00025 = 1/x + 1/(0.24 \cdot y)$
where:	$6x = y$
then:	$k_{La} = 0.00042 \text{ s}^{-1}$ and $k_{Ca} = 0.00252 \text{ s}^{-1}$
and:	$H_c \cdot k_{Ca} = 0.24 \cdot 0.00252 = 0.00060 \text{ s}^{-1}$

The requirement that  $k_{La} \ll H_c \cdot k_{Ca}$  is not fulfilled, in fact,  $k_{La} \cong H_c \cdot k_{Ca}$ . Therefore, the assumption that liquid side resistance dominates is not valid here.

Looking at a hypothetical case where  $k_{Ca}$  remains constant, but  $k_{La}$  increases ten-fold, we find that  $K_{La} = 0.00052 \text{ s}^{-1}$ . Thus, a ten-fold increase in  $k_{La}$  results in only a doubling of  $K_{La}$  when  $H_c \cdot k_{Ca}$  is on the same order of magnitude as  $k_{La}$ .

In the relationship between the mass transfer coefficients,  $\Psi$ , developed above, the assumption was liquid phase resistance dominates and  $K_L a = k_L a$  :

$$\Psi = \frac{k_L a_{VOC}}{k_L a_{O_2}} = \left( \frac{D_{LVOC}}{D_{LO_2}} \right)^n \quad (17)$$

Since this does not hold true for the less volatile compounds studied here in engineered systems, a new  $\Psi$  can be defined (Hsieh, 1990):

$$\Psi_m = \frac{K_L a_{VOC}}{k_L a_{O_2}} \quad (18)$$

In order to find the relationship between the two  $\Psi$ 's, we must go back to the over-all mass transfer coefficient:

combining equations 17 and 18:

$$\Psi_m = \frac{K_L a_{VOC}}{k_L a_{O_2}} = \frac{k_L a_{VOC}}{k_L a_{O_2}} \cdot \frac{K_L a_{VOC}}{k_L a_{VOC}} = \Psi \cdot \frac{K_L a_{VOC}}{k_L a_{VOC}} \quad (19)$$

rearranging equation 6:

$$\frac{R_L}{R_T} = \frac{K_L a}{k_L a} = \frac{1}{1 + \frac{k_L a}{k_G a \cdot H_c}} \quad (20)$$

and substituting in equation 19:

$$\Psi_m = \Psi \cdot \frac{1}{1 + \frac{k_L a_{VOC}}{H_c \cdot k_G a_{VOC}}} = \Psi \cdot \frac{R_L}{R_T} \quad (21)$$

The over-all mass transfer coefficient,  $K_{La_{VOC}}$ , will be used to denote the measured VOC mass transfer coefficients in the following sections, while for the oxygen mass transfer coefficients, the film coefficient  $k_{La_{O_2}}$  will be used to emphasize the difference.

In summary, if the liquid side resistance dominates for VOC transfer, then the ratio between the over-all mass transfer coefficients for oxygen and the VOC's ( $\Psi$ ) should remain approximately constant as power density varies and proportional to the ratio of the diffusion coefficients raised to a power  $n$ . If both gas and liquid side resistance play a role, then the ratio of the over-all mass transfer coefficients will vary as power density varies, because of its dependence on the ratio of liquid side to total resistance.

To illustrate the possible variation in  $\Psi$  just due to the variation in the exponent  $n$  predicted by the three common theories, from  $(D_{LVOC}/D_{LO_2})^{1.0}$  to  $(D_{LVOC}/D_{LO_2})^{0.5}$ , the calculated  $\Psi$  for the three compounds used in this study are listed in Table 2. Since the Wilke-Chang correlation used to calculate the diffusion coefficients is only considered valid within  $\pm 15\%$ , the possible variation in  $\Psi$  due to the error in the VOC diffusion coefficient is also listed. For example,  $(D_{LVOC}/D_{LO_2})$  for toluene is 0.42. The possible range of  $\Psi$  due to a change in the exponent  $n$  from 1.0 to 0.5 and the  $\pm 15\%$  error in  $D_{LTOL}$  is 0.36-0.70.

Table 2. Variation in  $\Psi$  according to mass transfer theories.

THEORY	Two-film			Surface renewal		
Compound	exponent (n) = 1.0			0.5		
% error	-15%	$\Psi$	+15%	-15%	$\Psi$	+15%
DCM	0.51	0.60	0.69	0.72	0.78	0.83
Toluene	0.36	0.42	0.49	0.60	0.65	0.70
1,2-DCB	0.34	0.40	0.46	0.58	0.63	0.68

### 2.1.5 Volatilization in engineered systems

In surface aeration studies on the relationship between the oxygen and organic compound mass transfer coefficients in clean water for six volatile chlorinated hydrocarbons, Roberts et al.(1984a) found the ratio of the two mass transfer coefficients to be constant,  $\Psi \cong 0.6$ , and independent of power input over the range of  $P/V = 0.8$  to  $320 \text{ W/m}^3$ . They also ran the experiments in filtered secondary effluent from a wastewater treatment plant and found the ratio remained the same. Comparing the mass transfer coefficients for the clean water to those for the filtered secondary effluent, they found  $\alpha_{VOC} = 0.89$ , while  $\alpha_{O_2} = 0.77$ , and they both increased with increasing power input.

Roberts et al. (1984) also made bubble column experiments to simulate diffused aeration basins. The column had a diameter of 22.5 cm with the liquid height varying from 35 to 60 cm. They found that for all but the most volatile compound,  $\text{CCl}_2\text{F}_2$ , the gas phase was substantially saturated upon exiting the column. Using the differential gas phase mass balance and integrating over the height of the column, they developed a model to estimate the mass transfer

coefficient when gas phase saturation is negligible, or the Henry's constant when saturation is complete, or either  $k_L a$  or  $H_c$  (if the other is known) for the intermediate range of gas phase saturation.

Truong and Blackburn (1984) investigated the volatilization of several volatile as well as non-volatile compounds in a bubble column. Various contaminants were added to tap water: surfactants, an oil phase, a pulp mill wastewater, and nonviable biomass to investigate their effect on volatilization. In analyzing their work, Allen et al.(1986) found that the Henry's constant for benzene calculated from their experimental data was comparable to values reported in the literature, suggesting that equilibrium for the organic compounds was reached in their apparatus. Therefore, a true mass transfer coefficient was not measured in their experiments and the relationship between the mass transfer coefficients cannot be checked with their data.

## 2.2 Driving force

Before considering how mass transfer coefficients are measured, we have to first delve deeper into the mass transfer theory and discuss the driving force. The driving force is the difference in the concentration of the compound in the phase itself and at the interface. As discussed above, the driving force can be defined in either phase, and if the Henry's absorption isotherm is linear for desorption:

$$\dot{m} = K_L a (c_L - c_L^*) \quad (22)$$

since:

$$H_c = \frac{c_G^*}{c_L} = \frac{c_G}{c_L^*}$$

In a mass transfer apparatus if the receiving phase reaches the equilibrium concentration, e.g., in volatilization if the gas becomes saturated such that  $(c_L - c_L^*) = 0$ , a mass transfer coefficient can no longer be used to calculate the mass transfer rate. For the case of nonsteady state with a saturated gas phase, the mass transfer rate can be calculated from:

$$V_L \frac{dc_L}{dt} = -Q_G \cdot c_L \cdot H_c \quad (23)$$

$$\text{since: } c_G = c_G^* = c_L \cdot H_c$$

where:  $Q_G$  = gas flow rate

$V_L$  = reactor volume

Mackay et al. (1979) suggests calculating Henry's constants with this equation from data collected in a bubble column. Figure 6 illustrates the rapid approach to equilibrium for air bubbles rising in a benzene/water solution (Allen et al., 1986).

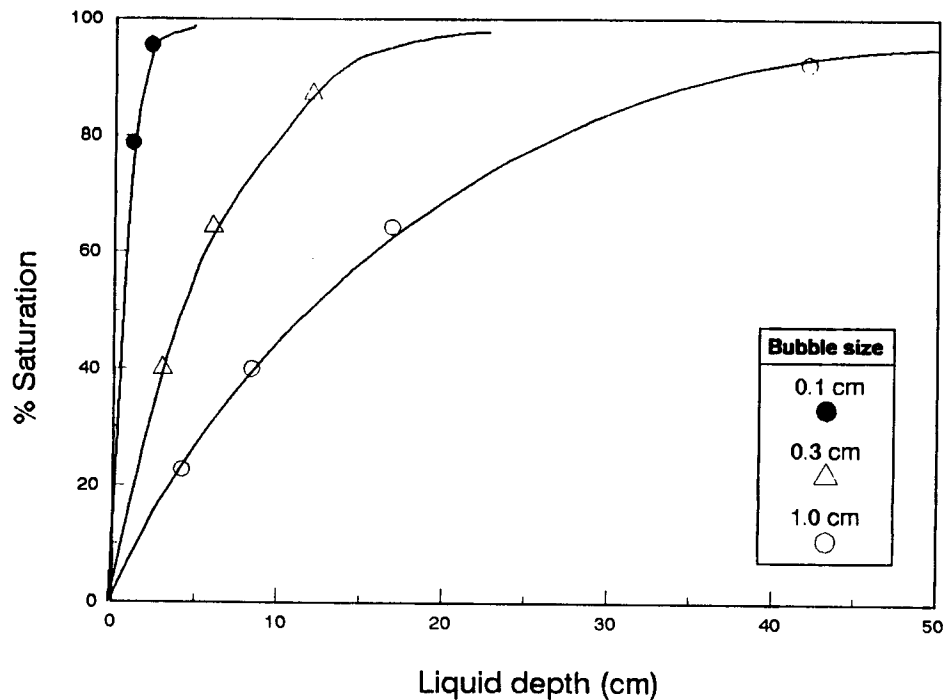


Figure 6. Approach to equilibrium as a function of liquid depth for benzene absorbed during bubble rise in water (Allen et al., 1986)

Since a mass transfer coefficient can only be measured in phases not at equilibrium, care must be taken to insure that samples of the gas and liquid phases collected for the evaluation of  $K_L a_{VOC}$  are not saturated. The experimental ratio of the  $K_L a$ 's cannot be constant for varying operating conditions if one of them is measured incorrectly, i.e with the phases in equilibrium.

### 2.2.1 Equilibrium concentration - $c^*$

Bringing in the equilibrium concentration ( $c^*$ ), we introduce a source of error in the calculation of the driving force. This applies to both oxygen and VOC's. The correction of  $c^*$  for the change in the oxygen saturation concentration in contaminated water is often made with an empirical factor, the beta factor. The beta factor has been defined as:

$$\beta = \frac{c_{WW}^*}{c_{TP}^*} \quad (24)$$

where:

$c_{WW}^*$  = oxygen saturation concentration in wastewater

$c_{TP}^*$  = oxygen saturation concentration in tap water

The beta factor has been found to be correlated to the total dissolved solids content of the water. Another common problem in determining  $c^*$  for oxygen is correctly accounting for hydrostatic pressure. In CFSTR's used in this study, this effect is negligible, but can be quite significant in deep diffused aeration systems. Campbell et al. (1976) present a good review of the problem.

In calculating the equilibrium concentration for VOC's, the error caused by using an inappropriate Henry's constant can be significant since the relationship  $c_L^* = c_G/H_C$  is used. The determination of the Henry's constant in clean water is difficult and the difference in values found by various investigators can be large. Mackay and Shiu (1981) reviewed published Henry's constants for environmentally relevant compounds and found that considerable discrepancies exist in the literature, even for fairly common compounds. The use of a Henry's constant obtained for a substance dissolved in a pure water in the calculations for a heavily contaminated water can lead to false estimates of the mass transfer rate. Two methods are commonly used for measuring Henry's constants, the bubble column as mentioned previously, and the equilibrium partitioning in closed systems (EPICS) method (Lincoff and Gossett, 1984) as described in Section 3.5.



For six chlorinated volatile organic compounds, Roberts et al. (1984b) found differences of up to 50% between the  $H_c$  found for filtered effluent from a wastewater treatment plant and for clean water in measurements in a bubble column. If we write the beta factor defined above for oxygen in terms of Henry's constants, we find:

$$\beta = \frac{c_{WW}^*}{c_{TP}^*} = \frac{c_G/H_{c_{WW}}}{c_G/H_{c_{TP}}} = \frac{H_{c_{TP}}}{H_{c_{WW}}} \quad (25)$$

Using this definition and the values of  $H_c$  reported by Roberts et al. for volatile chlorinated hydrocarbons, beta factors for the filtered secondary wastewater used in the study can be calculated that range from 0.62 for chloroform to 0.99 for carbon tetrachloride. They did not report a beta factor for oxygen. Accepting these values for the moment, and considering the wide range of beta factors found for the various compounds in the same waters: 0.62-0.99, it seems that the oxygen beta factor cannot be used to adjust for changes in  $H_c$  for other compounds.

Yuteri et al. (1987) investigated the effect of additives in distilled water on Henry's constants for trichloroethylene (TCE) and toluene using the EPICS method. They found differences in the Henry's constant for TCE of  $\sim +15\%$  when the ionic strength of the water was increased and  $\sim -15\%$  when surfactants were added. In experiments with natural waters, they found the  $H_c$  for toluene varied as much as 24%, but there was no apparent trend with alkalinity, pH, or TOC. They warn that unpredictable deviations from the pure water values of the Henry's constants should be expected in contaminated water because of

such molecular phenomena as association, solvation, and salting-out. In considering the significance of these variations, one must keep in mind that their comparison of their  $H_c$  data for 15 compounds in distilled water with other published experimental values shows deviations of up to 30%.

Lincoff and Gossett (1984), in comparing the two methods, found that the Henry's constants from the EPICS method was consistently higher than the bubble column results (~14%). An interesting explanation for this may be the equation proposed by Lord Kelvin in 1871 relating the change in vapor pressure with drop curvature as a function of surface tension. The interface for the EPICS method is a plane surface and the interface for the bubble column is spherical. If we consider that the vapor pressure of a small drop of liquid is greater than that of a liquid with a plane surface and that the vapor pressure inside a bubble surrounded by bulk liquid is less than that at a plane surface, then theoretically,  $H_{c_{drop}} > H_{c_{plane}} > H_{c_{bubble}}$ . Padday (1969a) explains this by supposing that the attraction forces on a molecule in a convex surface are less than those at a plane surface. The attraction is diminished because, on the average, there are fewer molecules in the immediate vicinity to contribute to the total attraction. In a similar way, the vapor pressure at a concave surface is less than that at a plane surface because the number of molecules contributing to the total attraction is greater at a concave than at a plane surface. Therefore, theoretically, a compound is more volatile in surface aeration than in fine bubble aeration. The question, of course, is the magnitude of this difference. Looking at the values of Henry's constants gathered by Yuteri et al. (1987) from the literature, there is no clear trend in the values from the two methods; the variation in the same method used by various researchers is sometimes greater than the varia-

tion between the two.

### **2.3 Surface tension**

Many studies of the effect of surfactants on mass transfer have found mass transfer to decrease with decreasing surface tension. Reports of increased mass transfer have also been made. In order to understand the effect of surfactants on mass transfer, we have to understand the general concept of surface tension. This is discussed below, as well as the factors affecting surface tension, followed by a discussion of literature results relevant to the effect of surface tension on mass transfer.

Surface molecules possess energy in excess of the energy they already possess in the bulk liquid state. In order to create new surface, work has to be done on the system to overcome the excess energy. This surface free energy equals the surface tension of a pure liquid.

Padday (1969a) presents an interesting review of the historical development of surface tension starting from Leonardo da Vinci's observation of capillarity to the present day theoretical and experimental results. Studying the historical development helps understand the theory of surface tension. The following table summarizes some of the historical highlights.

That contaminants, such as soap and grease, lower the surface tension of water has been known since the first measurements were made with capillary tubes; it took much longer before it was discovered that the addition of inorganic electrolytes increased the surface tension of water. This phenomenon, however, is not of interest in this work, because such large quantities are required that

Table 3. Historical development of the theory of surface tension.

Leonardo da Vinci	(1452 -1519)	-observed and recorded rise of liquid in a tube of small bore
Sir Isaac Newton	1721	-explained rise of liquid in a capillary tube as the product of cohesive and adhesive forces. -recognized that the forces were intermolecular in origin and that mutual attraction gave rise to a pressure inside the liquid.
J.A. von Segner	1751	-proposed the first theory of capillarity: cohesive forces create a pressure which is resisted by a uniform tension in the surface (surface tension). -surface tension denoted the presence of a contractile skin at the surface of a liquid.
Thomas Young	1804	-proposed particles of matter act on one another with two kinds of forces, attraction and repulsion, the former acting over greater distances than the latter.
P.S. de Laplace	1805	-the attraction force gives rise to a pressure on surface particles: the surface tension as proposed by von Segner.
J.D. van der Waals	1899	-showed existence of physical forces of attraction between molecules.
Lord Rayleigh	1902	-related the physical forces of attraction to surface tension.
J. Willard Gibbs	1906	-developed quantitative thermodynamic relationships between the energetics of surface formation and intensive properties of the liquid.

increases in surface tension due to salts in wastewater applications are not expected. The discussion here will be limited to the effect of surface active agents on surface tension. Various methods exist to measure surface tension; Padday (1969b) and Masutani (1988) present good reviews of the methods.

The addition of organic liquids or surface-active agents lowers the surface tension of water. The ability of an organic molecule to lower the surface tension is due to its tendency to adsorb at the liquid /air interface, orienting itself with the

hydrophobic group at the air interface and the hydrophilic group in the water phase. Characteristic of surface-active agents is their ability to lower the surface tension at relatively low bulk concentrations by adsorbing strongly at the surface.

### **2.3.1 Effect on mass transfer**

Surfactants can affect mass transfer in two ways, changing the interfacial area or the mass transfer coefficient  $k_L$ . A small amount of a surfactant can potentially cause a large change in interfacial area. Bubbles break away from an orifice when the ascending force is greater than the force due to surface tension; therefore, a decrease in surface tension can reduce the size of primary bubbles, increasing the interfacial area. Bubble coalescence is also hindered by surfactants, thereby, preserving the increase in interfacial area. This phenomena is discussed more thoroughly in Section 2.4.

Two theories are commonly used to explain the effect of surfactants on the mass transfer coefficient: the barrier effect and the hydrodynamic effect. In the barrier theory, the presence of the surfactants at the phase interface creates an additional resistance to mass transfer due to diffusion through the surfactant layer.

In studies of the effect of surfactants on the absorption of  $\text{SO}_2$  in water in a stirred system, Springer and Pigford (1970) found that surface films of a soluble surfactant (sodium lauryl sulfonate) showed no barrier effect, though the insoluble 1-hexadecanol surface film showed definite resistance. Llorens et al.(1988) in studying  $\text{CO}_2$  absorption into solutions of various surfactants in a wetted area column determined that the barrier effect was insignificant com-

pared to the hydrodynamic effect.

The hydrodynamic theory is based on two limiting cases. Considering a bubble in a pure water/gas system, the bubble behaves like a fluid sphere; it has a moving interface, retarded only by the viscosity of the gas, with a strong internal recirculation of the gas. Addition of surfactants retards the interface motion because surfactants have a strong tendency to adsorb on the bubble interface, accumulating at the bottom of the bubble. At high surfactant concentrations the bubble is thought to behave like a solid sphere, a Ping-pong ball with a rigid interface and no internal gas recirculation.

The mathematical model developed by Andrews et. al (1988) illustrates the hydrodynamic theory. Their model describes the hydrodynamics and mass transfer of bubbles rising through contaminated liquids using boundary layer and wake type hydrodynamics. The model divides the bubble into an upper boundary layer region where surfactant adsorbs and a lower wake region from where it desorbs. The model includes the mass transfer of surfactant from the liquid to the upper part of the bubble, its transfer around the interface by interfacial motion and diffusion, its desorption from the bottom of the bubble and the effect of these processes on the interfacial tension gradient in the boundary layer region. The results from the model only apply strictly for surfactant concentrations greater than the concentration that causes interface saturation; thus, the model may not be valid for very low surfactant concentrations.

The model predicts that at "low" surfactant concentrations the high concentration gradients produce large gradients of interfacial tension, which keeps the bubble interface almost immobile. Conversely, at surfactant concentrations

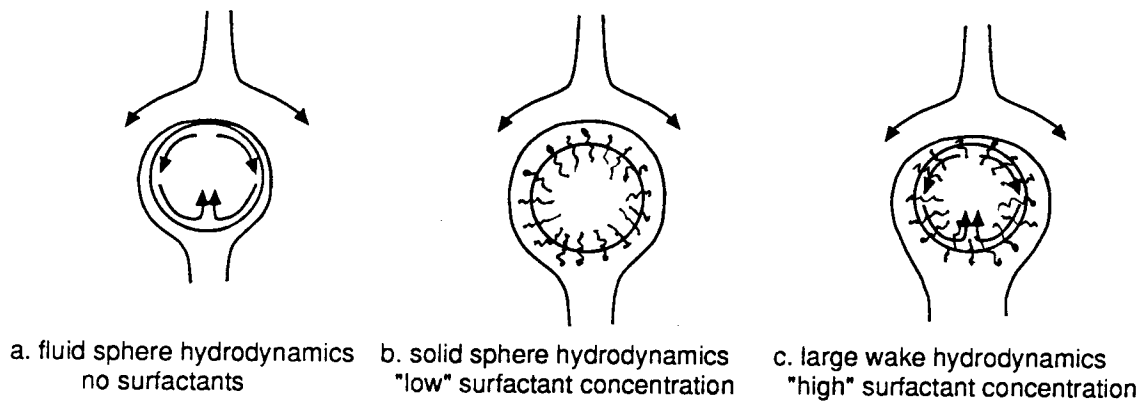


Figure 7. Change in bubble surfactant layer in the two hydrodynamic regimes.

above those required to make a bubble behave as a solid sphere (solid-sphere hydrodynamics), the gradients of adsorbed surfactant and interfacial tension are small so the interface is mobile (Figure 7).

They introduced a third hydrodynamic regime to describe this phenomena: the "large-wake" hydrodynamics, associated with the saturation of the interface in the wake region with surfactant. In this regime increasing the surfactant concentration increases the mobility of the interface in the boundary region so the boundary layer is thinner and the local mass transfer coefficients are correspondingly larger. At the same time the boundary layer occupies less of the total surface area of the bubble. Therefore, between the two hydrodynamic regimes the mass transfer coefficient from the bubble goes through a maximum and then declines. This maximum has been observed experimentally (Ziemin-ski, et al., 1967) with bubbles in a water/air system with low molecular weight

surfactants (carboxylic acids and alcohols). With high molecular weight surfactants, normally only the decline in  $k_L$  with a leveling off at high surfactant concentrations has been observed. Their explanation is the transition from fluid-sphere to solid-sphere to "large-wake" hydrodynamics happens in such a narrow range of surfactant concentrations that a maximum is not detectable.

In studying the mass transfer of acetone across a plane interface in a liquid/liquid system (water/carbon tetrachloride), Ollenik and Nitsch (1981) found that below the critical micelle concentration (cmc) of dodecyl sodium sulfate the interface was almost rigid and  $k_L$  fell to approximately one third the value in clean water. As the surfactant concentration neared the cmc, they observed an increase in interfacial velocities and  $k_L$ . Above the cmc, the values of  $k_L$  and interfacial velocity reached those of clean water. Assuming that the results from a liquid/liquid system are extrapolatable to liquid/gas systems, it is possible that this recovery corresponds to the maximum predicted by the bubble model of Andrews et al. (1988). In their model,  $k_L$  goes through a maximum as surfactant concentration increases because the two trends, the decrease in surface tension gradient and the decrease in surface area due to accumulation of surfactants in the bubble wake, cause opposite effects on mass transfer. In a system with a plane interface the decrease in the boundary layer due to accumulation of surfactants is reduced, so that  $k_L$  steadily increases due to the decrease in surface tension gradient and the resulting increase in interface mobility as discussed above.

Lee, Tsao, and Wankat (1980) investigated the hydrodynamic effect of surfactants using an oxygen ultra-microprobe. They studied the effect of sodium lauryl sulfate, bovine serum albumin, and glucose oxidase on oxygen transfer and



found  $k_L$  to decrease with increased surfactant concentration at a constant power input. However, the hydrodynamic effect decreased with increase in impeller speed.

The adsorption of surface active agents at the surface is time dependent. In aqueous solutions, a freshly formed surface possesses a higher surface tension than the value at equilibrium. Reports of the time required to reach equilibrium surface tension vary according to the surface active agent, from 0.01 s to many hours. The time required for the compound to migrate to the surface depends partly on the size of the molecule, its polarity, and the free energy of the surface (Addison, 1944). In studies of n-alcohols, Addison (1945) showed that the migrational velocity increases with chain length. He also found that at very low concentrations the migrational velocity decreases with decreasing concentration.

The difference between the dynamic and static surface tension may explain the dependence of mass transfer on power input. In discussing their results, Lee et al.(1980) point out that the common assumption that the surfactants recover their equilibrium surface tension immediately after the disruption by the eddies approaching the surface is an oversimplification. In reality, there may be a time lag before the surfactant recovers its equilibrium surface tension. If so, it is not the static but the dynamic value of surface tension that is responsible for the hydrodynamic effect. This dynamic surface tension is expected to depend on the properties of the surfactant. Springer and Pigford (1970) postulated that the dynamic surface tension is related with the time constant of recovery to equilibrium for a given surfactant, and stated that a surfactant with a fast recovery time exhibits the hydrodynamic effect even at high liquid turbulence.

Attempts to correlate equilibrium or static surface tension with mass transfer coefficients have been made with limited success (Stenstrom and Gilbert, 1981). This led Masutani (1991) to investigate the relationship between  $k_L a_{O_2}$  and dynamic surface tension. She studied the effect of two anionic surfactants on oxygen transfer in a tank with fine bubble diffusers. The maximum bubble pressure method was used to measure the change in surface tension with time and the Du Noüy ring method for the static surface tension values. She was able to develop a correlation for  $k_L a_{O_2}$  as a function of the air flow rate, dynamic surface tension, and static surface tension.

A model proposed by Koshy et al. (1988) for drop breakage and mass transfer in liquid/liquid systems offers insight into the dynamic/static surface tension effects. The model can help explain gas/liquid transfer as well. When a pressure fluctuation due to an eddy is experienced by a drop across its diameter, the drop starts deforming. The deformation most probably starts by the formation of a depression on the drop interface and this depression propagates resulting in breakage. When the surfactants are present at the interface, the pressure fluctuation, besides causing depression at the interface, also removes the adsorbed surfactant molecules thereby exposing a fresh interface. This fresh interface has dynamic interfacial tension which is higher than the static interfacial tension. Thus, at the base of the depression, the interfacial tension is higher. This difference in interfacial tension causes a flow towards the base and this adds to the flow already taking place due to the pressure fluctuation. Thus internal recirculation of the drop is generated due to the difference in dynamic and static interfacial tension. This in turn increases the mass transfer between the drop and its surroundings.

The effect of increasing power input can be explained based on this model. Since the effect of surfactants is to reduce the internal recirculation of a bubble and to dampen turbulence, the increase in surface renewal of the bubble interface due to increased turbulence, not only increases transfer by removing the barrier, but also through the increased interfacial turbulence caused by the difference in the dynamic and static surface tension at the point where the surface is renewed.

## 2.4 Coalescence

Mass transfer is affected by the coalescence behavior of the bubbles because of the decrease in interfacial area that occurs when the bubbles coalesce. As seen in the development of equation 9 in Section 2.1.2, a term describing bubble coalescence is needed for the correlation of the mass transfer coefficient, however, none is yet available. Therefore, separate correlations are made for coalescing and non-coalescing systems. Water/air is a coalescing system. Addition of electrolytes to water hinders bubble coalescence and increases the volumetric mass transfer coefficient. Organic compounds, such as surfactants, acids and alcohols, also affect coalescence, generally hindering it and thereby, increasing the volumetric mass transfer coefficient.

Osorio (1985) studied the influence of ionic strength with the steady state hydrazine method. He found  $k_L a_{O_2}$  increased with increased ionic strength up to a concentration of 0.2 mol/L NaCl where it then plateaus off with increased NaCl addition. He called this the region of complete coalescence inhibition. The  $\alpha$  value was approximately 1.5. He also studied the effect of iso-propanol on mass transfer, for the same energy input and superficial gas velocities, a "small" amount of iso-propanol (0.04 mol/L) caused more than a two-fold increase in

$k_L a_{O_2}$  ( $\alpha \approx 2-2.5$ ). Although he said coalescence in the salt solution of 0.2 mol/L was completely inhibited, he based this increase due to iso-propanol on the almost completely inhibited coalescence. Here it is possible that the amount of iso-propanol was large enough that the primary bubble size was decreased by the reduction in surface tension, although the surface tension was only reduced 1.5%.

The effect of coalescence inhibition on  $k_L a$  depends on the type of aerator, the greater the possibility of coalescence, the greater the effect. Zlokarnik (1978) found a strong dependence of salt concentration on the increase in  $k_L a_{O_2}$ , stronger than other published results, ( $\alpha = 5-7$ ), which he explained on the basis of his stirrer type (a self-aspirating stirrer) which produced very fine bubbles. Once fine bubbles are formed they do not easily coalesce. Zieminski and Hill (1962) developed a system which exploited this observation to increase oxygen transfer with a very low organic concentration. They introduced a concentrated solution of 4-methyl-2-pentanol continuously at the surface of the porous plate diffuser, and thus, compared to a system with the same bulk liquid concentration, achieved a higher oxygen transfer.

Keitel and Onken (1982) studied coalescence inhibition with n-alcohols, aliphatic mono-carboxylic acids, ketones, bivalent alcohols. They found that the compounds reduced the surface tension and with a certain concentration level caused coalescence inhibition. This concentration is lower for carboxylic acids than for alcohols and ketones. The presence of a second OH group pushes the concentration level necessary higher. Increasing chain length in a homologous group decreases concentration level necessary.

Drogaris and Weiland (1983) studied the coalescence frequency and coalescence times of bubble pairs in the presence of n-alcohols and carboxylic acids. They found that if the contact time between two bubbles is larger than the coalescence time, the bubbles coalesce. Since different reactors have different available contact times, the degree of coalescence inhibition produced by a certain concentration of an organic compound depends on the type of reactor and aerator used.

Guroi and Nekouinaini (1985) investigated the effects of various organics on the characteristics of oxygen transfer from air bubbles to water, (acetic acid, 8 phenols, tertiary butyl alcohol, toluene and chlorobenzene). They used a bubble column with a glass frit or capillary to introduce the air. The effects of gas flow rate, pH, and ionic strength were also examined.

Values of  $k_L a$  in the presence of phenolic compounds, acetic acid and tertiary butyl alcohol were consistently higher than those measured in pure water. Toluene and chlorobenzene (0.4mM = 36.8 mg/L toluene) did not affect the  $k_L a$ . The type of substitution on the phenol molecule made a significant difference on the magnitude of  $\alpha$ . Their attempt to correlation their  $\alpha$  values for the phenolic compounds at pH 2.5 with the octanol-water partition coefficient ( $K_{OW}$ ) showed the general trend that the more hydrophobic the compound (higher  $K_{OW}$ ), the higher the  $\alpha$  value. The effect of acetic acid on  $k_L a_{O_2}$  could not be explained with this. The pH also had an influence on the change in  $k_L a$  for the organics that deprotonate: the protonated form of the molecule showed a much larger effect. Above pH 7 acetic acid had little to no effect on  $\alpha$ . Because of the higher pKa of m-cresol, its affect on  $k_L a_{O_2}$  decreased only after ~pH 9 was reached ( $\alpha=2.5$ , 21.6 mg/L).

Because bubbles coalesce more rapidly at high gas flow rates in a water/air system, the presence of substances that suppress coalescence becomes more important the higher the flow rate:  $\alpha$  increased with an increase in  $Q_G$ . As already discussed above, an increase in ionic strength increased  $k_L a_{O_2}$ . They found ions and organics have additive effect. This is probably due to the concept of total coalescence inhibition, which was not yet reached by the addition of salts, so  $k_L a_{O_2}$  increased until the complete inhibition was achieved.

In order to investigate whether the increase in  $k_L a_{O_2}$  was due to coalescence or surface tension variations, Gurol and Nekouinaini (1985) studied the behavior of single bubbles in the presence of the organics. In experiments in which bubble coalescence was prevented by non-frequent formation of bubbles, neither  $k_L a_{O_2}$  nor bubble size was affected by the organics. Measurements with a tensiometer (Du Noüy ring method) showed no significant change in surface tension due to the presence of the organics in the concentration ranges studied.

They studied the effect of a surfactant in the system. The typical behavior of surfactants was seen-first  $k_L a_{O_2}$  decreased with concentration (up to  $\sigma = 69$  mN/m) then it recovered (after  $\sigma = 62$  mN/m) and increased to  $\alpha = 1.3$  as the concentration increased. ( $\sigma = 72.8 \rightarrow 56$  mN/m). They found the presence of both a surfactant and an organic compound have an additive effect.

#### **2.4.1 Increased coalescence**

Certain compounds in very low concentrations can cause a large increase in coalescence. Zlokarnik (1980) reported experimental results with a nonionic surfactant that is often used as an antifoam agent. He found that certain anti-foamers at concentrations as low as 3 mg/L can reduce the oxygen transfer to

half that found in pure water. In experiments with biomass, he found an  $\alpha$  value of 0.5. He postulated that the activated sludge flocs act as "crystallization seeds", promoting bubble coalescence and, thus decreasing the oxygen transfer. In comparison, in experiments with 6 g/L cellulose and 6 g/L activated carbon in pure water, the finely dispersed solids alone did not strongly promote coalescence.

In diffused aeration systems increases in air flow rate can sometimes reduce the volumetric mass transfer coefficient, because the increased gas flow and resulting increase in liquid flow promotes bubble coalescence. Zlokarnik warned that laboratory experiments have no validity, because the process of the gas distribution and the opposing process of bubble coalescence are both extremely dependent on the scale.

## 2.5 Determination of mass transfer coefficients

The various methods used to determine mass transfer coefficients are based on the material balance on the reactor (Figure 8). The following equations are written for absorption, however, the equations need only a slight modification for desorption:  $(c_L - c_L^*)$  instead of  $(c_L^* - c_L)$ .

liquid phase:

$$V_L \cdot \frac{dc_L}{dt} = Q_L(c_{L_o} - c_L) + K_L a \cdot V_L(c_L^* - c_L) - R_{Bio} \quad (26)$$

gas phase:

$$V_L \cdot \frac{dc_G}{dt} = Q_G(c_{G_o} - c_G) - K_L a \cdot V_L(c_L^* - c_L) \quad (27)$$

total material balance at steady state:

$$Q_G(c_{G_o} - c_G) = Q_L(c_{L_o} - c_L) \quad (28)$$

where:

$c_{L_o}$  = influent liquid concentration (mg/L)

$c_L$  = reactor and effluent liquid concentration (mg/L)

$c_{G_o}$  = influent gas concentration (mg/L)

$c_G$  = reactor and effluent gas concentration (mg/L)

$Q_L$  = liquid flow rate (L/h)

$Q_G$  = gas flow rate (L/h)

$V_L$  = reactor volume (L)

$R_{Bio}$  = biological reaction rate (mg/h)

Aerobic biological reactors are used for many applications, in treating wastewaters, industrial or municipal, or in industrial fermentation processes. The oxy-



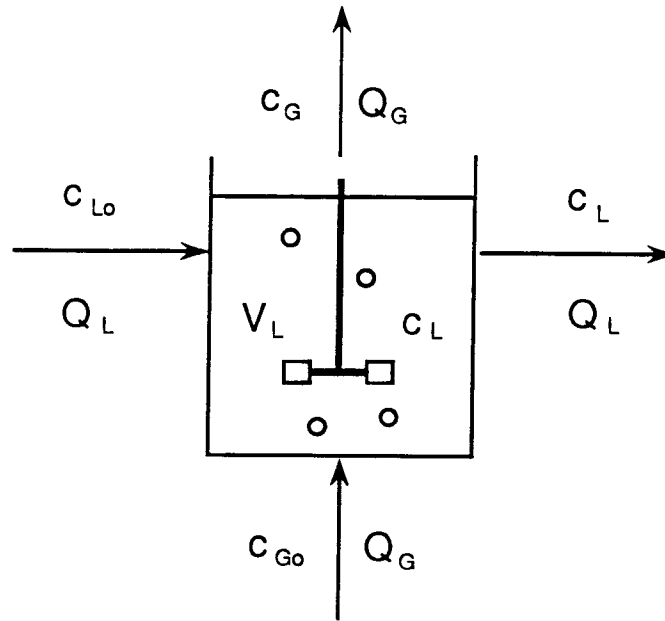


Figure 8. Mass balance on the reactor.

gen transfer required varies depending upon the process. Wastewater treatment plants generally require less oxygen transfer than industrial fermentation processes. This means that the mass transfer coefficient and therefore the energy input for wastewater treatment plants is usually much lower than for the industrial fermentation. The typical energy and mass transfer coefficient ranges are shown in Figure 9. The experiments made in this study span both regions, since the treatment of industrial wastewaters may require a higher oxygen transfer.

The following section presents the common methods used to determine the mass transfer coefficient and the problems inherent in each. The errors associated with the methods generally become large in the region of high power densities and high mass transfer rates. This can be seen in Figure 9. Oxygen absorption is used to discuss the methods, however, the methods and problems are similar for VOC desorption.

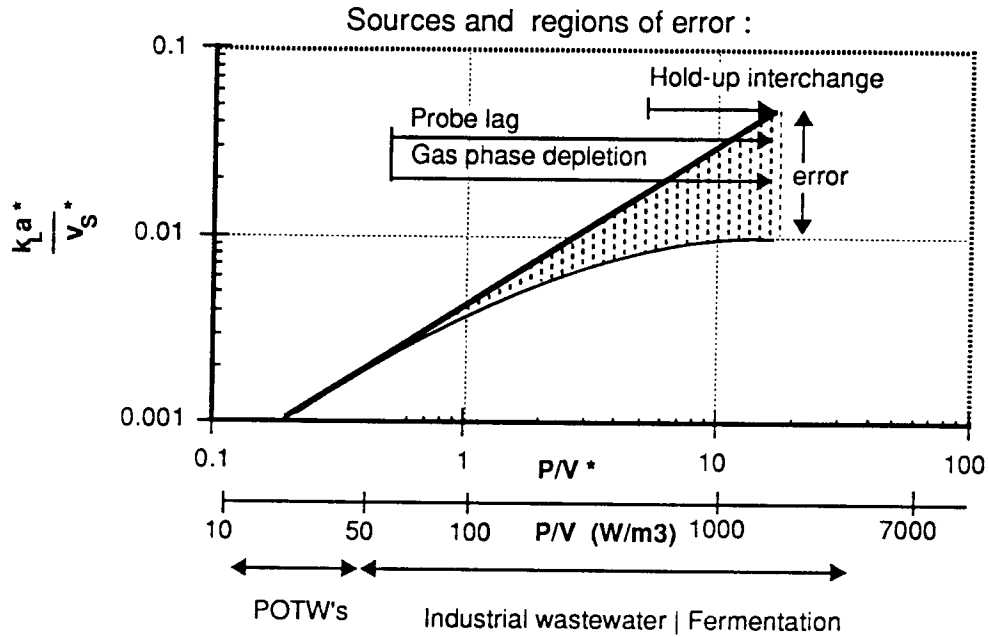


Figure 9. Typical ranges for mass transfer coefficients and energy input.

### 2.5.1 Nonsteady state methods

#### Batch model

A common approach in the laboratory or in new aeration basins is to use a batch set-up (with respect to the liquid) where deoxygenated water is gassed with air. The change in the liquid oxygen concentration over time is measured with an oxygen probe. The mass balance reduces to:

$$\frac{dc_L}{dt} = K_L a (c_L^* - c_L) \quad (29)$$

with the assumption that the gas and liquid phases are ideally mixed, and no reaction takes place.

The mass transfer coefficient can be found either from a linear or nonlinear regression of the integrated form of the equation:

$$\frac{c_L^* - c_{Lo}}{c_L^* - c_L} = e^{K_L a \cdot t} \quad (30)$$

### Continuous model

In operating systems with continuous flow, the nonsteady state approach is a bit more complicated. A perturbation in the dissolved oxygen concentration (DO) is made and the change in DO over time is measured as the system returns to steady state. The change can be either an increase in DO, i.e. addition of hydrogen peroxide or use of technical oxygen, or a decrease in DO, i.e. a chemical reaction. The liquid phase mass balance, equation 26, is used. The integrated form of the equation is:

$$\ln \left[ 1 - \left( \frac{c_L - c_{Li}}{c_{L\infty} - c_{Li}} \right) \right] = -K_2 \cdot t \quad (31)$$

where:  $K_2 = \frac{Q_L}{V_L} + K_L a$

$c_{Li}$  = oxygen concentration at  $t = 0$

$c_{L\infty}$  = oxygen concentration at  $t = t_{\infty}$

This equation can be used in systems with or without biological activity, as long as the reaction is at steady state.

### Gas phase oxygen concentration

In order to evaluate the experimental data, the correct  $c_L^*$  must be used. The general problems with  $c_L^*$  due to changes in Henry's constants from contam-

inants, and the effect of hydrostatic pressure discussed in Section 2.2.1 apply here as well, but one of the specific problems associated with nonsteady state reaeration is the oxygen depletion of the gas phase.

In experiments using air, the oxygen concentration in the gas phase decreases as the oxygen is transferred to the liquid phase. In the initial phase of reaeration where the liquid oxygen concentration increases sharply, gas phase oxygen depletion is the severest. Use of a constant  $c_L^*$  in the evaluation of the data can produce a greatly underestimated  $k_L a$ . Reports of  $k_L a$ 's underestimated by 40% when gas phase depletion was neglected in stirred tank reactors have been made (Chapman et al., 1982). The underestimation is more pronounced with higher oxygen transfer efficiencies. In investigating coalescing and non-coalescing systems, Osorio (1985) found the degree to which the nonsteady state method underestimates  $k_L a_{O_2}$  increases with decreasing superficial gas velocity, and with increasing inhibition of coalescence. In the extreme region of complete coalescence inhibition and low superficial gas velocity,  $k_L a$  was underestimated by 50%. In non-coalescing systems, an ideally mixed gas phase can no longer be assumed, especially in bubble columns. A more complicated model of the gas phase is then needed to include gas mixing and the change in the oxygen concentration.

In systems using a gas, i.e  $N_2$ , to deoxygenate the water, the problem of the oxygen concentration change due to transfer into the liquid phase is compounded by the dilution effect of the  $N_2$  transferring into the gas phase. Instead of assuming that  $c_L^* = c_{Gin}/H_c$ , a good model of the gas phase must consider the simultaneous transfer of oxygen out of and nitrogen into the gas phase. The reactor type determines the required complexity of the model; the

assumption of no change over the height of the vessel is a good approximation for a lab-scale stirred tank, but may not be valid for a deep diffused aeration system.

Various models describing the change in the gas phase oxygen concentration have been proposed over the years since question of the effect of gas phase depletion on  $k_L a$  evaluation was first raised. Linek et al. (1982) provide a good summary and review of the work done in lab-scale stirred tank reactors.

Brown and Bailod (1982) discuss this problem in evaluating  $k_L a$  in large scale aeration basins.

If pure oxygen is used there is no gas phase depletion as the oxygen is transferred, but to avoid the dilution effect, the water must be deoxygenated without the use of another gas. Another possibility besides vacuum degassing, is the use of a chemical reaction. Sodium sulfite and cobalt as the catalyst have often been used. If a large amount of salt must be used, which is the case for high mass transfer coefficients, the change in ionic strength due to the salt causes a change in bubble coalescence, and in the liquid diffusion coefficient, so that  $k_L a$ 's determined with this method cannot be compared directly to other methods (ASCE Standard, 1984).

### **Reactor hold-up**

When a gas, e.g.  $N_2$ , is used to deoxygenate the liquid, an instantaneous interchange between  $N_2$  and air to begin the reaeration is usually made in order to keep the fluid dynamics of the system constant. To account for the time it takes for the gas hold-up interchange between  $N_2$  and air to take place, additional equations describing this flush out must be used. Linek et al. (1982)

found that the neglect of this hold-up interchange has caused the inappropriate interpretation of experimental results as showing that  $k_L a$  with increasing power input reaches a maximum and then decreases.

A variant of the procedure without the above described problem of the hold-up interchange involves stopping the stirring and gas flow after the liquid has been deoxygenated to allow the bubbles to escape. Then the stirring and the air flow are simultaneously started. The start up period, i.e. the time required for the hold-up to reach the steady state value, must be included in the process model. This method combined with vacuum degassing and pure oxygen is the only nonsteady state one Linek et al. (1987) has found to give correct results in the regions of large mass transfer coefficients.

### **Oxygen probe dynamics**

Another problem specific to all nonsteady state tests is the influence of the response time of the dissolved oxygen probe. Philichi and Stenstrom (1989) showed that the importance of the probe time constant is negligible when the product of the probe time constant,  $\tau$ , and  $k_L a$  is less than 0.02 for first order probe dynamics. This means that for fine bubble diffusers where  $k_L a$  is usually of the order of  $0.001 \text{ s}^{-1}$ , the probe lag influence is negligible. If the initial data in the reaeration test is truncated at  $\sim 20\%$  of  $c^*$ , they found that the error in  $k_L a$  was still less than 1% for  $\tau \cdot k_L a < 0.05$  when using a nonlinear regression to calculate  $k_L a_{O_2}$ . Using a probe with a small time constant extends the range of  $k_L a$  to  $\sim 0.01 \text{ s}^{-1}$ . But for mass transfer devices with  $k_L a$ 's greater than  $0.01 \text{ s}^{-1}$ , the lag in probe response can significantly influence the determination of  $k_L a$ . Stirred tank reactors used in industrial fermentation have  $k_L a$ 's that can range

up to  $0.2 \text{ s}^{-1}$ . It is, therefore, important to consider the probe dynamics when measuring  $k_L a$ 's in these types of transfer devices. Various models have been proposed to describe probe lag. (Dang, et al., 1977, Linek et al., 1987)

### **Nonsteady State Model**

The complexity of the model necessary to determine  $k_L a$  with the nonsteady state reaeration method depends upon the range of the mass transfer coefficients measured. For the range normally found in wastewater treatment plants ( $0.001\text{-}0.005 \text{ s}^{-1}$ ), the problems mentioned above are not serious. Brown and Bailod (1982) found that error caused by neglecting gas phase depletion was less than 10% for  $k_L a < 0.0025 \text{ s}^{-1}$ . Since a chemical reaction is used to deoxygenate the aeration basins, the reactor hold-up interchange is not a problem.

In investigating mass transfer coefficients typical for industrial wastewater treatment or in the fermentation industry, Chapman et al.(1982) found the  $k_L a$ 's measured with nonsteady state reaeration tests using  $\text{N}_2/\text{air}$  and assuming a constant driving force were underestimated up to 40%. They suggest the direct measurement of the gas phase oxygen concentration as a means of correcting for the gas phase depletion. Linek et al. (1987) criticized this method by pointing out the dynamics of both the gas and liquid phase probes can then significantly affect the calculation of  $k_L a$ . He recommends the use of pure oxygen combined with vacuum degassing of the liquid to remove the oxygen as discussed above, or the use of an appropriate model of the gas phase oxygen concentration.

Therefore, in industrial wastewater treatment or fermentation processes with large mass transfer coefficients, the appropriate nonsteady state model combines both a process and probe model to calculate  $k_L a$  using a regression method. The concentration profile calculated from the process model is converted to a probe response which includes the distortion due to the probe dynamics (Linek et al., 1987).

### 2.5.2 Steady state methods

For investigations of the oxygen mass transfer coefficient under real process conditions with biological activity, steady state tests are generally simpler to perform than nonsteady state tests. No interruptions of the continuous process are necessary. In laboratory investigations, the steady state method can be used with a semi-batch set-up (gas phase continuous) or a continuous flow set-up (both gas and liquid phases continuous). The semi-batch set-up uses a chemical reaction to remove the absorbed oxygen, e.g. a sulfite or hydrazine reaction. In the continuous flow set-up, the liquid is first deoxygenated and then flows into the absorber. The liquid can then be recycled or discharged.

Two methods based on the liquid and gas phase steady state mass balances (equations 26 and 27) are possible. The liquid phase steady state method requires that an accurate determination of the reaction rate of oxygen is possible, i.e. either the chemical reaction rate or the biological oxygen uptake rate (OUR). In the case of biological activity, the OUR is normally determined from batch endogenous tests which often do not realistically project operating conditions (Mueller and Stensel, 1990). Consequently, because the method based on the gas phase mass balance eliminates the need for an accurate determination



of the OUR, it is often used for evaluating the efficiency of aeration equipment under process conditions with wastewater. This method is a variant of the off-gas method (Redmon et al., 1983).

1. liquid phase:

- with biological or chemical reaction

$$K_L a = \left[ \frac{Q_L}{V_L} (c_{Lo} - c_L) + OUR \right] \left[ \frac{1}{(c_L^* - c_L)} \right] \quad (32)$$

- without reaction

$$K_L a = \frac{Q_L}{V_L} \cdot \frac{(c_{Lo} - c_L)}{(c_L^* - c_L)} \quad (33)$$

2. gas phase:

- with or without reaction

$$K_L a = \frac{Q_G}{V_L} \cdot \frac{(c_{Go} - c_G)}{(c_L^* - c_L)} \quad (34)$$

Assumptions for both methods are:

- The phases are ideally mixed.
- Negligible oxygen transfer occurs at the liquid surface.
- The liquid and gas flow rates to the reactor are constant.

and specifically when nitrogen is used to produce oxygen free influent:

- the volume of nitrogen desorbed in the reactor approximately equals the volume of oxygen absorbed, so that  $Q_{Co} = Q_{Ce} = Q_G$ .

If the mixing deviates too far from ideality,  $k_L a$  is no longer uniform throughout the reactor. Neither method as described can then be used. Instead a more complicated model of the mixing zones in the reactor would be necessary. The

assumption of an ideally mixed phase can be checked by determining the residence time distribution in the reactor. Another aspect to be considered is that the error associated with the steady state method becomes large as the liquid phase concentration approaches the saturation concentration. Care must be taken to avoid this region.

### **2.5.3 Method chosen for volatilization studies**

Although the remedy for the deviations of nonsteady state batch methods exist, i.e. use of vacuum degassing and pure oxygen or an appropriate model, the method of the mass transfer coefficient determination must be evaluated with the purpose of this study in mind: the investigation of the mass transfer coefficients of oxygen and an organic compound and the relationship between them. The method for the mass transfer coefficient determination must be adequate to measure both coefficients accurately. The nonsteady state method in the simplest form produces apparent mass transfer coefficients. Analogous to Khudenko and Garcia-Pastrana's analysis of the temperature correction factor (discussed in Section 2.1.3) the ratio of apparent oxygen mass transfer coefficients is dependent on hydrodynamic conditions. In order to achieve a valid relationship between the organic compound and oxygen mass transfer coefficients, the true mass transfer coefficient for both substances must be used. Linek et al. (1987) have shown that the "correct" method for nonsteady state testing in STR's produces good results for  $k_L a_{O_2}$ . However, the validity of this method for the determination of  $K_L a_{VOC}$  must be questioned.

Not gas phase depletion, but rather gas phase saturation may be a problem. As seen in the work by Truong and Blackburn (1984), which was carried out to consider the effect of solids, surfactants, and other water contaminants on the

mass transfer rate in bubble columns, the saturation of the gas phase prevents using their work to determine the effect of these substances on the mass transfer coefficient. Even if a reactor designed to minimize the percent saturation achieved in the gas phase is used, samples of the gas phase should be made to ensure the assumption of  $c_G = 0$  is correct, or the appropriate model should be used to account for the gas phase concentration change.

Another possibility is to circumvent the problems associated with changing concentrations of the gas and liquid phases altogether. In the steady state method, the streams sampled have a constant concentration. The oxygen gas and liquid phases can be measured on-line with high accuracy ( $\pm 1\%$ ). Enough samples of the VOC concentration in the gas and liquid can be analyzed to provide statistical confidence in the values. In the studies of the effect of an anionic surfactant on mass transfer, the advantages of the steady state method become even more apparent. Surfactant gradients in the reactor and loss of surfactant due to foaming have been found in nonsteady tests (Hwang, 1983, Masutani, 1988). In continuous flow reactors, a new supply of surfactant is constantly entering the reactor and gradients can be detected by sampling the effluent and the bottom of the reactor. Therefore, the steady state method was chosen as the best method to obtain true mass transfer coefficients for oxygen and the organic compounds.

### 3 Experimental methods

Oxygen mass transfer experiments were made in four water systems: water/air, water/VOC/air, water/DSS/air, and water/biomass/air. VOC mass transfer experiments were made in two systems: water/VOC/air and water/DSS/-VOC/air. The nonsteady (batch and continuous flow) and steady state methods were used and compared for oxygen mass transfer in the water/air system. The steady state method was used for all the other systems and for VOC mass transfer.

The liquid residence time distribution was measured in order to check that the assumption of ideal mixing was valid for the liquid flow rates used. Values of the Henry's constants for the three VOC's used were necessary for the evaluation of  $K_{La_{VOC}}$ , so experiments using the EPICS method were made to measure  $H_c$ . Surface tension measurements of dilutions of the anionic surfactant solution (DSS) were made with a Du Noüy ring tensiometer and compared to values measured by other authors.

A sensitivity analysis of the steady state method was made. The experimental method and data evaluation were designed to minimize the error in the mass transfer coefficients.

#### 3.1 Equipment

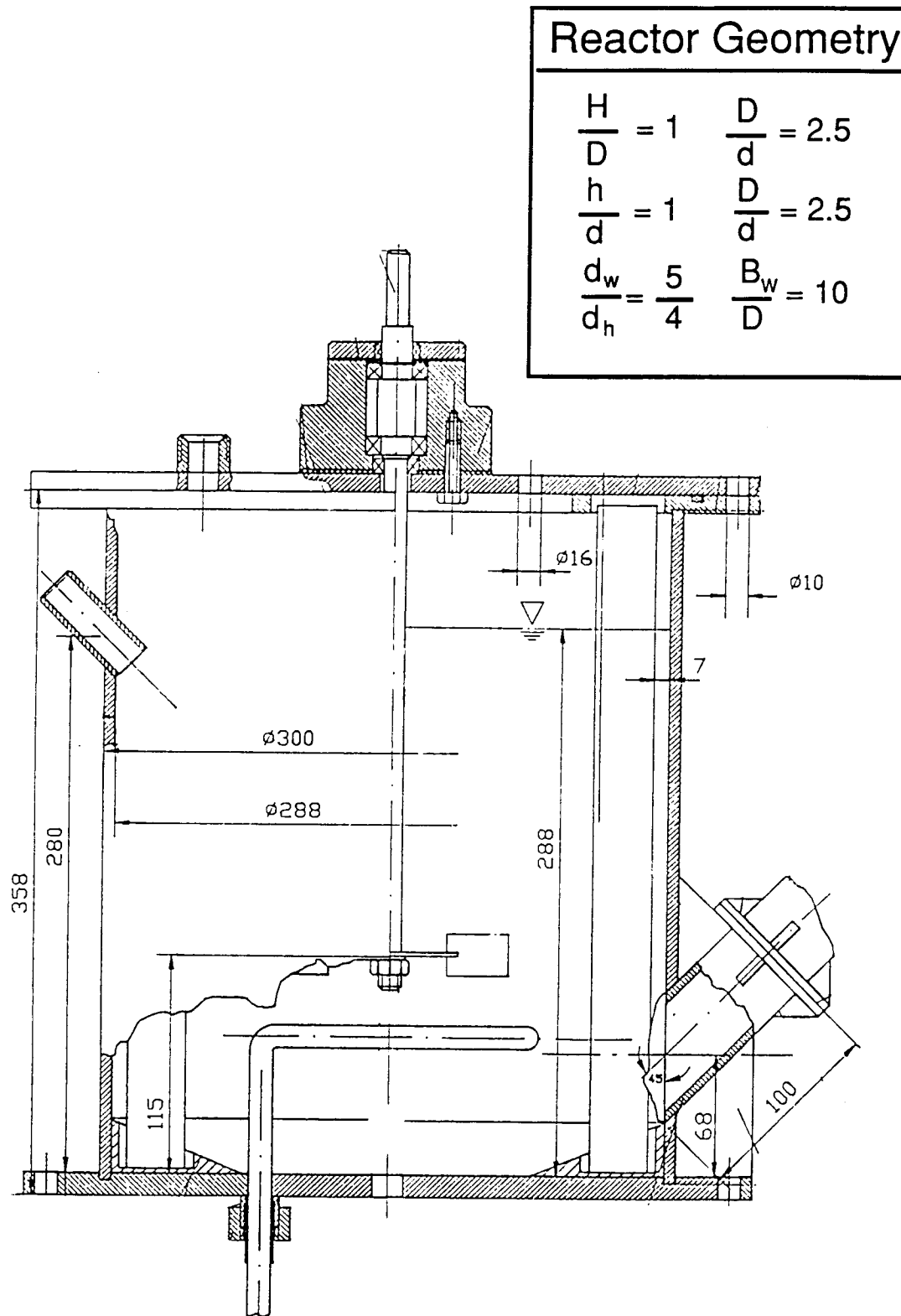
Two identical reactors were used in this study. They can be operated separately, or in series with gravity flow in between. The reactors were designed to operate under pressure, so each reactor has a flanged cover with the appropriate openings for the influent flow, gas outlet, and necessary instruments. Figure 10 shows the details of the reactor.

The reactor is made of 0.12 cm thick plexiglass; the diameter and fill height are both 28.8 cm. It has four baffles (baffle width to tank diameter, 1:10). The gas flow is introduced into the vessel through a 9 holed ring sparger with a diameter of 13.6 cm. The sparger pipe passes through the bottom of the vessel. An inclined tube clarifier is attached to the side of the reactor through which the effluent flows when the reactor is operated in the steady state mode.

The stirrer is a standard stainless steel Rushton turbine with 6 blades and a diameter of 11.5 cm. The details of the stirrer are given in Figure 10. The two stirrers are connected by a belt and driven by a variable speed motor. The speed is controlled with a voltage regulator. A stroboscope is used to measure the stirrer speed. The power is calculated from a correlation from Judat (1976) (described in the Appendix). The correlation is valid for a water/air system with  $Re > 2.6 \cdot 10^4$ . To check its validity for this reactor, the correlation was compared to experimental values measured with a torquemeter, and a correlation from Ihme (1975).

The air was taken from the house supply. Nitrogen (technical grade) was supplied from cylinders. The rotameters (Turbo-Werke, Köln, 0-250 L/h) were calibrated with a soap bubble meter at atmospheric pressure; the air flows were then adjusted for the air pressure measured by a pressure gauge located before the rotameter. The dissolved oxygen probe was inserted through an opening in the side of the reactor at a 45° angle and located at a height of 24 cm.

Figure 10. Reactor details. (dimensions in mm)



The oxygen content of the off-gas in the continuous flow experiments was analyzed using a Magnos 4G from Hartmann and Braun. The principle of the analyzer is based on the different magnetic characteristics of gases. The Magnos 4G is an on-line analyzer with 2 channels; one for a reference gas and one for the off-gas. The reference gas used was a slipstream off the influent gas to the reactor. Oxygen is strongly paramagnetic. All other gases, with the exception of nitrogen and chlorine oxides, are weakly diamagnetic and are not affected by a magnetic field. By subjecting the gas to an inhomogenous magnetic field, oxygen is drawn in the direction of the increasing field strength. Due to the difference in the oxygen content of the reference gas and off-gas, the magnetic field causes a pressure difference, which is proportional to the concentration difference. The analyzer used has three ranges: 0-1%, 0-2%, and 0-5%(volume). The ranges were calibrated with the appropriate gases. The instrument has a detection limit of <1% of the range and a reproducibility of  $\pm 0.5\%$  of the range.

The gas streams must be dry and dust-free before entering the analyzer. In order to ensure an accurate measurement of the oxygen concentration, the CO<sub>2</sub> must either be removed when biological activity is present or else measured. The gas analyzer has two parallel treatment trains (reference and off-gas). The gas is first bubbled through a 10M NaOH solution to remove the CO<sub>2</sub>, then it is dried in a gas cooler followed by a silica gel filter. The flow is controlled at 20 L/h with a rotameter. In the last step the gas passes through a membrane filter and then into the analyzer.

### **3.2 Batch experiments**

In the batch nonsteady state experiments one reactor with a liquid volume of 17.5 L was used. The reactor was filled with tap water, which was allowed to

come to room temperature. Water temperatures ranged between 16.4° to 24.2° C. The water was first deoxygenated with N<sub>2</sub> to ~0.10 mg/l O<sub>2</sub>. Then, through the use of a three-way valve, the gas was switched to air and the change in the dissolved oxygen concentration over time was recorded with a MINC computer (DEC). The oxygen concentration was measured with a WTW (Wissenschaftlich-Technische Werkstätten GmbH) oxygen probe (EO 166) with a time constant on the order of 7 seconds. Visual observation of the probe showed the bubbles did not lodge on the membrane. The air flow was varied from 122 to 178 L/h and power input was varied from 195 to 3060 W/m<sup>3</sup>.

The data were evaluated using the nonsteady state regression program from the ASCE Standard (1984). Because of possible probe lag effects, the data was truncated at 20 % of c\*.

### **3.3 Continuous flow experiments**

#### **3.3.1 Residence time distribution**

In order to ensure the assumption of a well-mixed liquid phase was valid for the high flow rates necessary for steady state operation, the liquid residence time distribution was determined. The reactor was first filled with a NaCl solution (conductivity ~5 s). Tap water (conductivity = 0.63 s) was then fed to the reactor and the change in conductivity of the effluent over time was recorded for various flow rates and stirrer speeds. The reactor was not gassed. This operating mode represents the minimum level of mixing; gassing increases the turbulence and increases mixing.

The data were evaluated with the integrated form of the nonsteady state mass balance on the system:



$$V_L \frac{dc}{dt} = Q_L(c_o - c) \quad (35)$$

integrating from  $t = 0$  and  $c = c_1$ , to  $t = t$  and  $c = c_o$ :

$$\ln \left[ \frac{(c_o - c_1)}{(c_o - c)} \right] = \frac{t}{\theta_H} = \tau \quad (36)$$

where:

$c_o$  = conductivity of the tap water

$c_1$  = initial conductivity of reactor contents

$V_L$  = reactor volume

$Q_L$  = liquid flow rate

$\theta_H = \frac{V_L}{Q_L}$  = hydraulic retention time

$\tau$  = dimensionless time

Plotting the ideal residence time distribution values calculated from equation 36 with the experimental data allows the approach to ideal mixing to be judged. Figure 11 shows a typical plot. By reducing the stirrer speed and increasing the liquid flow rate, a limit to the assumption of ideal mixing was searched for. However, even with a high flow rate ( $Q_L=124$  L/h) and no stirring, the experimental data approximate ideal mixing. A visual test with a few drops of dye injected into the reactor content confirmed the experimental data.

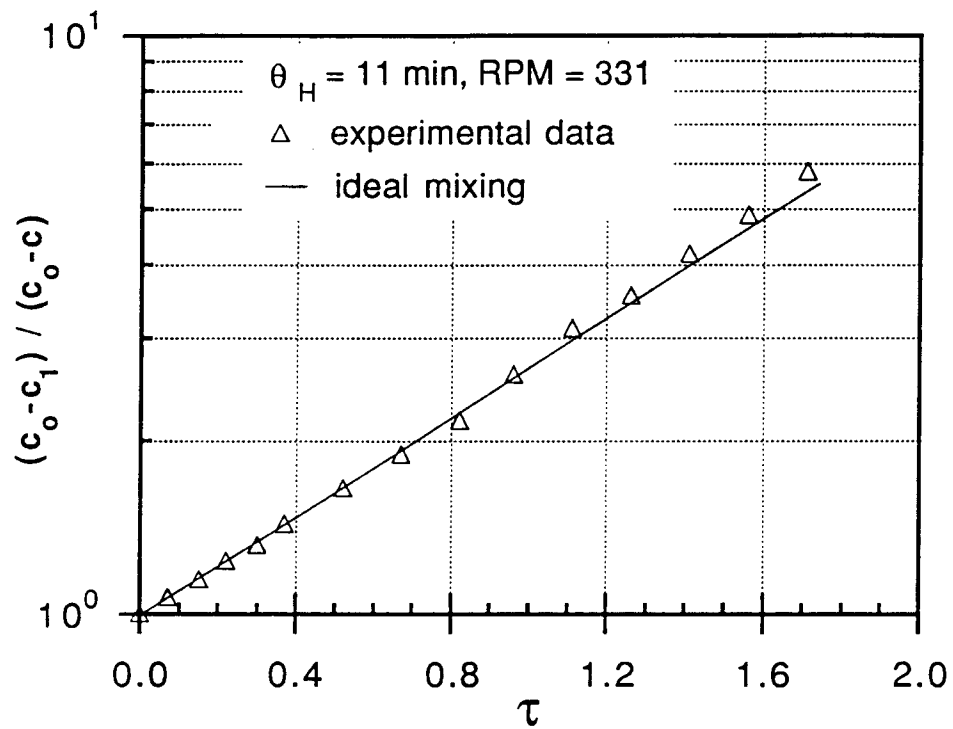


Figure 11. Residence time distribution for typical experimental conditions.

$\theta = 11 \text{ min, RPM} = 331.$

### 3.3.2 Water/Air system

For the continuous flow experiments, the reactors were operated in series. Each reactor had a volume of 19.2 L. In the continuous flow mode, reactor 1 was used to deoxygenate the tap water and reactor 2 was used to aerate the tap water. Tap water was fed to reactor 1, which flowed by gravity into reactor 2. The effluent flow rate from reactor 2 was measured manually with a graduated cylinder. The temperature of the reactors ranged from 16° to 19°C for the various runs. Figure 12 shows the experimental set-up including all the modifications made for later experiments.

The liquid oxygen concentration of each reactor was measured with an oxygen probe (WTW EO 191), located as described in the nonsteady state section. The EO 191 probe has a slightly faster response time than the EO 166 probe used in the nonsteady state experiments. The time constant was ~3.5 s.

The gas phases of the reactors were kept separate through the use of pressure equalizers. In order to measure the off-gas oxygen concentration, the reactors were pressurized slightly (~0.07 bar gauge) to insure a constant flow to the gas analyzer.

### **Steady state**

Steady state was assumed to have been reached when  $c_L$  and  $c_G$  were constant for at least 30 minutes. The average time required for the reactors to reach steady state was ~1 hour, i.e. approximately five times the hydraulic retention time. The mass transfer coefficient for oxygen was measured in reactor 2. Both the liquid phase and gas phase mass balance as discussed in Section 2.5.2 were used to calculate a  $k_L a$  for each run.

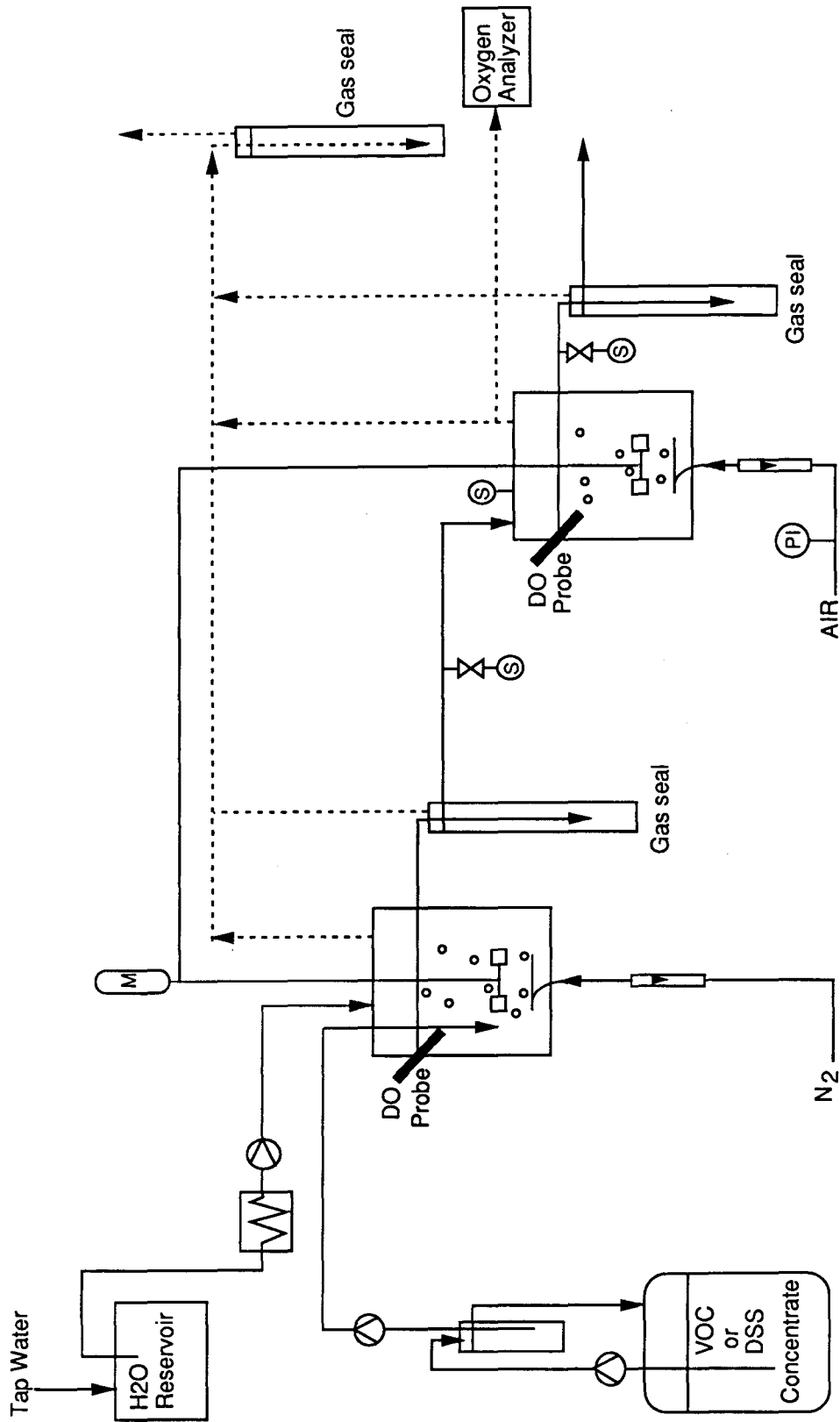


Figure 12. Steady state experimental set-up.

### **Nonsteady state**

The continuous flow nonsteady state measurements were made after the reactors had reached steady state, as defined above. Then an appropriate amount of cobalt catalyst ( $0.05 < \text{Co}^{+2} \text{ mg/L} < 0.1$ ) was injected into both reactors; after waiting one minute, the appropriate amount of  $\text{Na}_2\text{SO}_3$  was injected into the second reactor. An immediate fall in the DO concentration to  $\sim 0 \text{ mg/L}$  indicated that the Co catalyst and  $\text{Na}_2\text{SO}_3$  concentrations were correct. Enough  $\text{Na}_2\text{SO}_3$  was added to keep a zero DO concentration for at least one minute. The subsequent increase in DO was recorded by a strip chart and the MINC computer. The data were evaluated according to the equation 31 in Section 2.5.1, the slope from the linear regression is  $-(Q_L/V_L + k_L a_{O_2})$ .

### 3.3.3 Water/VOC/Air system

A slight modification of the reactor setup was necessary for the volatilization experiments. To improve operation in the steady state mode, the inclined tube clarifiers were removed and additional outlets drilled in the reactor wall, resulting in reactor volumes of 18.5 L. A common pressure equalizer for both exit gas streams ensured equal pressure in both reactors. The effect of temperature on  $k_L a_{O_2}$  is well-known and quantified, however, the effect on VOC mass transfer has not been quantified. Therefore, in the VOC experiments, the temperature of the liquid was kept constant to exclude temperature influences. The placement of a water bath between the tap water reservoir and the pump to reactor 1 allowed the temperature in reactor 2 to be held at  $20 \pm 1$  C.

The first reactor was used to deoxygenate the water and to mix in the organic chemicals, which were continuously added as a concentrated solution from a separate 65 L tank. In order to ensure the tank remained mixed and the flow rate constant during the experiments, the solution was first pumped into a small vessel with an overflow back into the tank and an outlet to the peristaltic pump. The concentration of chemicals in the tank was chosen so as to be below the solubility limit of each chemical. The desired VOC concentration for the experiments was achieved by adjusting the concentrate flow rate to the reactor. The concentrate was prepared by adding the organic chemicals to 60 L warm water in the tank, which was immediately closed and first manually shaken and then mixed overnight with the pump/overflow system. Since stripping of the VOC's occurs in the first reactor as a result of the deoxygenation with N<sub>2</sub>, the calculated VOC influent concentration from the concentrate flow rate to the reactor and the concentration in the tank is only approximate, and thus, cannot strictly be used as a control of the analyzed GC concentrations.



The sample system was designed to minimize volatilization losses. This was especially important since, in order to reduce disturbances in the steady state operation, influent samples had to be drawn off slowly. The order of sampling was chosen to avoid possible cross-influences: first the effluent, then the reactor gas phase, then the influent. Sample points for the liquid phase were installed in the influent tubing to the second reactor and the effluent tubing as shown in Figure 12. The sample point consisted of a tee with a valve attached to screw cap for 100 ml glass sample bottles. For sampling, the bottles were screwed onto the caps and filled to the brim. The bottles were rinsed three times before a new sample was taken. The sample was then transferred with a Pasteur pipette to two GC autosampler bottles (1.8 ml glass bottles with a crimp top and teflon lined rubber septum). One bottle was analyzed the same day, and one was frozen as a reserve. Samples were also stored in 100 ml serum bottles with teflon lined rubber crimp caps, with no gas space, in the refrigerator. Four samples of the liquid phase were generally taken for each experimental run.

The gas phase of reactor 2 was sampled with a 10 microliter syringe inserted through a valve and septum into the gas space. The plunger was removed to allow the syringe to be purged with reactor gas and inserted to take the sample. The sample was then immediately injected into the GC. The 10 microliter sample volume allowed good GC quantification. Again four samples of each run were generally taken.

The mass transfer coefficients for both oxygen and the VOC's were measured in the experiments with the steady state method.

### **3.3.4 Water/DSS/Air and Water/VOC/DSS/Air system**

The reactor setup was identical to the VOC experimental setup, except for the addition of a small vessel in the gas line to the gas phase oxygen analyzer in an attempt to catch the foam caused by the surfactant. The 65 L tank was used to mix a concentrated solution of dodecyl sodium sulfate (DSS) (99% purity) or of DSS and VOC's in the same manner as explained above for the organic chemicals, except that distilled water was used to avoid DSS precipitation. The liquid sample program included two extra sample points: from the bottom of both reactors. This was to check if there was a surfactant gradient in the reactor. No gradient was found; the surface tension of the reactor effluent was the same as that of the sample from the bottom of the reactor.

The samples for surface tension measurement were filled into 100 ml serum vials with crimp caps and teflon lined rubber septums or 100 ml screw cap bottles. The surface tension was usually measured the same day or within 24 h. Gas and liquid phase sampling for GC analysis was as above.

### **3.3.5 Water/Biomass/Air system**

Biomass from one of Berlin's municipal wastewater treatment plants, Marienfelde, was used. The concentrated waste activated sludge from the flotation unit was diluted 1 to 10 in the 65 L tank to achieve a suspended solids concentration of ~3 g/L. This was then pumped through the water bath into reactor 1. Samples were taken for COD, TOC, IC (inorganic carbon), and surface tension measurements.

Since the gas phase balance can be used to calculate  $k_L a_{O_2}$  in reactors with biological activity, the oxygen uptake rate (OUR) need not be measured. In fact, the combination of the gas phase balance and the dissolved oxygen concentrations in the influent and effluent allow the calculation of the OUR. The OUR was also measured from a batch run and compared to the steady state measurements.

### 3.4 VOC analysis

The three volatile compounds used in this study were: toluene, dichloromethane, and 1,2-dichlorobenzene. All chemicals used were reagent grade. They have Henry's constants ranging from 0.240 to 0.095. A non-volatile compound, m-cresol ( $H_c \sim 10^{-4}$ ) was used as an internal standard. The Henry's constants and solubilities are listed in Table 4.

Table 4. Henry's constants and solubilities for the compounds investigated.

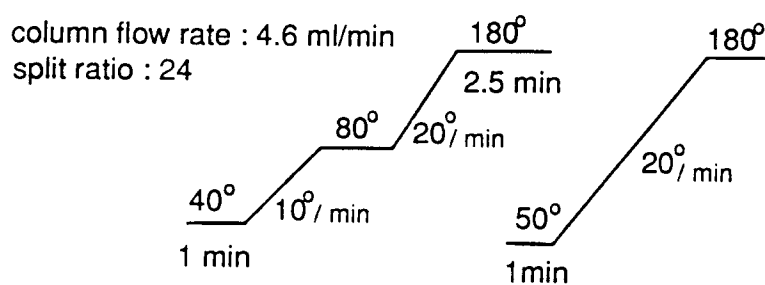
Compound	$H_c^*$ (dimensionless) at 293 K	Solubility <sup>*</sup> (mg/L)
toluene	0.240	520
dichloromethane	0.105	19,400
1,2-dichlorobenzene	0.095	140
m-cresol	$\sim 10^{-4}$	23,500

# measured this study

\* Mackay et al.(1981) and Verschueren (1977)

The organic chemicals were analyzed by gas chromatography using a Hewlett Packard GC Model 5890 A, equipped with an automatic sampler and a flame ionization detector. A polar capillary column, FEAP-DF-0.25, was used from the company Macherey-Nagel. The aqueous sample was put into a 1 ml (nominal) vial with a teflon-lined rubber septum and a crimp cap and directly injected (2 microliters) with the autosampler; no pre-concentration of the samples was required. The gas sample of 10 microliters was manually injected. The GC operating conditions are found in Table 5.

Table 5. GC operating conditions.



Experiments were made to investigate the behavior of the VOC's in the sample vials. Aqueous standards (4 dilutions) were made and filled into the GC sample

vials, and analyzed immediately, or frozen over a period of one week. The frozen samples showed a loss of 10-30%. Therefore, all samples were analyzed in the following 24 hours, except for one run, in which the frozen samples were analyzed 3 days later. A four point standard curve with all four compounds was made each time new GC samples were run. All but toluene had a linear response over the concentration range, however, in the experimental range of toluene concentrations used, the response was linear.

One method to make gas standards is to put a known amount of a substance into a leak-tight vial and let it evaporate. Gas phase standards in the low concentration range proved to be difficult to make because the small size of the available leak-tight vials (119 ml) required an accurate introduction of 0.1-2.0 mg of the chemicals into the vials. The use of the combination of volume and weight of the substance added increased the reliability of the method. Another possibility to find the response factor for the gas phase is to use the results from Henry's constant measurements in both the gas and liquid phase. This procedure was used in the experiments and is described below. The response factors from the two methods agreed quite well.

### **3.5 Henry's constants**

Henry's constants for the four compounds used in this investigation were measured in tap water using the equilibrium partitioning in closed systems (EPICS) method. A detailed description of the method can be found in Lincoff and Gossett (1984). Two 119 ml serum vials with different volumes of liquid and gas (e.g. bottle 1-10 ml liquid, bottle 2-100 ml liquid), but with the same total mass,

were allowed to equilibrate 24 h in a water bath at 20°C. From the mass balance of the two bottles, an equation to calculate the Henry's constant were made for both phases:

Liquid phase:

$$H_c = \frac{\frac{c_{L_2}}{c_{L_1}} \cdot V_{L_2} - V_{L_1}}{V_{G_1} - \frac{c_{L_2}}{c_{L_1}} \cdot V_{G_2}}$$

Gas phase:

$$H_c = \frac{\frac{c_{G_1}}{c_{G_2}} \cdot V_{L_1} - V_{L_2}}{V_{G_2} - \frac{c_{G_1}}{c_{G_2}} \cdot V_{G_1}}$$

If both the gas and liquid phases are analyzed by GC and the liquid response factor is known, then the gas phase concentration and response factor can be calculated from the measured  $H_c$  and  $c_L$ .

The mass introduced into each bottle need not be known to calculate the Henry's constant nor must it be known to find the gas phase GC response factor; however, it can be used as a check on the whole procedure. The  $H_c$  measured are listed in Table 6, as well as published values from studies using the EPICS method.

Table 6. Comparison of experimental and published values of  $H_c$  at 293 K.

$H_c$ (at 293 K)	Reference			
Compound	This study	Kapartis (1991)	Yuteri et al.(1987)	Lincoff and Gossett(1984)
Toluene	0.240	0.260	0.244	
Dichloromethane	0.105	0.098	0.077	0.094
1,2-Dichlorobenzene	0.095	0.092		

### 3.6 Surface tension measurements

The effect of the organic compounds and of dodecyl sodium sulfate (DSS) on the surface tension was measured with a tensiometer (Krüss GmbH, Hamburg) using the Du Noüy ring method. Since surface tension decreases with increasing temperature, all measurements were made at 20°C. A calibration curve of surface tension as a function of concentration was made for each compound, as well as for a combination of the four organic compounds alone and with the surfactant. Difficulties were encountered in finding a stable surface tension reading. The surface tension increased with time for both the organic compounds and surfactant. Volatilization as a cause was excluded by comparing covered and uncovered dishes filled with the solutions. The value leveled off after ~ 30 minutes. Differences were also found depending on the prehistory of the sample, i.e. whether the bottle was shaken or not before filling the dish. The results of these studies are illustrated in Figure 13. Comparison to other authors (Hwang and Stenstrom (1979), Masutani (1988)) shows similar variations.

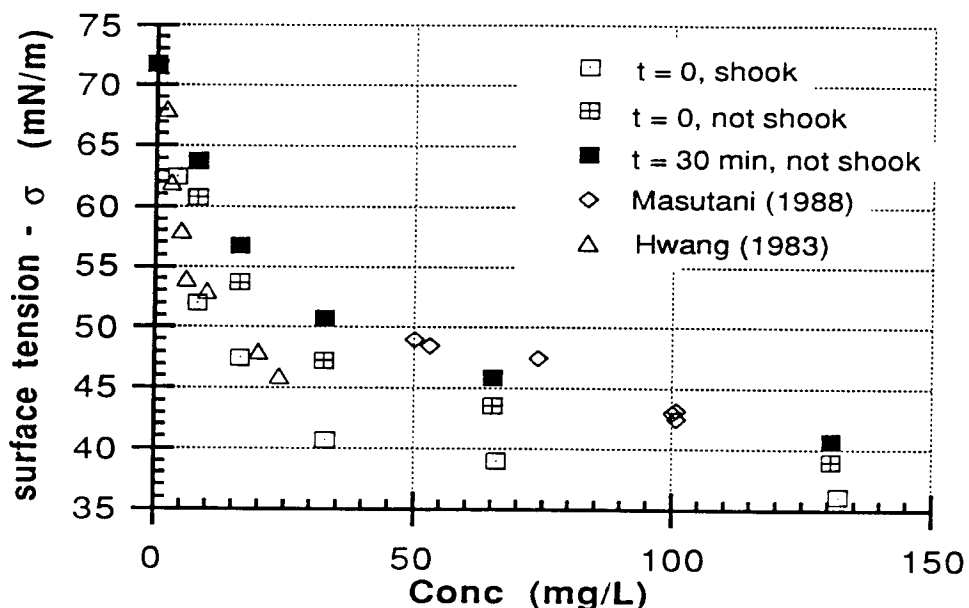


Figure 13. Surface tension of dodecyl sodium sulfate solutions as a function of sample treatment; and compared to other authors.

An experiment to see whether the surface tension values were reproducible with the same method was made. A dilution curve for DSS was measured in which the bottles were shaken before they were poured into the dish and the surface tension was read immediately. The readings were repeated over 10 minutes. The values rose with time. The solution was poured back into the bottle, shaken, and returned to the dish. The surface tension readings were repeated. This procedure was repeated a third time. The values and the trend were reproducible. The experimental error in the surface tension values is  $\pm 3$  mN/m (=dyne/cm). This method, shaking the bottle with immediate reading, was then chosen for use in the experiments.



### 3.7 Experimental design

The steady state method avoids many of the sources of experimental error associated with the nonsteady state method, however, it has its own distinct sources of error. Because data analysis of the nonsteady state method uses the form of the response curve (with nonlinear regression) or the slope (with linear regression), the absolute value of the concentration is not important. A systematic error in measuring DO or the VOC concentration does not affect the  $k_L a$  value. In the steady state method, error in the values of  $Q_G$ ,  $Q_L$ ,  $V_L$ ,  $c_G$ , results in an error in  $k_L a$  of the same magnitude, i.e. 1%  $\rightarrow$  1%. However, error in the liquid concentration and equilibrium concentration is magnified. The amount of error introduced into  $k_L a$  by a certain error in concentration depends on the approach of the liquid concentration towards the equilibrium concentration for oxygen transfer, or the gas phase concentration towards saturation for VOC transfer, because it is the difference of the two concentrations that is used and it is in the denominator, e.g. a 1% error in  $c_L$  can cause a 10% error in  $k_L a$ . In the following section, the types of error in the variables and their effect on  $k_L a$  are examined. The data collection program developed to minimize error is discussed.

There are three different ways to calculate  $K_L a$  depending upon which phase was sampled (the following equations are written in terms of VOC mass transfer).

If only the liquid phase is measured, the steady state mass balance can be used to calculate  $c_G$  (Method GB):

$$K_L a = \frac{Q_L (c_{Lo} - c_L)}{V_L (c_L - c_L^*)} \quad (37)$$

where: 
$$c_G = \frac{Q_L}{Q_G}(c_{Lo} - c_L)$$

and:

$$c_L^* = \frac{c_G}{H_c}$$

If both phases are measured, two methods are possible. One based on the liquid phase mass balance (Method GA- $Q_L$ ), and the gas phase concentration used to calculate  $H_c$ :

$$K_L a = \frac{Q_L (c_{Lo} - c_L)}{V_L \left( c_L - \frac{c_G}{H_c} \right)} \quad (38)$$

The third method (GA- $Q_G$ ) is based on the gas phase mass balance:

$$K_L a = \frac{Q_G}{V_L} \cdot \frac{c_G}{\left( c_L - \frac{c_G}{H_c} \right)} \quad (39)$$

The error in  $K_L a$  due to error in  $c_L$ ,  $c_{Lo}$ , and  $c_G$  is affected by which equation is used to evaluate it. Obviously  $c_G$  has no effect on  $K_L a$  when equation 37 is used, similarly  $c_{Lo}$  has no effect on  $K_L a$  when equation 39 is used. The effect of error in the three variables on the error in  $K_L a$  is analyzed in Table 7. Looking at Table 7, it is evident that equation 37 based on the steady state mass balance is the most sensitive to error in  $c_{Lo}$  and  $c_L$ .

The different effects of error in the variables on  $K_L a$  due to method of calculation can be seen in Figure 14. The error bars in Figure 14 illustrate the variation due to the three equations. The method based on the liquid phase mass balance using the gas phase concentration to calculate  $c_L^*$  minimizes the error in  $K_L a$  (equation 38). It was, therefore, used in the data analysis.

Table 7. Sensitivity of  $K_{La_{Tot}}$  to concentration variations.

% error		Conc. (mg/L)			$K_{La_{Tot}}$ (1/s)			Change %		
		$C_{Lo}$	$C_{Le}$	$C_G$	GB	GA- $Q_L$	GA- $Q_G$	GB	GA- $Q_L$	GA- $Q_G$
Ref. (0)		19.1	12.3	2.0	0.0015	0.0015	0.0015			
$C_{Lo}$	-10%	17.2	12.3	2.0	0.0007	0.0010	0.0015	-54	-28	0
	-7%	17.8	12.3	2.0	0.0008	0.0012	0.0015	-42	-20	0
	-3%	18.5	12.3	2.0	0.0011	0.0013	0.0015	-22	-8	0
	+3%	19.7	12.3	2.0	0.0019	0.0016	0.0015	31	8	0
	+7%	20.4	12.3	2.0	0.0029	0.0017	0.0015	98	20	0
	+10%	21.0	12.3	2.0	0.0043	0.0019	0.0015	194	28	0
$C_{Le}$	-10%	19.1	11.1	2.0	0.0051	0.0025	0.0021	252	69	43
	-3%	19.1	12.0	2.0	0.0019	0.0017	0.0016	32	16	10
	+3%	19.1	12.7	2.0	0.0012	0.0013	0.0013	-21	-13	-8
	+10%	19.1	13.6	2.0	0.0007	0.0009	0.0011	-51	-37	-23
$C_G$	-10%	19.1	12.3	1.8	0.0015	0.0012	0.0011	0	-17	-25
	-3%	19.1	12.3	1.9	0.0015	0.0014	0.0013	0	-6	-8
	+3%	19.1	12.3	2.0	0.0015	0.0015	0.0016	0	6	10
	+10%	19.1	12.3	2.2	0.0015	0.0018	0.0020	0	25	37

Since both the gas and liquid phase oxygen concentrations were measured in most of the experimental runs, it was possible to check the effect of the oxygen depletion of the gas phase on  $k_L a$ . Although gas phase oxygen depletion was minor in this investigation,  $\Delta c_G$  was always less than 1%, the effect of this small change in  $c_L^*$  was examined. As expected, there was no effect in the region of low power density where the driving force is large, however, as power density increased, the effect increased because the difference between the saturated and liquid concentration becomes very small (Figure 15). The steady state method

must then be used with caution in the region where the driving force becomes small. This problem may not be present in systems where chemical or biological reactions consume the transferred oxygen.

In order to ensure statistical confidence in the GC values, an internal standard was used in the experiments to compensate for GC variability. A non-volatile compound was chosen, m-cresol. Four samples of each point were taken, with two replicates, so that a total of eight GC values were made for each point. The coefficient of variation ranged from 1.5 to 12% and the standard error varied from 0.02 to 0.9 mg/L. Differences in liquid effluent concentrations of  $\pm 10\%$  would be highly significant considering these values (t-test,  $\alpha=0.95$ ).

Because the DO probe needs a minimum flow past the membrane to give a correct reading, a small stirrer was used in the second reactor to ensure a correct reading at the low power densities. The probes used required a minimum flow of 15 cm/s. The VOC/m-cresol mixture caused the DO reading to oscillate; the use of the stirrer smoothed out the signal.

The use of a continuous on-line method to measure the VOC  $c_L$  and  $c_G$  would greatly enhance statistical confidence in  $K_L a_{VOC}$ . Since the concentrations studied were high enough to measure without preconcentration of the samples, the liquid concentration could be measured with a spectrophotometer equipped with a flow-through cell and the gas concentration with a GC.

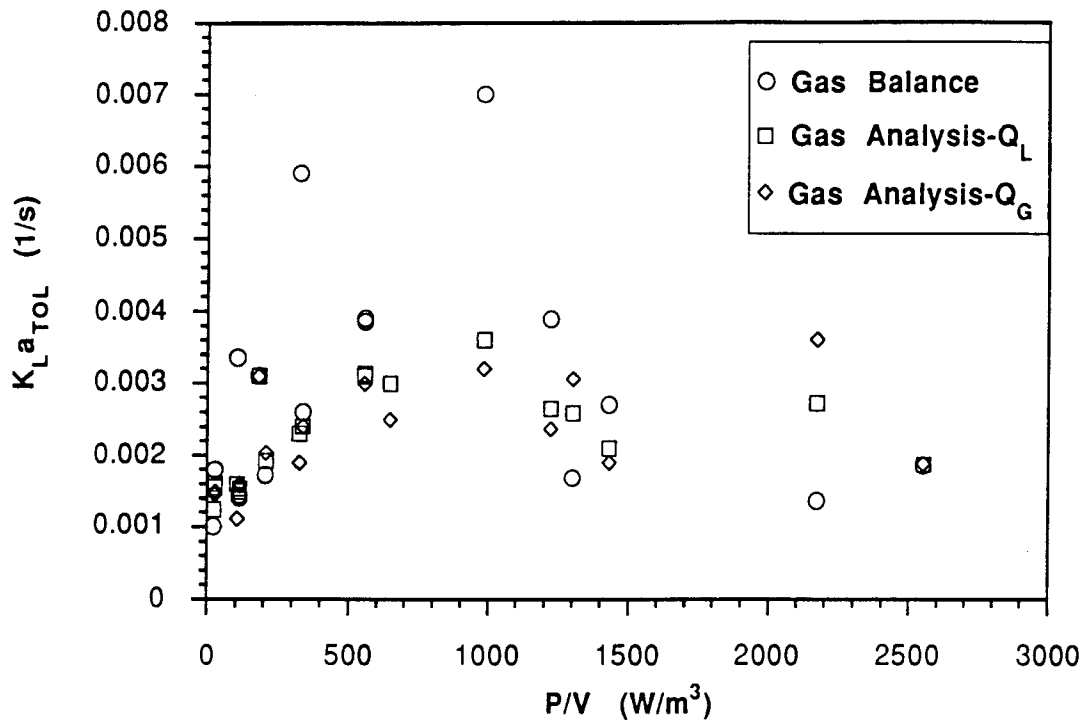


Figure 14. Comparison of the three methods used to calculate  $K_L a$ .

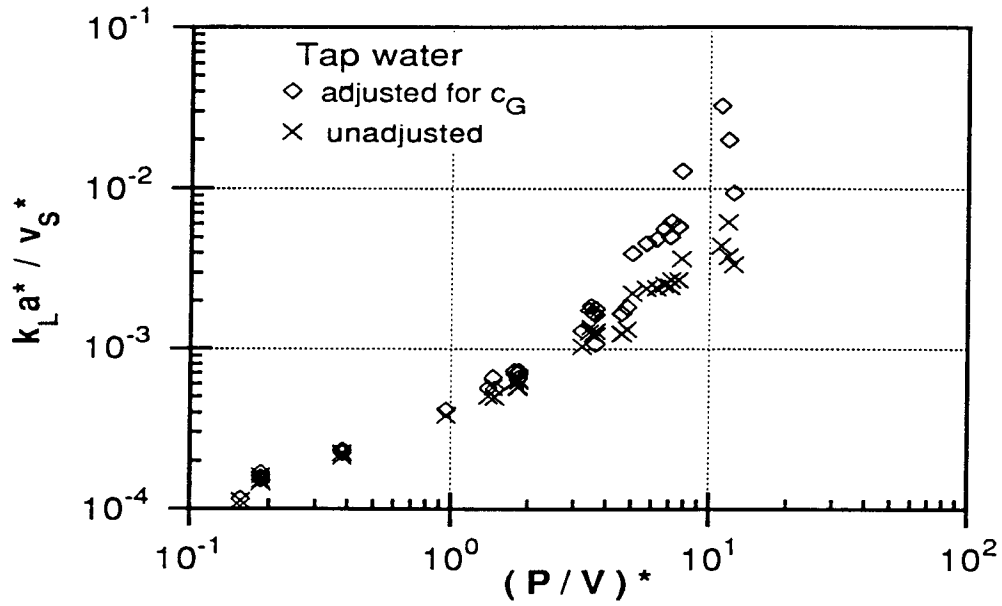


Figure 15. Comparison of  $k_L a_{O_2}$  values calculated with and without adjustment of gas phase concentration.

## **4 Results and discussion**

The results of the experiments studying the mass transfer of oxygen into the liquid phase and the experiments studying the mass transfer of the VOC's into the gas phase of the various water systems (tap water, m-cresol, DSS solutions, and biomass) are discussed separately. First the results of the experiments using the nonsteady and steady state methods to determine  $k_L a_{O_2}$  are presented and compared to published correlations. Then the results of the experiments of mass transfer into solutions of VOC/m-cresol and DSS solutions are discussed.

The results of the volatilization experiments are analyzed in terms of the two resistance theory and the implications for predicting stripping loss from wastewater treatment plants during aerobic biological treatment are presented. Finally, the effect of the anionic surfactant (DSS) on the mass transfer of the VOC's is compared to its effect on oxygen.

### **4.1 Oxygen transfer**

#### **4.1.1 Water/Air system**

The transfer of oxygen into water has been the focus of much research over the past decades. Many correlations exist describing the relationship between power input, superficial gas velocity and  $k_L a$ . In order to verify the reactor set-up and evaluation methods before beginning the volatilization studies, oxygen transfer experiments in tap water were made and compared to published correlations.

#### **Batch nonsteady state experiments**

The data were evaluated and compared to published correlations that have been used with a certain degree of success for correlating data obtained from

nonsteady state experiments in tap water. In analyzing  $k_L a_{O_2}$ 's reported in 12 publications found by nonsteady state reaeration tests in geometrically similar stirred tanks using water/N<sub>2</sub>/air systems, Judat (1982) used the modified version of the relationship developed from dimensional analysis (equation 12) to fit the data within  $\pm 30\%$ . He found  $k_L a^* = A(P/V)^{0.43} v_s^{0.57}$ .

A comparison of my data with the correlation developed by Judat is shown in Figure 16. The agreement is acceptable considering that upon closer inspection of his graph of the 12 authors' data (Figure 5), many of the groups of data taken individually have a steeper slope than the given correlation. In fact many of the authors themselves correlated their data with a larger exponent for  $(P/V)^n$ .

In reviewing published correlations, one must keep in mind that many investigations of  $k_L a$  in stirred tank reactors, including this one, were based on nonsteady state experiments that contained error because the investigators ignored gas phase oxygen depletion, hold-up interchange, or any of the other problems discussed in Section 2.5.1. Such is the case for most of the published values used by Judat (1982).

Another correlation available for geometrically similar reactors is the dimensional inconsistent relationship from Linek et al.(1987):

$$K_L a = 4.95 \times 10^{-3} \frac{P^{0.593}}{V} v_s^{0.4} \quad (40)$$

The comparison to the correlation by Linek et al.(1987) seems less satisfactory (Figure 17), however, the deviation is explainable in light of the fact that my

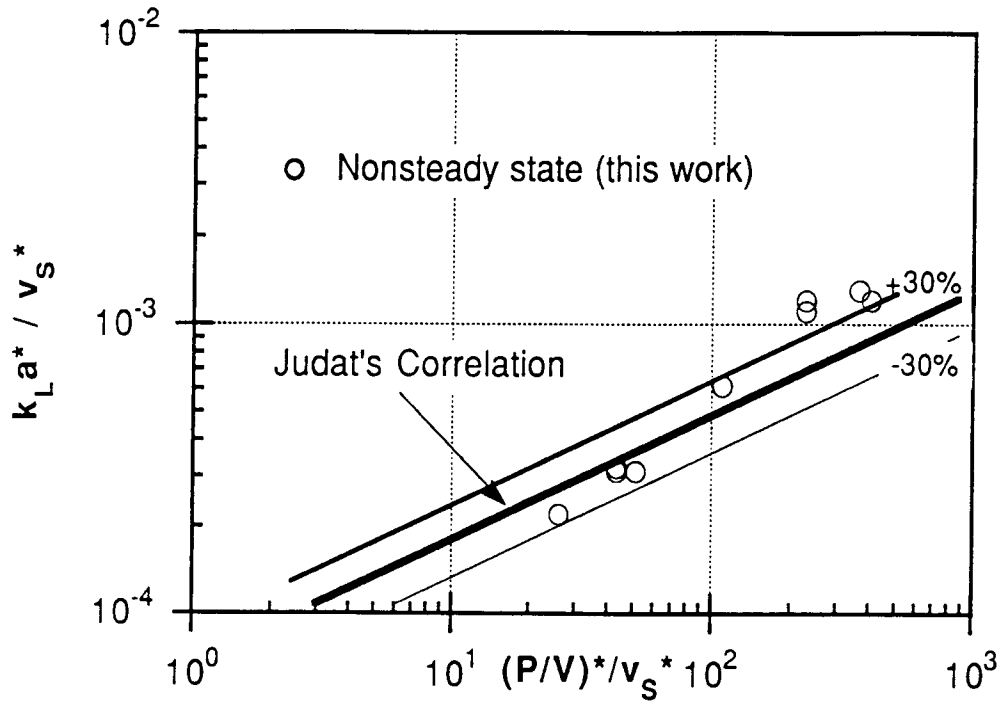


Figure 16. Comparison of nonsteady state  $k_L a_{O_2}$  values (this work) to the correlation from Judat (1982).

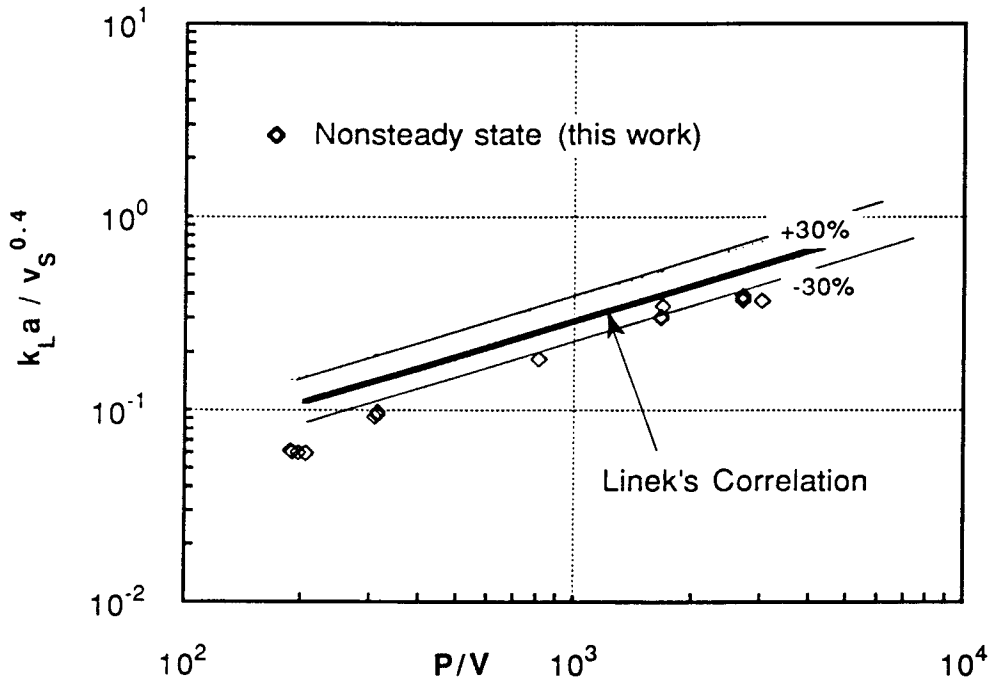


Figure 17. Comparison of nonsteady state  $k_L a_{O_2}$  values (this work) to the correlation from Linek et al. (1987).



data were not evaluated using the gas phase depletion model, nor was the flushing out period of the hold-up interchange considered. Since their correlation is based on the "correct method" (vacuum degassing and pure oxygen), both omissions could clarify the observed deviation. The plateau observed in the last six data points can be explained by the observation of Linek et al.(1987) that the error in  $k_L a$  due to the phenomenon of the hold-up interchange becomes more pronounced at higher  $P/V$  values.

## **Continuous flow experiments**

### **Steady state**

Figures 18 and 19 compare the steady state data to the two methods discussed above, the correlations from Judat (1982) and Linek et al. (1987). On first inspection, the scatter seems daunting. However, careful inspection of the data shows that the scatter is systematic with increasing superficial gas velocity. The development of the relationship used by Judat in Figure 16 requires the assumption that the exponents of the power term,  $a$ , and gas velocity term,  $b$ , sum up to one:  $a+b=1$ , and groups the superficial velocity term with both the  $k_L a$  and  $P/V$  terms. If the assumption is removed, and the dimensionless  $k_L a$ , ( $k_L a^*$ ) is plotted versus  $P/V^*$ , one can see in Figure 20 that the  $k_L a^*$  can be correlated with the superficial velocity term,  $v_s^*$ . By plotting  $k_L a^*$  vs.  $v_s^*$ , the exponent  $b$  was determined to be one. Figure 21 shows the good correlation for  $k_L a^*/v_s^*$ , with an  $r=0.979$ . Linek et al.(1987) did not measure  $k_L a$  as a function of superficial gas velocity, but rather used the exponent of 0.4 as reported by Robinson and Wilke (1973) and Smith et al.(1978). Changing the exponent for  $v_s$  from 0.4 to 1.0, the plot of  $k_L a/v_s$  vs.  $P/V$  becomes a straight line again, just as in Figure 21.

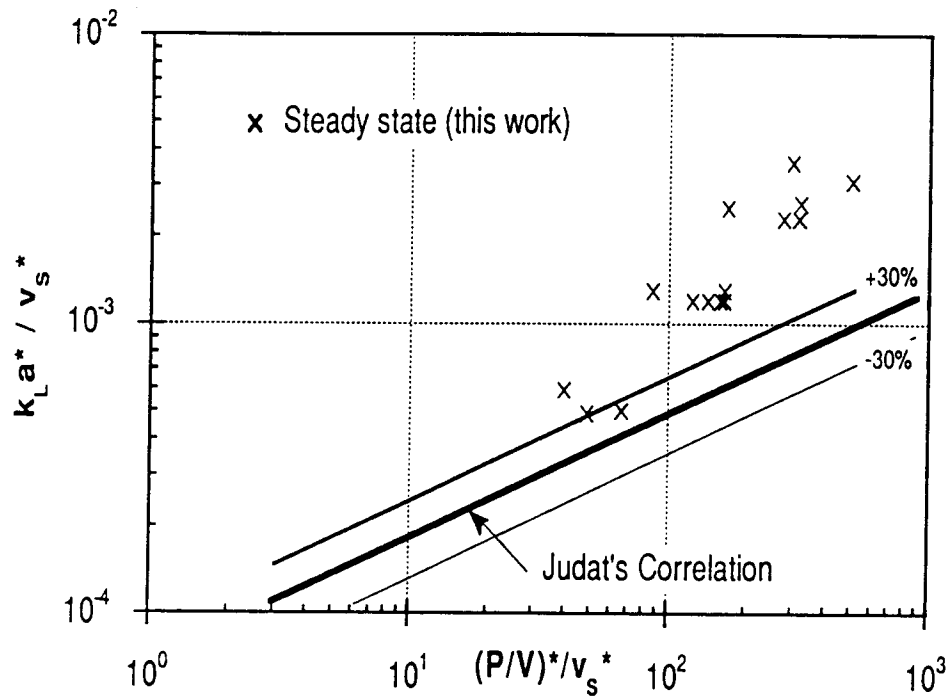


Figure 18. Comparison of steady state  $k_{L}a_{O_2}$  values (this work) to the correlation from Judat (1982).

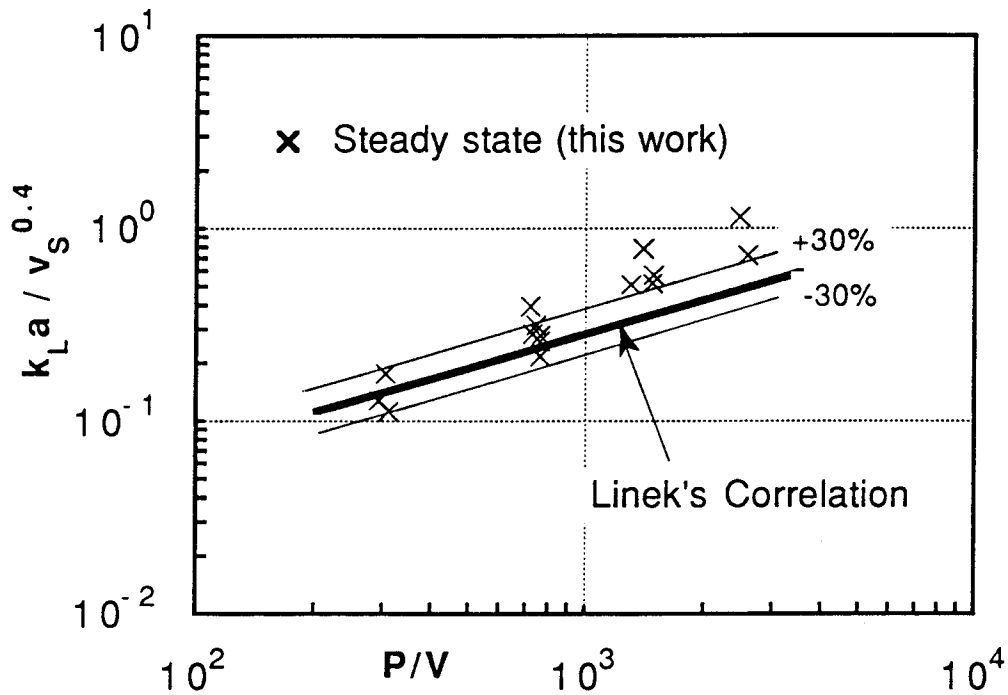


Figure 19. Comparison of steady state  $k_{L}a_{O_2}$  values (this work) to the correlation from Linek et al.(1987).

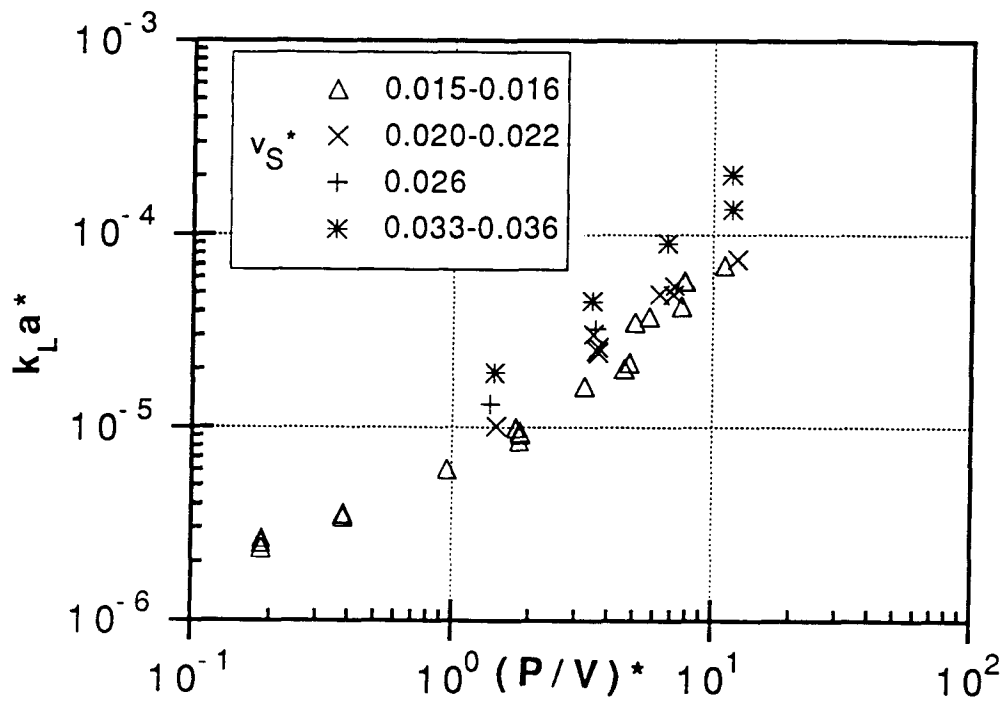


Figure 20. Analysis of  $k_L a^*$  versus  $(P/V)^*$  as a function of  $v_s^*$ .

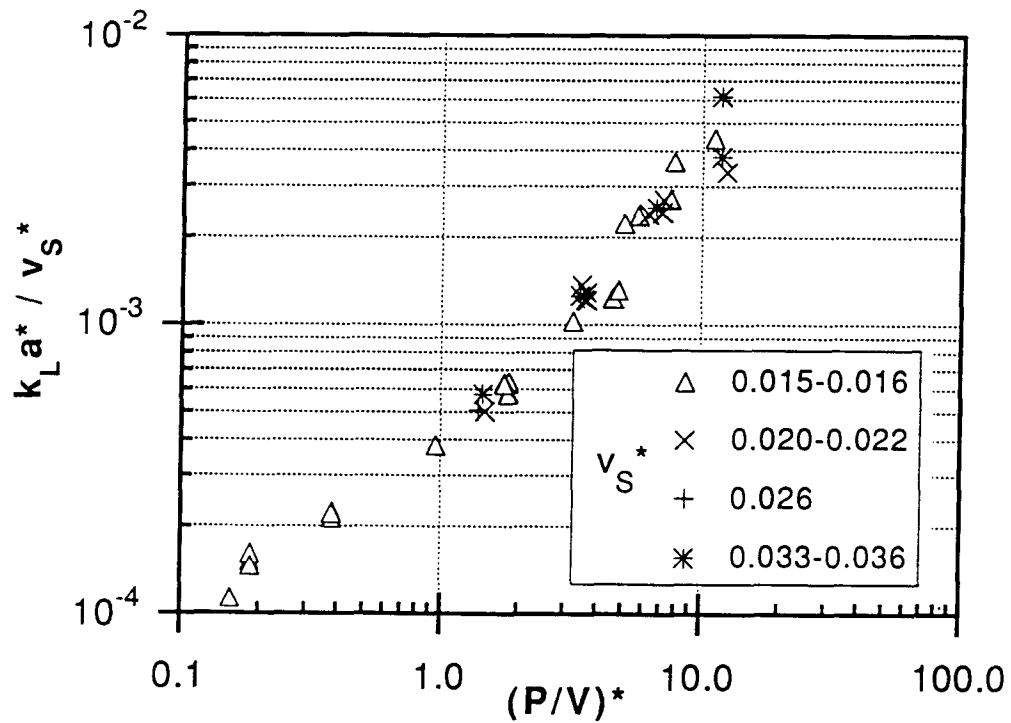


Figure 21. Plot of  $k_L a^* / v_s^*$  versus  $(P/V)^*$ .

A comparison of my nonsteady state and steady state data using the dimensionless variables,  $k_L a^* / v_s^*$  and  $P/V^*$ , illustrates the problems in the experimental methods (Figure 22). The data from both nonsteady state methods, i.e. deoxygenation with  $N_2$  and  $Na_2SO_3$ , do not agree in all regions. The difference at the higher  $P/V^*$  values can be explained with the observation of Linek et al.(1987) discussed above that the hold-up interchange when switching from  $N_2$  to air becomes important at high  $P/V$  values, since there is no hold-up interchange with the chemical method. The importance of probe lag time is illustrated in Figure 22 by the difference between the values obtained from a probe with a lag time of 7 s and one with a lag time of 3.5 s.

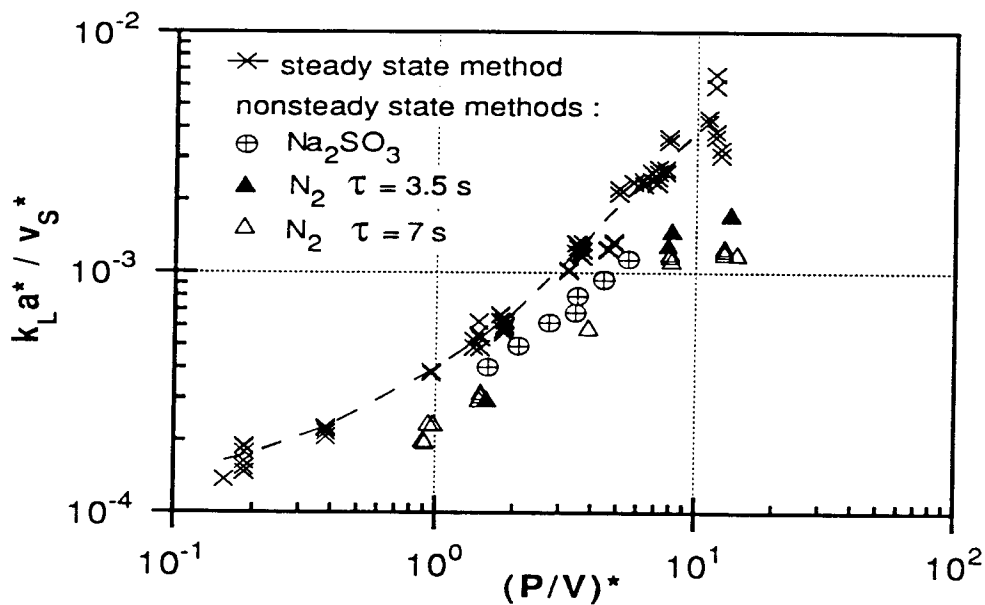


Figure 22. Results from the three experimental methods: nonsteady state with  $N_2$ , and with  $Na_2SO_3$  deoxygenation, and steady state (this work).

The difference between my nonsteady and steady state data can be explained by considering all the problems in the nonsteady state method discussed in Section 2.5.1. In comparing a steady state method, the hydrazine method, with the nonsteady method using the N<sub>2</sub>/air method, Osorio (1985) also found that the nonsteady state method gave lower  $k_L a$  values. He observed the greatest deviation between the two methods at small superficial gas velocities and high energy input, the region where errors from both gas phase depletion and probe lag time can be important.

One approach to avoiding the problems associated with the nonsteady state method is to use an appropriate model considering both the gas and liquid phase mass balances (Linek et al., 1982). Another approach is to modify the experimental method to overcome these problems. Comparing the results from experiments using a modified method with the correlation from Judat (1982), we see that they are higher than his correlation predicts (Figure 23). The various correlations and the methods used are listed in Table 8.

Table 8. Correlations developed from methods modified to account for error sources.

Author	Correlation	Method improvement
Judat (1982)	$k_L a^* = \left[ \frac{P}{V} \right]^{*0.43} \cdot v_s^{*0.57}$	
Linek et al. (1987)	$k_L a = 4.95 \times 10^{-3} \cdot \left[ \frac{P}{V} \right]^{0.593} v_s^{0.4}$	Vacuum degassing and pure oxygen Evaluation included probe and hold-up dynamics
Gibilaro et al. (1985)	$k_L a = 0.49 \cdot \left[ \frac{P}{1000 \cdot V} \right]^{0.76} \cdot v_s^{0.45}$	Double response/initial response methods Gas phase concentration measured
Osorio (1985)	$k_L a^* = A \cdot \left[ \frac{P}{V} \right]^{*0.6} \cdot v_s^{*0.6}$	Steady state method: hydrazine

Since two methods are available to measure the mass transfer coefficient in the steady state mode, both were used and compared: the liquid phase mass balance and the gas phase mass balance, equations 33 and 34. Another check on the system is the total mass balance on the system. This can be used to check if the measured values are consistent within themselves; for example, the most unreliable parameter can be checked. The agreement between the two  $k_L a$ 's was good, <10% difference in most cases. The total mass balance was used to check the dissolved oxygen concentration in the aerated reactor. The  $k_L a_{O_2}$ 's from the liquid and gas balances are compared in Figure 24.

Although the steady state method is free from the major problems caused by the concentration changes over time of the nonsteady state method, it also has regions in which error can become large. The sensitivity analysis of the steady state method presented in Section 3.7 illustrated the problem caused when the liquid concentration approaches saturation. Because the difference

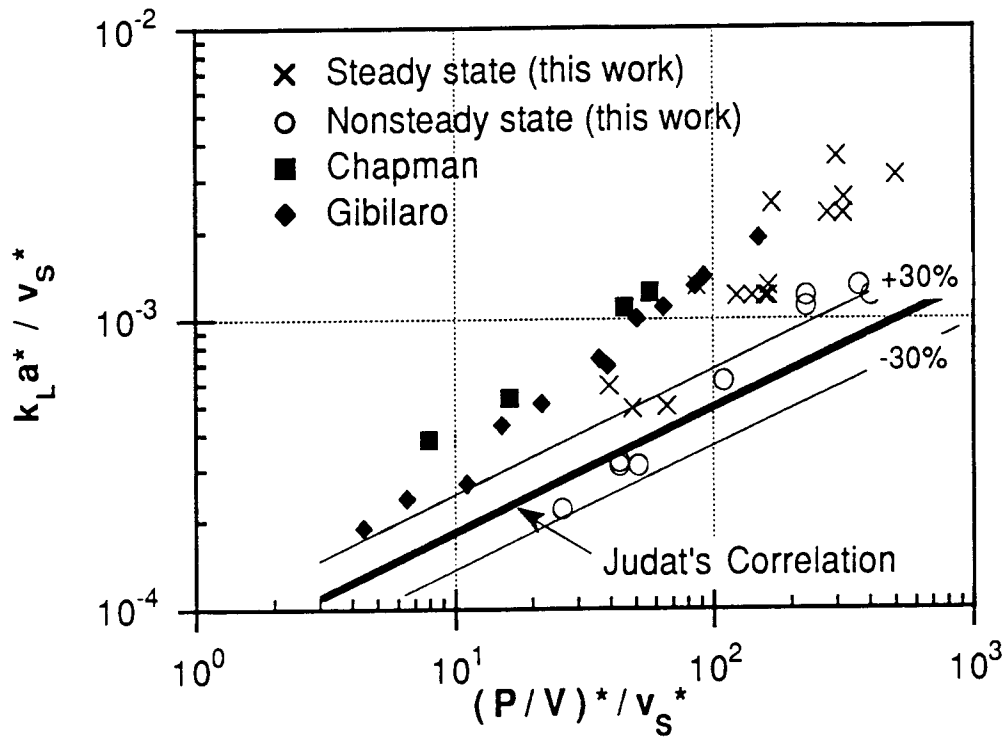


Figure 23. Comparison of Judat's correlation to experimental  $k_{L}a_{O_2}$  values from various modified methods.

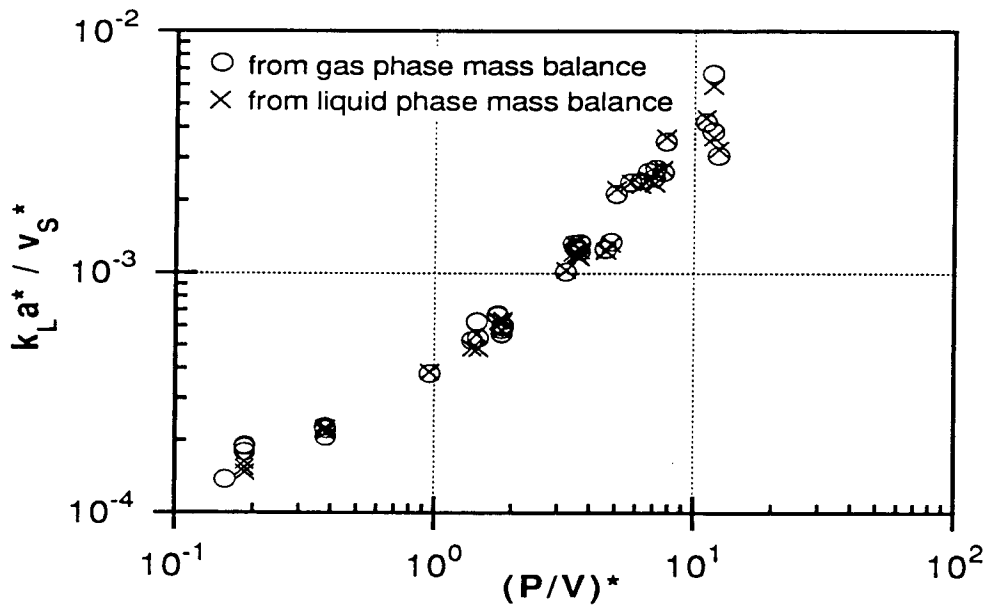


Figure 24. Comparison of  $k_{L}a_{O_2}$  values calculated from the two steady state methods: gas phase and liquid phase balances (this work).

between the saturation and liquid concentration is in the denominator, a small difference greatly magnifies the error. As the difference, i.e. the driving force, approaches zero, the mass transfer coefficient becomes undefined, both theoretically and mathematically.

In examining the correlations in Table 8, we see that most correlate the dependence of  $k_L a_{O_2}$  on power density to a power of 0.6, with the exception of Judat who found the exponent to be 0.4. Analyzing my results using dimensional analysis,  $k_L a^*$  as a function of  $(P/V)^{*a}$  and  $v_s^{*b}$ , it appears that the curve can be broken into two regions, from  $0.1 < (P/V)^* < 2.0$  and  $(P/V)^* > 2.0$ . The lower region has a slope of 0.64 ( $r^2=0.965$ ), while the higher region has a slope of 1.0 ( $r^2=0.991$ ). These parameters do not fully describe the mass transfer process in the low power range (20-200 W/m<sup>3</sup>). In this region the bubbles are not sheared as much by the stirrer; they remain large, and have a higher velocity and shorter retention time than the smaller bubbles produced at higher power densities. It is possible that the use of bubble velocities and residence time distributions could correlate the data better. However, using the superficial gas velocity, the results can be separated into two power regions, with  $a=0.64$  for 20-200 W/m<sup>3</sup>, and  $a=1.0$  for  $>200$  W/m<sup>3</sup>;  $b=1.0$  for both regions.

Different regions in the relationship between the mass transfer coefficient and power density have been observed by various authors. A minimum agitator speed for dispersing gas bubbles ( $n_0$  (s<sup>-1</sup>)) was correlated by Van Dierendonck et al.(1968) in their work on the specific contact area in gas liquid reactors.



for pure liquids:

$$\left(\frac{n_o d^2}{D}\right)(gD)^{1/2} = 0.07 \quad \text{for } D < 1.0 \text{ m} \quad (41)$$

Using this correlation, the minimum stirrer speed for the reactors used in this study is  $n_o = 154$  RPM or  $(P/V)^* = 0.4$ . Few data was taken below this speed, so this minimum cannot be confirmed. This is not the point where the data in this study can be broken into two regions. The break occurs at a higher power density and is not explained by the minimum stirrer speed.

A similar increase in the mass transfer coefficient at high power densities was observed by Figueiredo and Calderbank (1979). They postulated that surface aeration was taking place. Van Dierendonck et al.(1968) also correlated the characteristic stirrer speed for aspirating gas bubbles ( $n_o^*$  ( $s^{-1}$ )) in a baffled stirred tank reactor.

$$\left(\frac{\mu n_o^* d^2}{D \sigma}\right) \left(\frac{\rho \sigma^3}{g \mu^4}\right)^{1/4} = 2 \left(\frac{H-h}{D}\right)^{1/2} \quad (42)$$

Calculating this characteristic speed  $n_o^*$  for the reactors used in this study, we find that  $n_o^* = 330$  RPM or  $(P/V)^* = 3.7$ . Looking at Figure 24, we see that this is where the second region begins. Therefore, it is probable that the increased dependence on  $(P/V)^*$  in the second region is due to the increased gas flow into the reactor because of bubble aspiration.

### Nonsteady state

Because of the difficulties experienced with the steady state method at high power densities, i.e. the liquid concentration approached saturation, a non-

steady state method to determine the oxygen mass transfer coefficient was used. A comparison of the continuous flow nonsteady state and the steady state method is shown in Figure 25. The two methods agree well at lower power densities but deviate at  $k_L a_{O_2}$ 's above  $0.01 \text{ s}^{-1}$ , the steady state  $k_L a_{O_2}$  is ~30% higher. Some of the same problems associated with the batch nonsteady state methods are encountered here, i.e. gas phase depletion, but because the continuous nonsteady state method experiences a lesser rate of increase in the dissolved oxygen concentration due to transport into the reactor of deoxygenated water, the error introduced by DO probe lag time begins to appear at higher  $k_L a$  values than discussed in Section 2.5.1. The hold-up interchange problem that caused large deviations in the high P/V region is no longer present.

The use of this method allowed the steady state method to be used to determine the  $K_L a_{VOC}$ 's and as well allowed as the  $k_L a_{O_2}$  to be determined.

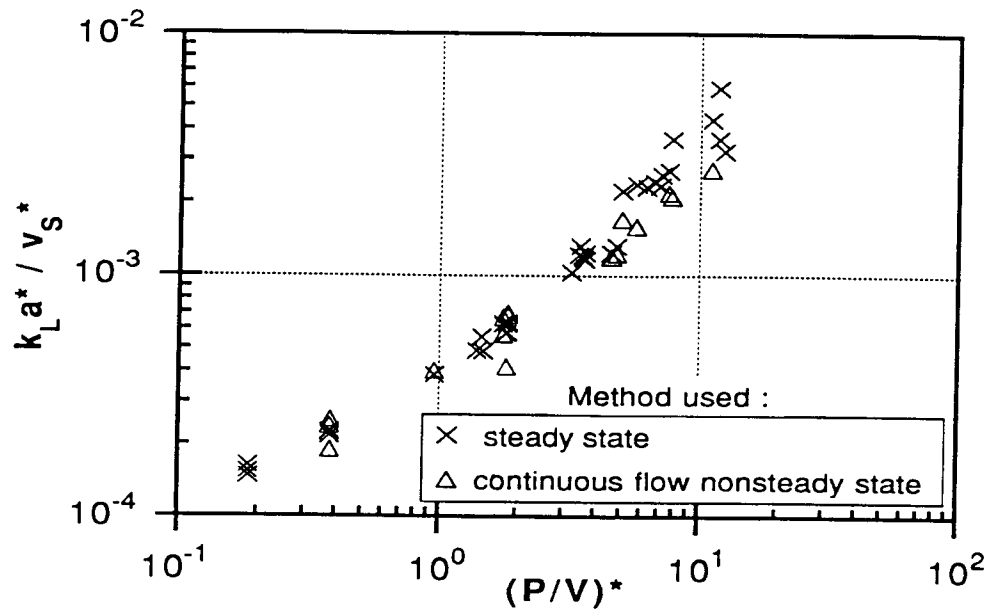


Figure 25. Comparison of the steady state method with the continuous non-steady state method.

#### 4.1.2 Water/VOC/Air system

Estimating the simultaneous transfer rate of VOC's and oxygen was the object of this study. In the investigations of the volatilization of the three organic compounds,  $k_L a_{O_2}$  was measured with the steady state and continuous non-steady state methods. As discussed in Section 2.4, organic compounds can affect the coalescence behavior of bubbles leading to changes in the oxygen mass transfer coefficient. Therefore, the effect of the organic compounds used in this study on oxygen transfer must be considered.

During the course of optimizing the volatilization experiments, various organic compounds and concentrations of the organic compounds were used. From these experiments it was seen that the concentrations of toluene, dichloromethane, and 1,2-dichlorobenzene studied had no effect on  $k_L a_{O_2}$ . The compound

m-cresol was used in this study as an internal standard. Gurol and Nekouinaini (1985) found m-cresol to increase  $k_L a_{O_2}$  in diffused aeration experiments. The increase was dependent on the concentration of m-cresol and the hydrodynamic conditions of the experiment, i.e.  $\alpha$  increased with increasing concentration and air flow rate. Similar results were seen in this investigation. The runs without m-cresol or with a low concentration ( $< 25$  mg/L) follow the  $k_L a_{O_2}$  curve for tap water (Figure 26).

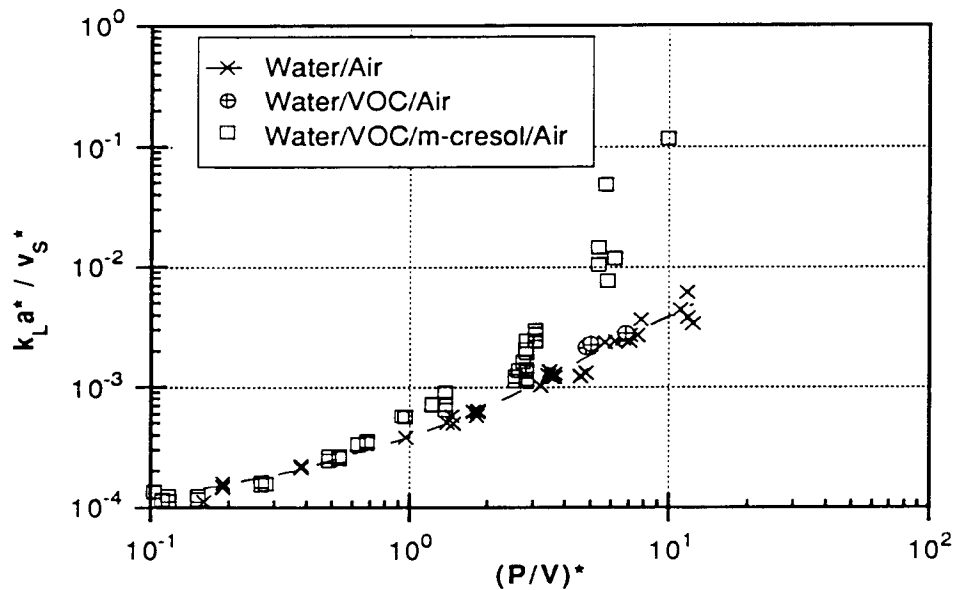


Figure 26. Comparison of  $k_L a_{O_2}$  measured in tap water to those measured in the presence of VOC's and VOC's with m-cresol.

The dependence on the hydrodynamic conditions for the runs where m-cresol had an effect is illustrated in Figure 26. At low power densities there is no effect on  $k_L a_{O_2}$ , the curves are the same. The sparger used to introduce the air produces large primary bubbles; the coalescence hindering property of

m-cresol is not yet important. However, as the power density increases, the curves diverge. The large primary bubbles are broken up by the stirrer at the higher power densities and the coalescence hindering property of m-cresol produces very fine bubbles. The  $k_L a_{O_2}$  values rapidly increase due to the increase in interfacial area.

#### **4.1.3 Water/DSS/Air system**

The anionic surfactant dodecyl sodium sulfate (DSS) was used to investigate the effect of changes in surface tension on oxygen transfer. The surfactant decreased  $k_L a_{O_2}$  at low power densities; the lower the surface tension, the more effect. As the turbulence of the system increased, the  $k_L a_{O_2}$  values approached those of tap water, and finally increased to four times the tap water values. Looking at Figure 27, we can see that the region where the  $k_L a_{O_2}$  values of the surfactant become larger than those of tap water is the same region where the  $k_L a_{O_2}$  values with m-cresol also become larger than the tap water values.

Other authors have also found this decrease and recovery in  $k_L a_{O_2}$  with increasing power (Mancy and Okun, 1965, Eckenfelder and Ford, 1968, and Hwang, 1983). In discussing the results of Mancy and Okun (1965) and their own results, Eckenfelder and Ford (1968) break the analysis into three hydrodynamic regions. Under laminar conditions they found little to no effect on  $\alpha$  since the resistance in the bulk liquid to oxygen transport exceeds the combined interfacial resistance. This region was not used in this study. Laminar conditions are rarely encountered in aeration practice. They found the maximum depression in  $k_L$  occurs under moderately turbulent conditions. They assume this is due to the barrier effect: the transfer rate is controlled by

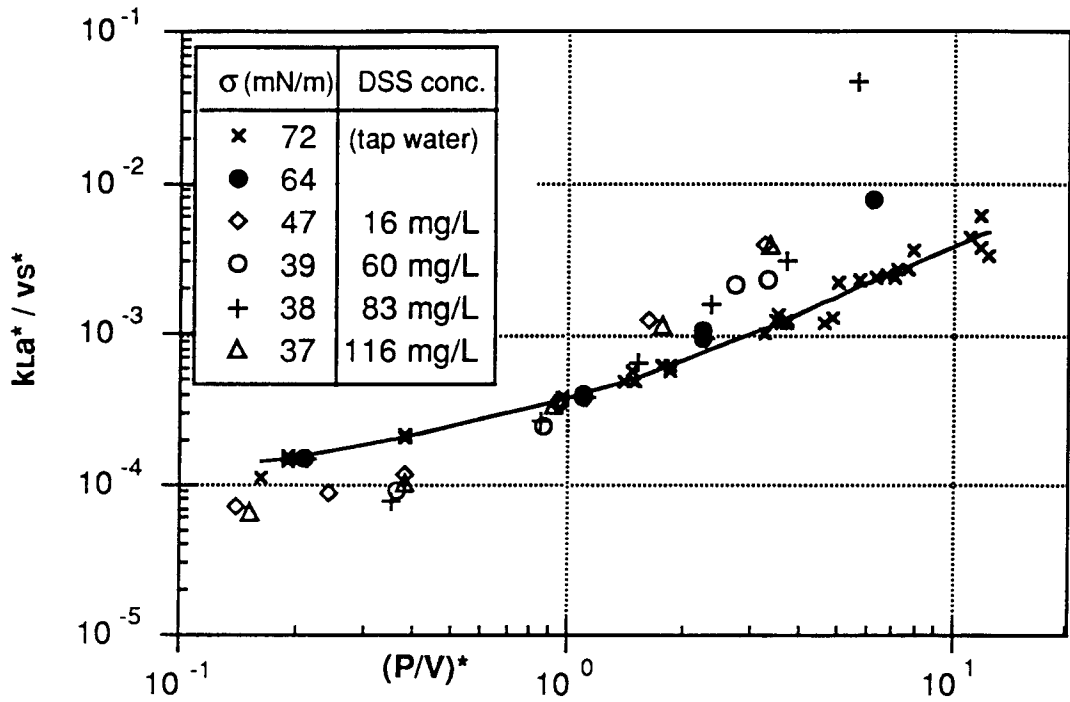


Figure 27. The effect of DSS on the oxygen mass transfer coefficient.

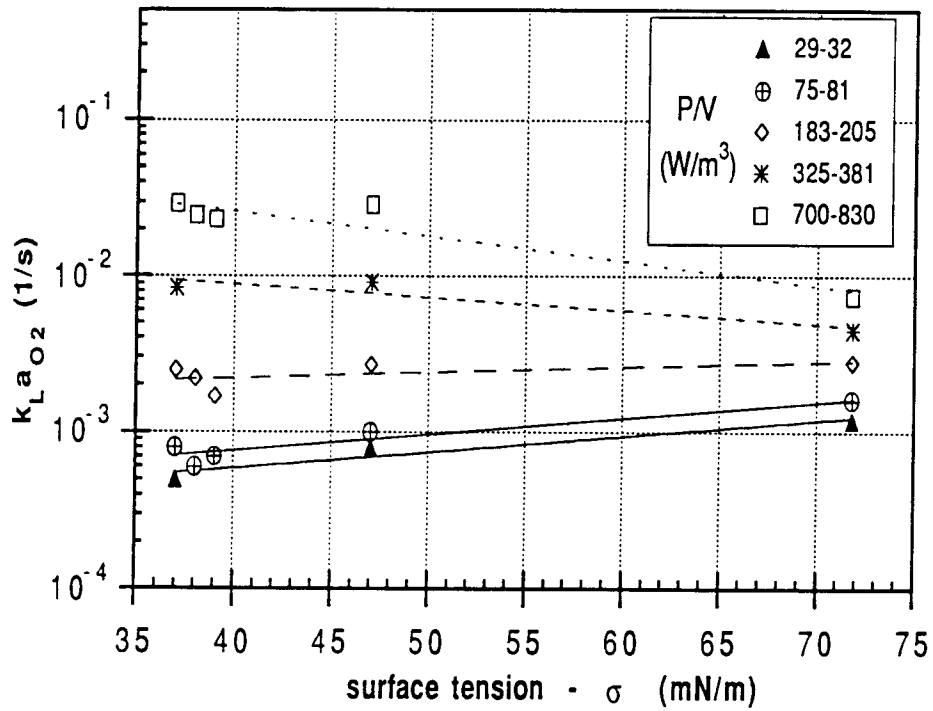


Figure 28. Dependence of the effect of DSS on reactor hydrodynamics.

the interfacial resistance to molecular diffusion caused by the adsorbed surfactant. From the work of Llorens et al.(1988) and Ollenik and Nitsch (1981), it seems that the hydrodynamic effect is more important: the suppression of the interfacial turbulence and reduction in internal gas recirculation due to the surface tension gradient. The magnitude of the effect on  $k_L$  in this region depends upon whether the life of the interface is sufficient to establish equilibrium with respect to absorption of the surfactant.

The effect of the change in surface tension on  $k_L a_{O_2}$  is seen in Figure 28 for increasing power densities. In the moderately turbulent region ( $P/V < 200 \text{ W/m}^3$ ), as surface tension decreases, the mass transfer of oxygen decreases. The recovery of the mass transfer coefficient to its original value (as discussed in Section 2.3.1) at the critical micelle concentration could not be investigated because of precipitation problems, i.e. at high concentrations, DSS formed a precipitate in the tap water used. Looking at the data from the more turbulent regions ( $P/V > 325 \text{ W/m}^3$ ), we see that  $k_L a_{O_2}$  increases as surface tension decreases.

In this third region described by Eckenfelder and Ford (1968), the turbulence at the higher power densities, in causing the same surface renewal experienced in water/air systems, indirectly caused increased interfacial turbulence and inner gas recirculation due to dynamic/static surface tension differences as discussed in Section 2.3.1 (Koshy et al., 1988). Therefore, the mass transfer coefficient measured in the presence of surfactants,  $k_{L,s}$ , approaches that of  $k_{LTP}$ , the mass transfer coefficient measured in tap water. However, the volumetric mass transfer coefficient of the surfactant system,  $k_L a_s$ , exceeds that of the tap water

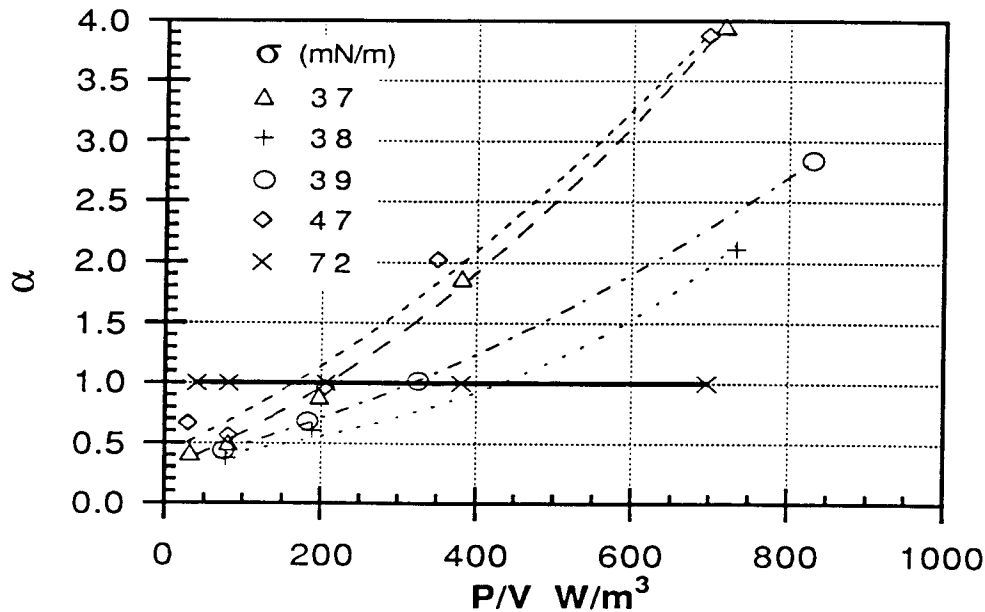


Figure 29. Change in alpha factor with increasing power density for the DSS solutions.

system at high power densities, i.e.  $\alpha > 1$ . This is due to the increased interfacial area, either caused by the formation of smaller primary bubbles or, in the case of this study, the inhibition of coalescence after the primary bubbles are broken up (Figure 29).

In studying the effect of DSS on surface aeration in three sizes of geometrically similar tanks, Hwang (1983) was able to correlate his data using surface tension as a parameter with the Weber number  $(=\rho n^2 d^3 / \sigma)$  raised to the power 0.8. The correlation was developed for a range of  $P/V$  from 3 to 40  $W/m^3$ , the lowest region of this study. Although the reactors in the two studies are not geometrically similar, a comparison can be made to see if the effect of surface tension can be described by this function. Figure 30 shows the data from this



study plotted in a similar manner. The y-axis was modified using the appropriate dimensionless numbers for a sparged turbine stirred tank,  $k_L a^* / v_s^*$ . The data is fairly well correlated with these parameters.

Osorio developed a correlation to describe his coalescence inhibited system (from the addition of salt and iso-propanol) using the dimensionless surface tension number,  $\sigma^*$ . He found  $k_L a$  to be inversely proportional to  $\sigma^{*1.04}$ . Plotting my data in his form, we see that the low and high ranges are not well described (Figure 31). His correlation was not developed for surfactants, so the reduction in  $k_L a_{O_2}$  at the lower P/V region due to hydrodynamic dampening is not considered in his correlation. The phenomena observed in his study are most probably due to the change in coalescence behavior, not due to changes in surface tension.

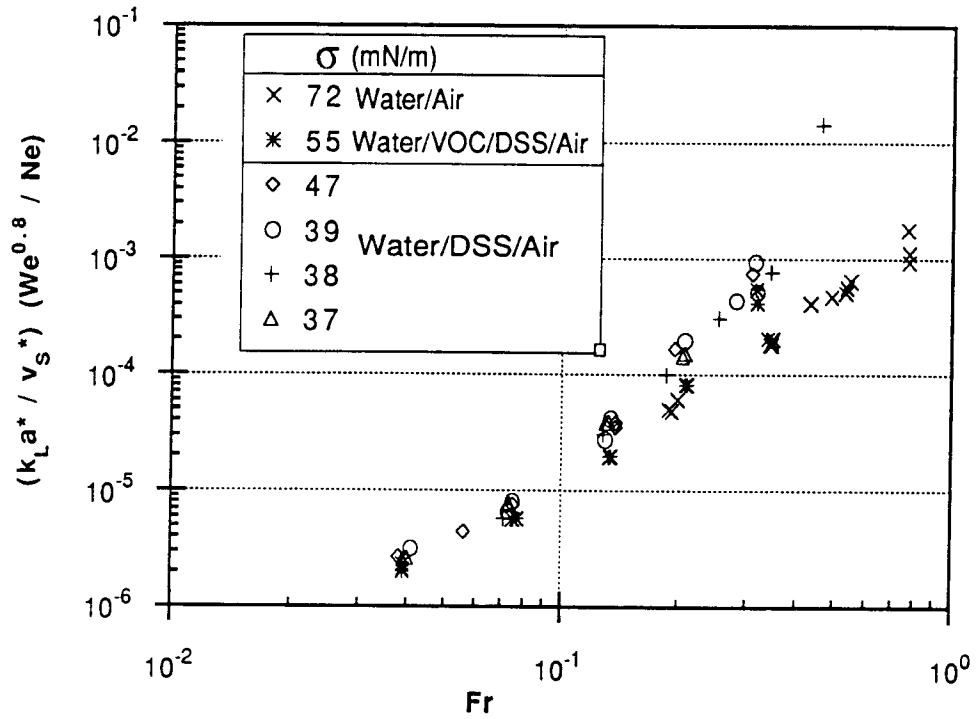


Figure 30. Comparison of data to the correlation developed by Hwang (1983).

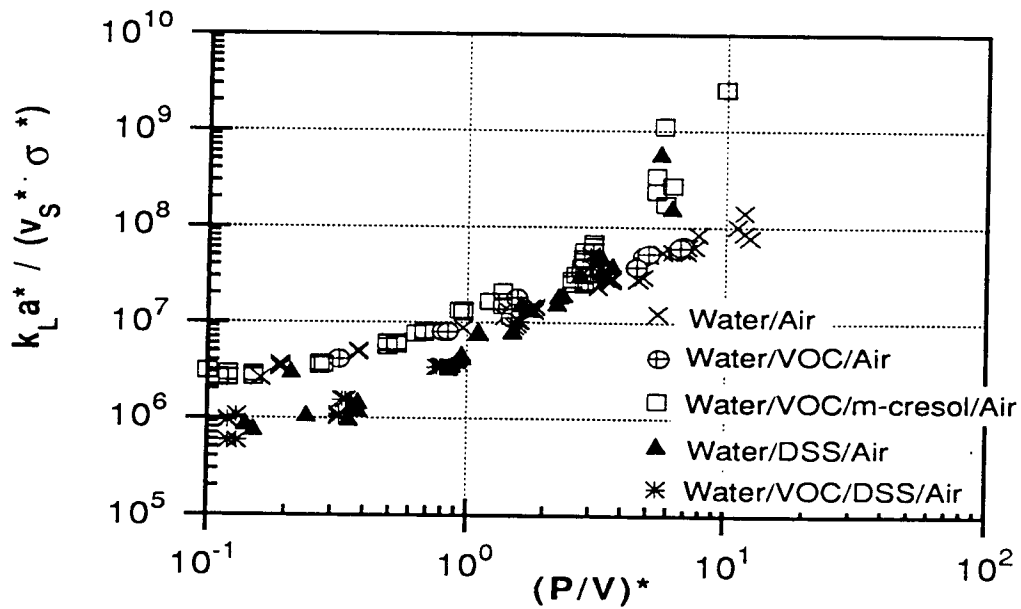


Figure 31. Comparison of data to the correlation developed by Osorio (1985).

#### 4.1.4 Water/Biomass/Air system

Experiments were made to measure the oxygen mass transfer coefficient in the presence of biomass. Thickened waste activated sludge was obtained from a Berlin municipal wastewater treatment plant and diluted to a suspended solids concentration of ~3 g/L. The mixed liquor was characterized in terms of surface tension, suspended solids, COD, IC (inorganic carbon), and TOC (Table 9). There was a reduction in  $k_L a_{O_2}$  compared to tap water values until high power densities were reached ( $P/V^* > 5$ ) (Figure 32). Comparing the effect of surfactant at this surface tension and the effect of the biomass showed that surface tension was not enough to describe the changes in  $k_L a_{O_2}$ . Since the presence of biomass in the reactor appeared to dampen the turbulence, a study of the effect of biomass on the hydrodynamics of the system may bring more insight into the effect of biomass on mass transfer.

Table 9. Characteristics of the biomass suspension.

$\sigma$	SS	COD	TOC	IC
mN/m	g/L	mg/L	mg/L	mg/L
63.2	3.15	48	6	27

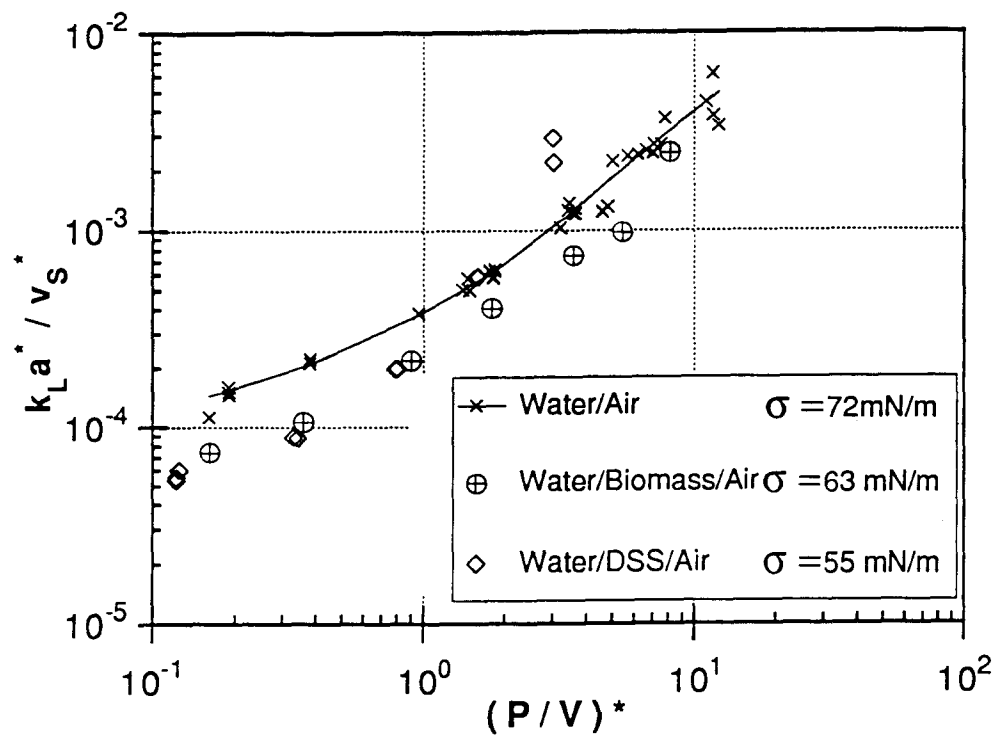


Figure 32. Comparison of  $k_L a_{O_2}$  values measured in the presence of biomass to those measured in tap water and a DSS solution.

## 4.2 Volatile organic compound transfer

The data from the volatilization experiments were evaluated for consistency by checking the mass balance closure, since both the gas and liquid phases were sampled. The closure was generally good; only data with a closure  $\pm 15\%$  were used. The coefficients of variation (standard deviation/mean) for the GC measurements were good, varying from 1.5-12%. The VOC mass transfer coefficients were calculated with the steady state equations 37-39. The mass transfer coefficient values from equation 38 were used in the discussion below because, as discussed in Section 3.7, it is the most reliable of the three equations. However, in the experiments with a good mass balance closure, the agreement between the  $K_L a_{\text{VOC}}$ 's from the three equations was good.

### 4.2.1 Water/VOC/Air system

In contrast to  $k_L a_{\text{O}_2}$ , the VOC mass transfer coefficients show little dependence on the power input in the reactor (Figure 33). Since  $k_L a_{\text{O}_2}$  increased with power density, the ratio of the two over-all mass transfer coefficients,  $\Psi_m$  decreases with increasing power (Figure 34). The curve can be approximated as a line in the log/log plot. However, the negative deviation at high power densities is not due to scatter, but rather due to the exponential increase in  $k_L a_{\text{O}_2}$  in non-coalescing systems at high power densities.

Some experimental values of  $k_L a_{\text{O}_2}$ ,  $K_L a_{\text{VOC}}$ , and  $\Psi_m$  are listed in Table 10.  $\Psi_m$  varies from 0.13 to 0.66 for toluene, and from 0.03 to 0.28 for dichloromethane and 1,2-dichlorobenzene. Comparing this to Table 2 in Section 2.1.4, we see that these values are not within the range predicted based on the theory of a

liquid film controlled mass transfer. The predicted range considering error in the diffusion coefficient and the variation possible in the exponent n is between 0.34 and 0.83 for all three compounds.

Table 10. Experimental results:  $k_{L}a_{O_2}$ ,  $K_{L}a_{VOC}$ , and  $K_{L}a_{VOC}/k_{L}a_{O_2}$  ( $\Psi_m$ ) for three power ranges.

Power	$k_{L}a_{O_2}$	$K_{L}a_{VOC}$			$K_{L}a_{VOC}/k_{L}a_{O_2}$		
$W/m^3$	1/s	1/s			$\Psi_m$		
		TOL	DCM	1,2-DCB	TOL	DCM	1,2-DCB
27	0.0023	0.0016	0.0007	-	0.66	0.28	-
113	0.0048	0.0015	0.0006	0.0007	0.32	0.13	0.14
555	0.0232	0.0031	0.0008	-	0.13	0.03	-

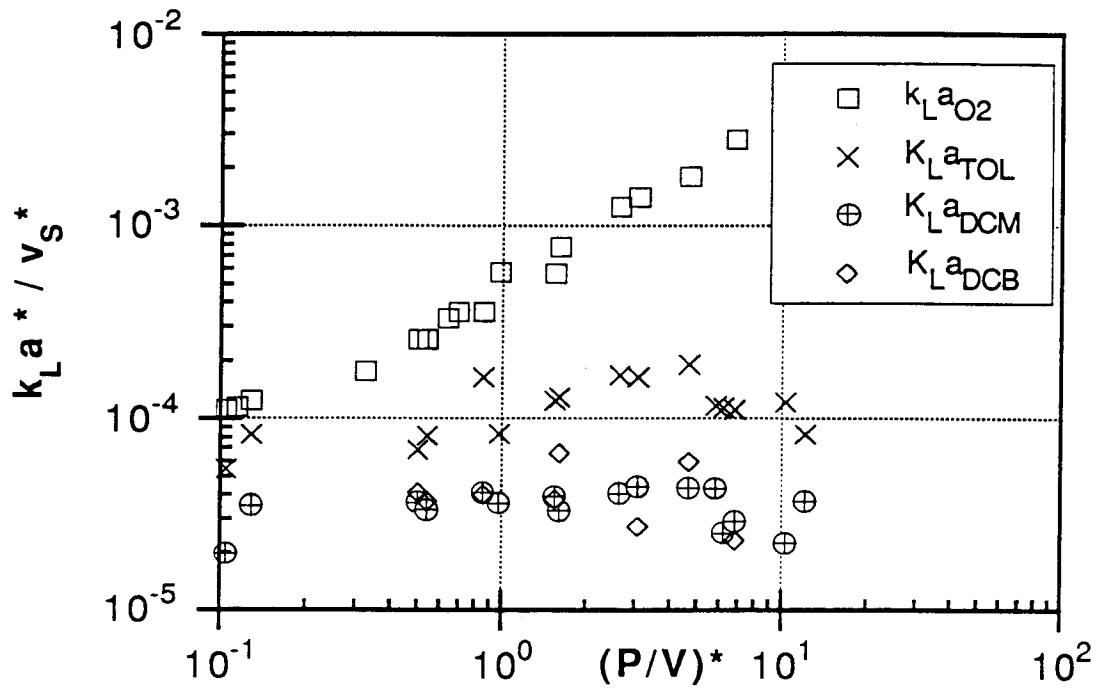


Figure 33. Dependence of the oxygen and VOC's mass transfer coefficients on power density.

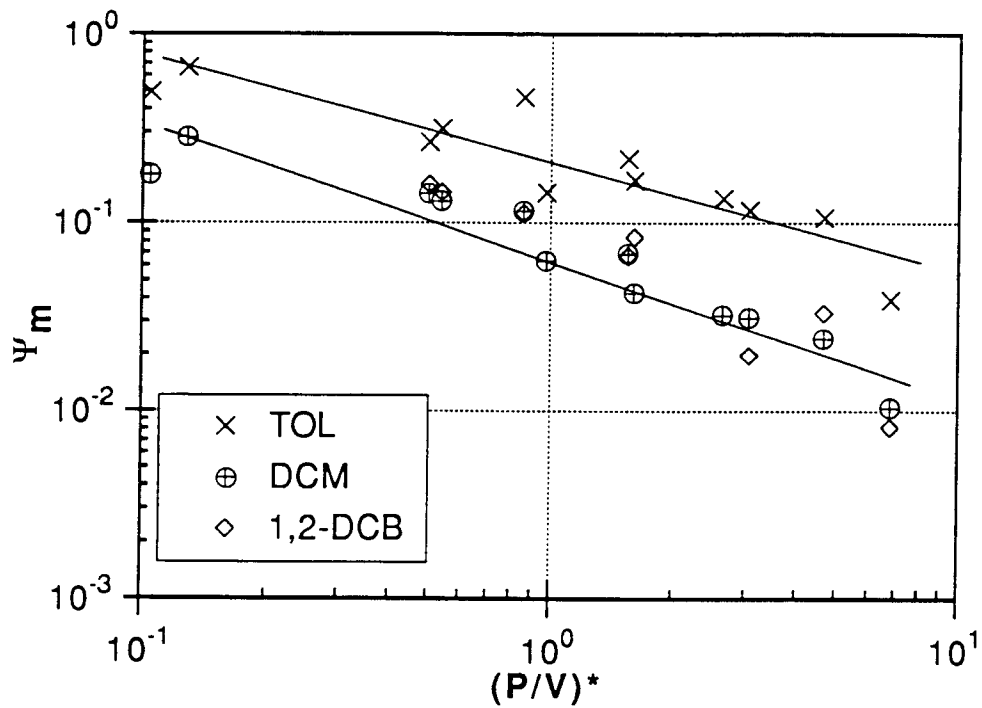


Figure 34.  $\Psi_m$  as a function of the dimensionless power density.

### Influence of gas phase resistance

Obviously, the resistance to mass transfer of the volatile organic compounds does not just lie in the liquid side. The gas phase resistance must also play a role in the over-all resistance. The importance of the gas side resistance is determined by the hydrodynamic conditions in the reactor and the Henry's constant of the compound. Both influence the relationship of the over-all mass transfer coefficients,  $K_L a_{\text{VOC}}/k_L a_{\text{O}_2}$ , because of the relationship of the film coefficients and  $H_c$ :

$$\frac{1}{K_L a} = \frac{1}{k_L a} + \frac{1}{H_c \cdot k_G a} \quad (40)$$

Using this equation, it is possible to approximate the experimental ratio of  $k_G a/k_L a$  from a plot of  $1/K_L a$  versus  $1/H_c$ .

The slope is the inverse of  $k_G a$  and the y-intercept is the inverse of  $k_L a$ . This equation applies strictly only for compounds with the same Schmidt number. The three VOC's have similar liquid diffusion coefficients, the diffusion coefficient of oxygen is only approximately two times larger, therefore, the variation in  $Sc$  is negligible. This method can be used to calculate the ratio  $k_G a/k_L a$  for the various power densities used. A drawback of this method is that it is extremely sensitive to experimental error. The smallest and most error prone  $K_L a$  becomes very important,  $K_L a_{\text{DCB}}$ , and a slight change in the slope ( $1/k_G a$ ) changes the y-intercept ( $1/k_L a$ ) from positive to negative. Not only is the uncertainty of the mass transfer coefficient magnified, but also the uncertainty of the Henry's constant. Because of the limited number of compounds used and the weight placed on the component with the most unreliable mass transfer



coefficient (1,2-dichlorobenzene), this method can only be viewed as approximate, especially in the determination of  $k_L a$ . However, since  $k_L a_{O_2} = K_L a_{O_2}$ , we can estimate  $k_L a_{VOC}$  from  $k_L a_{O_2} (D_{LVOC}/D_{LO_2})^n$ .

In order to check the results, a second form of the equation was also used:

$$\frac{K_L a}{H_c} = k_G a - K_L a \cdot \frac{k_G a}{k_L a} \quad (41)$$

This time the y-intercept is  $k_G a$  and the slope is  $k_G a/k_L a$ . This equation places much more emphasis on the oxygen mass transfer coefficient.

Another possibility to calculate the ratio  $k_G a/k_L a$  is based on the theory developed in Section 2.1.4:

$$\frac{1}{K_L a_{VOC}} = \frac{1}{k_L a_{O_2} \cdot \left(\frac{D_{LVOC}}{D_{LO_2}}\right)^n} + \frac{1}{H_c \cdot k_G a_{O_2} \cdot \left(\frac{D_{GVOC}}{D_{GO_2}}\right)^m} \quad (42)$$

Smith et al. (1981) suggest using this equation to calculate  $K_L a_{VOC}$  from known  $k_L a_{O_2}$ 's when gas phase resistance is also present. They investigated volatilization under conditions simulating natural bodies of water. Instead of  $k_G a_{O_2}$  though they use  $k_G a_{H_2O}$ , which is easy to determine experimentally in their experiments. Other authors have used this equation to calculate  $k_G a/k_L a$  (Munz and Roberts, 1984, Hsieh, 1990) using nonlinear regression. Because only three compounds were studied here, it was not possible to use this method with any certainty. However, if a value of  $n=0.5$  is assumed,  $k_G a/k_L a$  can be calculated from the following equations:

$$\frac{R_L}{R_T} = \frac{K_L a_{VOC}}{k_L a_{O_2} \cdot \left( \frac{D_{LVOC}}{D_{LO_2}} \right)^n} \quad (43)$$

$$\frac{k_G a}{k_L a} = \frac{1}{\left( \frac{R_T}{R_L} - 1 \right)} \cdot \frac{1}{H_c} \quad (44)$$

Unlike the other methods, the compounds are evaluated individually here. Therefore, although the ratio  $k_G a/k_L a$  should be the same for all compounds regardless of their  $H_c$  as in the other two methods, the ratio  $k_G a/k_L a$  calculated with this method for dichloromethane and 1,2-dichlorobenzene are similar, but the ratio for toluene is higher in all cases.

The ratio  $k_G a/k_L a$ ,  $k_G a$ , and  $k_L a$  calculated from these three methods are shown in Table 11. There is fairly good agreement between the methods. The ratio of the two film mass transfer coefficients decreases with power input as expected, while the gas film mass transfer coefficient remains constant (Figure 35). Experiments with more compounds covering a wider range of Henry's constants would be needed to reduce the scatter. Although there is scatter in the values, the trend is evident. Figure 36 shows the contrasting trends in  $k_G a/k_L a$ ,  $k_G a$ , and  $k_L a_{O_2}$ .

It is clear that  $k_G a/k_L a$  decreases with increasing power density because  $k_L a$  increases while  $k_G a$  remains constant. However, it is not clear why  $k_G a$  remains constant with increasing power. No correlations exist for  $k_G a$  in stirred tank reactors (Joshi and Pandit, 1981). Investigations have shown the dependence of  $k_G a$  on gas diffusivity in stirred cells (Versteeg et al., 1987) and

the gas flow rate is certainly another important parameter for  $k_{Ga}$ . Experiments studying the effect of  $Q_G$  and power density on  $k_{Ga}$  are necessary to develop a better understanding of  $k_{Ga}$ .

Table 11. Comparison of  $k_{Ga}/k_{La}$ ,  $k_{Ga}$ , and  $k_L a$  calculated from the three methods.

P/V (W/m <sup>3</sup> )	kGa/kLa			kGa			kLa			kLa-O2 (1/s)	RL/RT (%)
	Method 1	Method 2	Method 3	Method 1	Method 2	Method 3	Method 1	Method 2	Method 3		
22	1.3		5.3	0.0052		0.0093	0.0041	0.0018	0.0018	0.0026	30
24			2.6			0.0039	0.0032	0.0015	0.0015	0.0022	25
27	2.9	4.6		0.0086	0.0133		0.0030	0.0016	0.0016	0.0023	
105	1.6		2.8	0.0094		0.0115	0.0058	0.0041	0.0041		27
113	1.0	1.6	2.8	0.0068	0.0081	0.0093	0.0069	0.0033	0.0033	0.0048	28
146			2.6			0.0117	0.0058	0.0046	0.0046	0.0067	19
180	0.2	1.2	3.5	0.0081	0.0104	0.0160		0.0046	0.0046	0.0067	32
205	0.5		1.0	0.0084		0.0090	0.0180	0.0091	0.0091	0.0133	9
325	0.1	0.8	1.3	0.0073	0.0088	0.0097		0.0073	0.0073	0.0106	16
337		0.7	1.1	0.0060	0.0106	0.0115		0.0100	0.0100	0.0146	14
555		0.5	0.8	0.0073	0.0126	0.0134		0.0159	0.0159	0.0232	11
645		0.3	0.5	0.0079	0.0089	0.0093		0.0179	0.0179	0.0260	8
980		0.3	0.5	0.0077	0.0119	0.0123		0.0229	0.0229	0.0333	8
1220			1.6	0.0084							11
1300			0.0	0.0040		0.0077					1
1430		0.1	0.2	0.0051	0.0062	0.0062		0.0361	0.0361	0.0525	3

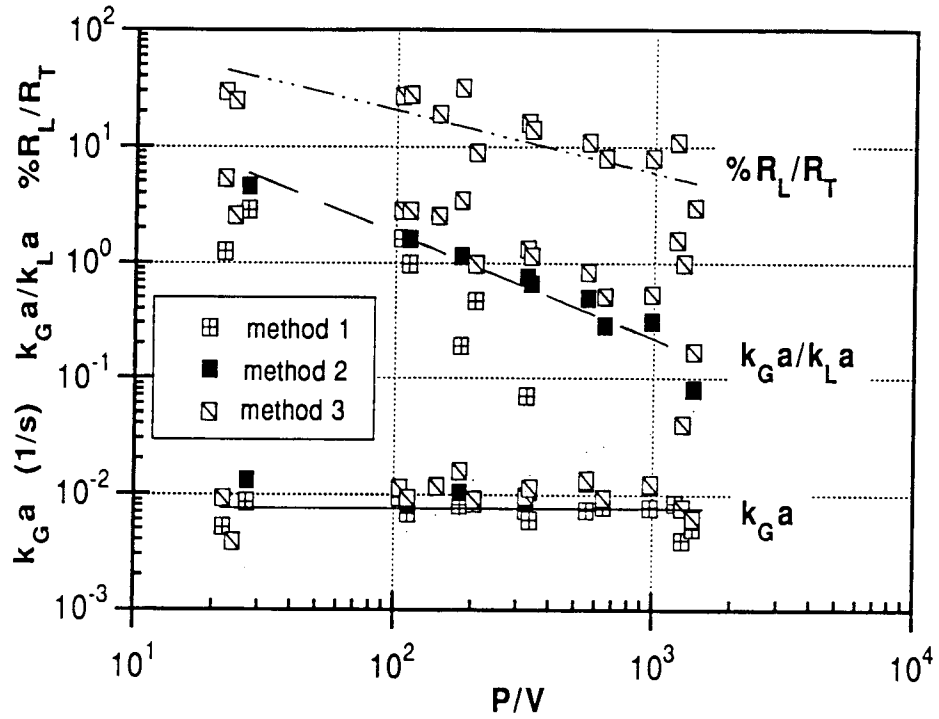


Figure 35. Comparison of the three methods of calculating  $k_G a$ ,  $k_G a/k_L a$ , and  $\%R_L/R_T$ .

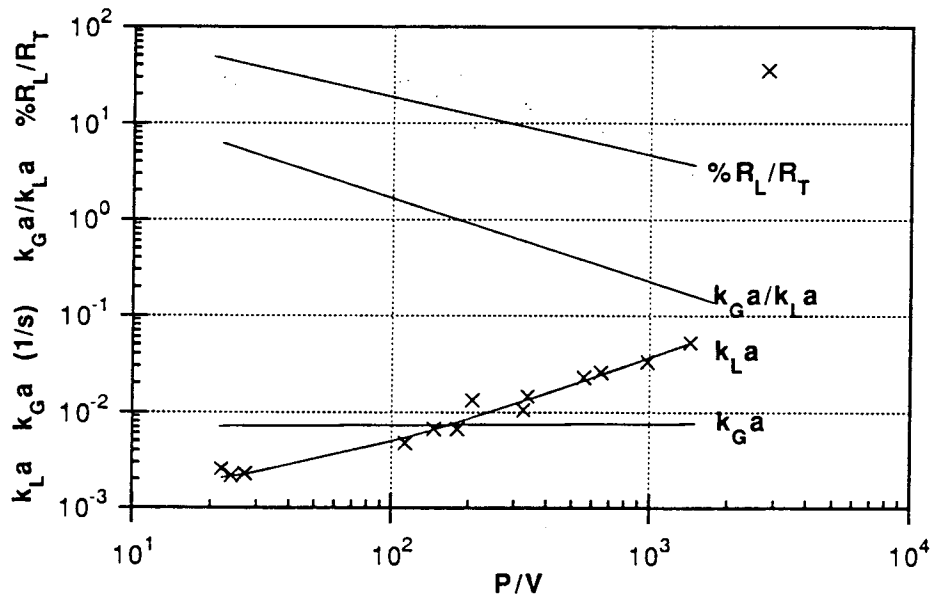


Figure 36. The film mass transfer coefficients and their ratio as a function of power input.

### Determination of $k_{Ga}/k_{La}$

The type of mass transfer contactor, the power input, and the gas superficial velocity are the major parameters in determining the ratio  $k_{Ga}/k_{La}$ . In this study of a stirred reactor, the power input ranged from 22-→2820 W/m<sup>3</sup>,  $v_s$  from  $3 \cdot 10^{-4}$  to  $1.1 \cdot 10^{-3}$  m/s, and  $k_{Ga}/k_{La}$  varied from 5 to 0.1. Munz and Roberts (1984) reported values for surface aeration that range from 90 to 20, for packed columns from 10 to 1, and for bubble aeration from 60 to 10, all with increasing power input. Table 12 lists their correlations developed from the experiments. Their correlation for surface aeration uses the Reynolds number. The dimensionless power density would be more appropriate to use, because at high Reynolds numbers the power number is actually independent of the Reynolds number.

The value of the ratio  $k_{Ga}/k_{La}$  depends on the value of both  $k_{Ga}$  and  $k_{La}$ . The value of  $k_{Ga}$  depends on the gas velocity over the surface in surface aeration. In the surface aeration experiments of Munz and Roberts (1984), forced air circulation was used, but this dependence was not quantified. Therefore, their correlation for surface aerators cannot be used to yield absolute values of  $k_{Ga}/k_{La}$ . It was not possible to develop a correlation for the stirred tank reactor because the superficial gas velocity was not varied much in this study. Therefore, the dependence of  $k_{Ga}$  on  $v_s$  could not be determined. However, the dependence on power was determined and is shown in Table 13.

All published reports on volatilization studies under conditions simulating natural bodies of water and for surface and bubble aeration have found  $\Psi_m$  to be independent of power input. In a study on surface aeration with power

Table 12. Correlations for the various types of mass transfer contactors.

Contactors Type	Correlation	Author
Surface Aerator	$\frac{k_G a}{k_L a} = 1.15 \cdot 10^7 \cdot Re^{-1.23}$	Munz and Roberts (1984)
Fine Bubble Dif- fuser	$\frac{k_G a}{k_L a} = 389 \cdot \left(\frac{P}{V}\right)^{-1.12}$	"
Packed Column	$\frac{k_G a}{k_L a} = 1.32 \cdot \left(\frac{Q_L}{Q_G}\right)^{-0.62}$	"
Stirred Tank	$\frac{k_G a}{k_L a} = f \left[ \left(\frac{P}{V}\right)^{* -0.77} \cdot v_s^{*b} \right]$	this study

input ranging from 0.8-320 W/m<sup>3</sup>, Roberts et al.(1984) found  $\Psi_m$  to be constant. In this investigation, power input was varied from 22-2820 W/m<sup>3</sup>. A decrease in  $\Psi_m$  was observed at power densities as low as 50 W/m<sup>3</sup>. This can be explained by the ratio  $k_{Ga}/k_{La}$ . The surface aeration experiments of Roberts et al. had  $k_{Ga}/k_{La}$  values ranging from 90 to 20. In the stirred tank reactor in this study, for the same range of power input, the ratio ranged from 5 to 1. Liquid side resistance accounted for 90 - 50 % of the total resistance in surface aeration, whereas in the stirred tank reactor it accounted for only 30 - 10 %.

#### Effect of Henry's constant on $\Psi_m$

It is possible to calculate the influence of the Henry's constant on  $K_L a_{VO_2}$  and  $\Psi_m$  for a given  $k_{LaO_2}$  and  $k_{Ga}/k_{La}$  from the relationships developed in Section 2.1.4.

Rearranging equation 17:

$$k_L a_{VOC} = k_L a_{O_2} \cdot \left( \frac{D_{LVOC}}{D_{LO_2}} \right)^n \quad (45)$$

Combining equation 17 and 21:

$$\Psi_m = \Psi \cdot \left( \frac{1}{1 + \frac{k_L a_{VOC}}{H_c \cdot k_G a_{VOC}}} \right) = \left( \frac{D_{LVOC}}{D_{LO_2}} \right)^n \cdot \left( \frac{1}{1 + \frac{k_L a_{VOC}}{H_c \cdot k_G a_{VOC}}} \right) \quad (46)$$

If we look at the experimental stripping data of Hsieh (1990) for 20 organic compounds at one set of hydrodynamic conditions and analyze it in terms of the influence of  $H_c$  on  $\Psi_m$ , we see that it follows the predicted curves quite well (Figure 37). The erratic course of the curves stems from the calculated diffusion coefficients. As  $H_c$  increases the value of  $K_L a_{VOC}$  tends toward  $k_L a_{VOC}$  and  $\Psi_m$  tends toward  $\Psi$ .

Changing the hydrodynamic conditions changes the dependence of  $\Psi_m$  on  $H_c$ .

Figure 38 illustrates this effect for three hydrodynamic conditions from this investigation and one from Hsieh (1990). Again, as the compounds become more volatile ( $H_c \uparrow$ ),  $\Psi_m$  tends towards  $\Psi$  and as  $D_{LVOC}$  approaches  $D_{LO_2}$ ,  $\Psi_m \rightarrow 1$ . Increasing turbulence decreases  $\Psi_m$ , because the ratio  $k_G a / k_L a$  decreases.



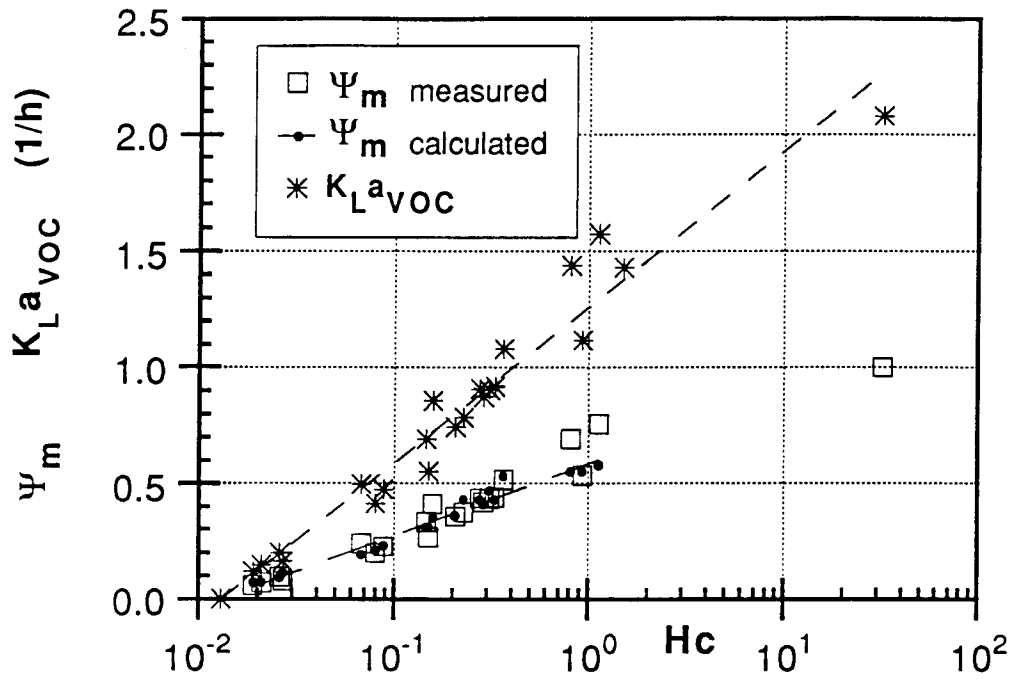


Figure 37. Relationship between  $K_L a_{VOC}$ ,  $\Psi_m$ , and  $H_c$  (data from Hsieh, 1990).

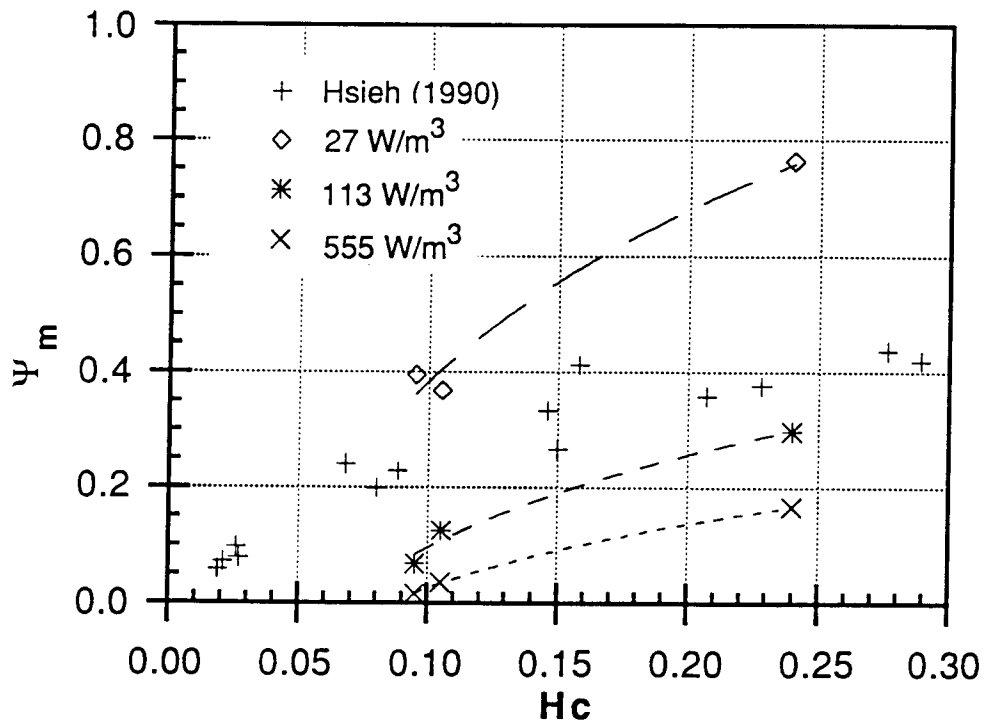


Figure 38. Dependence of  $\Psi_m$  on  $H_c$  for various power densities.

### Gas phase saturation

A constraint on the experimental evaluation of over-all mass transfer coefficients of VOC's is that the gas phase must not be saturated with the organic compound. Calculating the percent gas saturation (Table 14), we see that this constraint is fulfilled for the experimental conditions used in this research. No relation between power input and gas saturation is visible. Using the CFSTR model, we can look at the predicted gas phase saturation for various hydrodynamic conditions for the three compounds investigated. For a constant  $\Psi_m$ , the percent saturation is independent of the gas and liquid flow rates, but dependent on the power input into the system and  $H_c$ . The less volatile the compound, the faster it approaches 100% saturation with increasing power input. However, the gas saturation is also dependent on  $\Psi_m$ . Remembering that  $\Psi_m$  decreases with increasing power input and following the line of the experimental  $\Psi_m$  values across Figure 39, we see that as the power input increases the percent gas phase saturation remains fairly constant.

Table 13. Experimental stripping loss and gas phase saturation.

Power	$k_L a_{O_2}$	Exptl. Stripping Loss			Gas Phase Saturation	
$W/m^3$	$s^{-1}$	%			%	
		TOL	DCM	1,2-DCB	TOL	DCM
27	0.0023	36.7	20.7	19.8	67	65
113	0.0048	35.0	18.8	14.8	68	67
555	0.0232	40.6	20.3	15.2	81	70

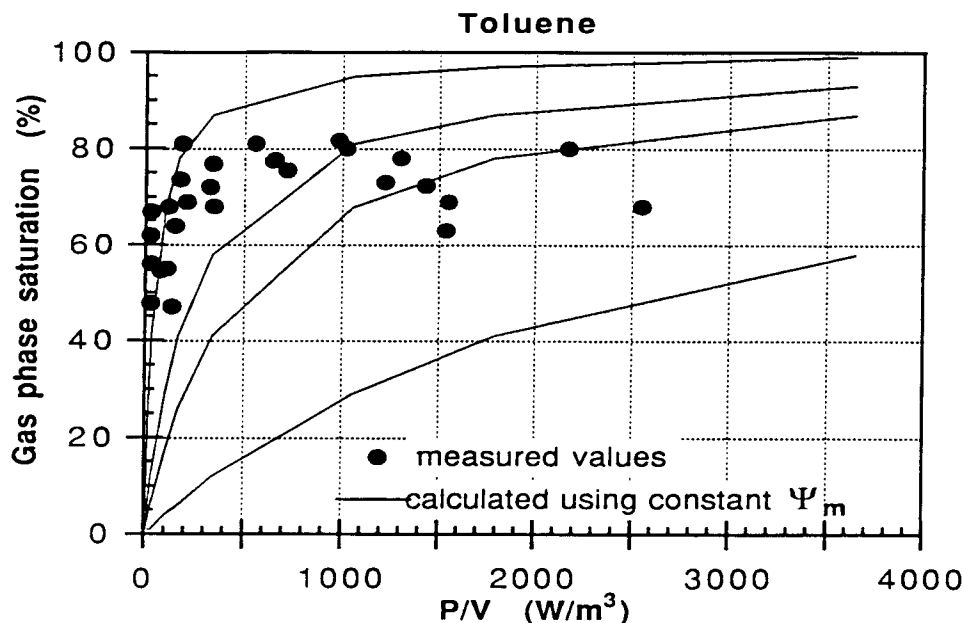


Figure 39. Gas phase saturation as a function of power density.

### Stripping loss

The stripping losses of the volatile organic substances from tap water for various reactor hydrodynamic conditions are listed in Table 14. Although the power densities used produce a range of  $k_L a_{O_2}$  from 0.0023 to 0.0232  $s^{-1}$ , the stripping loss seems to be independent of power input. An order of magnitude increase in  $k_L a_{O_2}$  shows no corresponding trend in stripping loss.

If we evaluate these results in light of the importance of both the gas and liquid phase resistances, we see that the independence of the stripping loss from  $k_L a_{O_2}$  is predictable. Using a model of the CFSTR, the relationship between stripping loss and  $k_L a_{O_2}$ , as a function of  $\Psi_m$  and  $H_c$ , can be calculated. Figure

40 shows the experimental results compared to the calculated results for toluene. From the preceding discussion we know that  $\Psi_m$  decreases as  $k_L a_{O_2}$  increases, so that in following the decreasing  $\Psi_m$  across the graph as  $k_L a_{O_2}$  increases we find that the percent stripping loss remains almost constant.

This can be explained in terms of the two resistance theory. Since the stripping loss is dependent on  $K_L a_{VOC}$ , we can look at it as a function of power input:

$$K_L a_{VOC} = \Psi \cdot \frac{k_L a_{O_2}}{1 + \frac{k_L a_{VOC}}{H_C \cdot k_G a_{VOC}}} \quad (40)$$

For small  $H_C$  and  $k_G a / k_L a$ :

$$K_L a_{VOC} \approx \Psi \cdot \frac{k_L a_{O_2}}{k_L a_{VOC}} \cdot H_C \cdot k_G a_{VOC} \quad (40)$$

and since: (40)

$$\frac{k_L a_{O_2}}{k_L a_{VOC}} = \frac{1}{\Psi}$$

then:

$$K_L a_{VOC} \approx H_C \cdot k_G a_{VOC} = \text{constant}$$

Therefore,  $K_L a_{VOC}$  becomes independent of power at the higher power inputs.

In order to expand these results to wastewater treatment design, we can consider the experimental data in a different form. The variables that affect stripping losses are:  $Q_G$ ,  $Q_L$ ,  $\Psi_m$ ,  $k_L a_{O_2}$ ,  $H_C$ . Because the hydraulic retention time,  $\theta_H$  ( $V_L/Q_L$ ), used in this study was small compared to those of wastewater treatment processes, it is interesting to look at the effect of  $\Psi_m$  on stripping

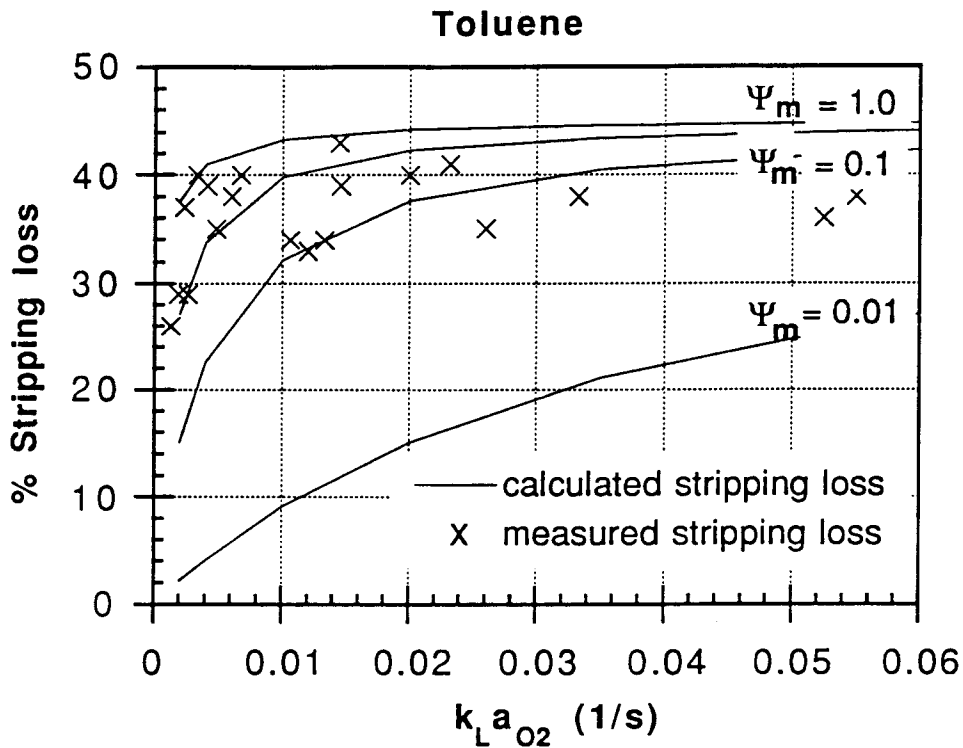


Figure 40. Toluene stripping loss as a function of  $k_L a_{O_2}$  for  $\Psi_m = 0.01 \rightarrow 1.0$ .

loss as a function of  $\theta_H$ . This allows us to see what would happen under full scale conditions. The percent toluene stripping loss is plotted against  $Q_L$  (or  $\theta_H$ ) in Figure 41 for two different power densities (or  $k_L a_{O_2}$ ) and  $\Psi_m$  for these experimental conditions.  $Q_G$  is held constant at 200 L/h and the  $H_c$  of toluene is used, 0.240.

As  $\theta_H$  becomes large (small  $Q_L$ ), the stripping loss increases to 100% for all  $k_L a_{O_2}$ . The experimental points are shown for  $\theta_H = 0.3$  h. For  $k_L a_{O_2} = 0.0023 \text{ s}^{-1}$ ,  $\Psi_m = 0.66$ ; for  $k_L a_{O_2} = 0.023 \text{ s}^{-1}$ ,  $\Psi_m = 0.13$ . These two curves are very close together, therefore, there is only a small increase in stripping loss for an order of magnitude increase in  $k_L a_{O_2}$ . This can be explained by the increased importance of the gas side resistance as power is increased.

Considering stripping loss for one power density ( $P/V=27 \text{ W/m}^3$ ,  $k_L a_{O_2}=0.002 \text{ s}^{-1}$ ,  $k_{Ga}/k_L a=5$ ) and for the range of  $\Psi_m$  from 0.001 to 1.0, the influence of  $\Psi_m$  on stripping loss is seen (Figure 42): as  $\Psi_m$  increases, stripping losses increase. This means as the gas side resistance decreases, more is stripped. The range of compound volatility covered by this range of  $\Psi_m$  can be calculated using equation 46;  $\Psi_m = 0.001$  would be typical for m-cresol ( $H_c=0.0001$ ) under these experimental conditions,  $\Psi_m = 0.05$  for naphthalene ( $H_c=0.020$ ),  $\Psi_m = 0.13$  for dichloromethane ( $H_c=0.105$ ), and  $\Psi_m = 0.66$  for toluene ( $H_c=0.240$ ). The increase in compound volatility greater than that of toluene ( $H_c>0.240$ ) does not significantly increase  $\Psi_m$  or stripping losses.

In summary, when estimating the potential stripping losses for one compound at various power densities, the change in  $\Psi_m$  with power must be taken into consideration. An increase in power causes a decrease in  $\Psi_m$ , thus causing only a small increase in stripping losses.

For the case of one power density and various compounds, the less volatile the compound, the more important the gas side resistance becomes, and the more  $\Psi_m$  deviates from  $\Psi$ , thus decreasing potential stripping losses.

The stripping losses in all cases must be calculated with  $\Psi_m$  to avoid overestimation.

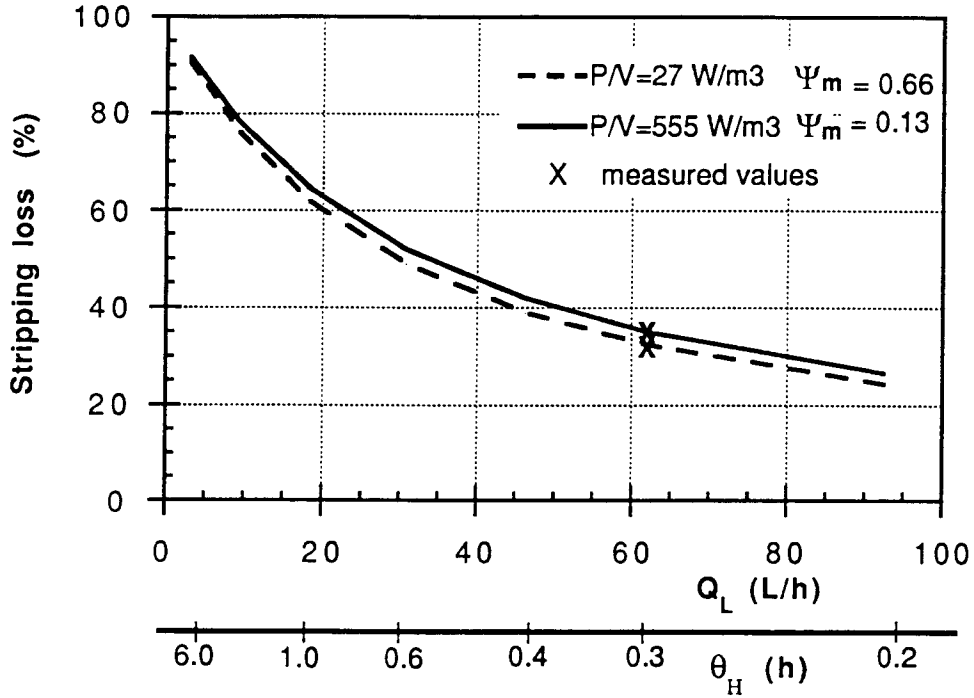


Figure 41. Stripping loss as a function of liquid flow rate (or  $\theta_H$ ) for two power densities and the corresponding  $\Psi_m$  values.

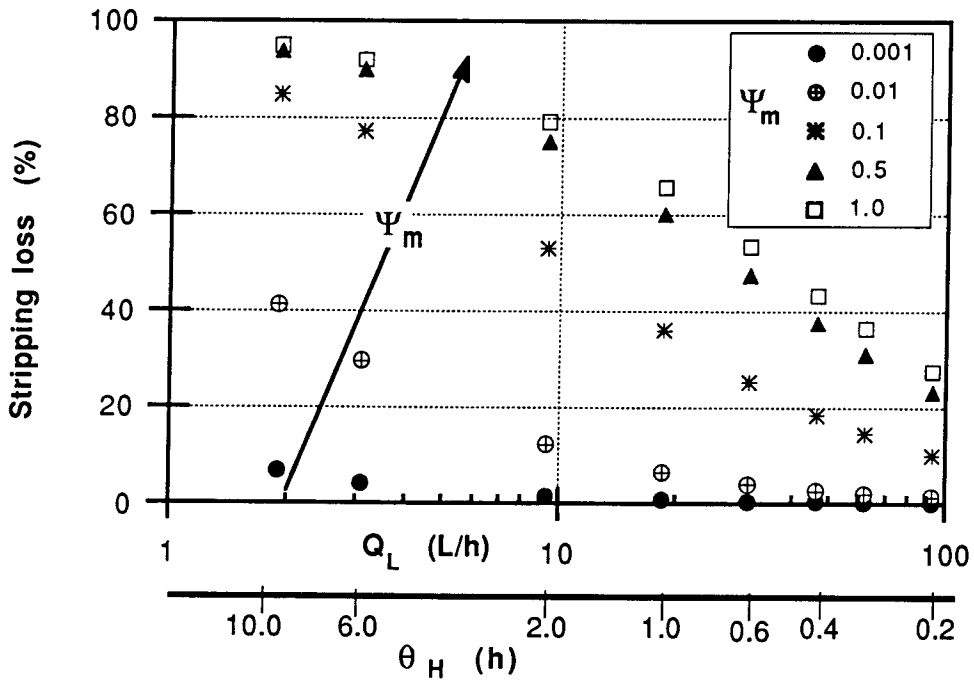


Figure 42. Stripping loss as a function of liquid flow rate (or hydraulic retention time) for one power densities and varying  $\Psi_m$  values.

#### 4.2.2 Water/DSS/VOC/Air system

The effect of surface tension on VOC mass transfer was studied by the addition of the anionic surfactant dodecyl sodium sulfate (DSS). A DSS solution with a surface tension of  $\sigma = 55$  mN/m was used. The results are compared to the  $K_L a_{\text{VOC}}$ 's measured in tap water in Figure 43. The addition of DSS caused a decrease in  $K_L a_{\text{VOC}}$  over the range of  $P/V$  studied. However, the degree of decrease changes as power input increases, e.g. for toluene from 50% reduction to 15%. This behavior is similar to that of  $k_L a_{\text{O}_2}$ . A plot of the  $\alpha$  values for oxygen and VOC transfer in the presence of DSS illustrates this point (Figure 44). As power density increases,  $\alpha$  increases for all three compounds. However, the  $K_L a_{\text{VOC}}$ 's just approach the tap water values at  $P/V = 652$  W/m<sup>3</sup>, while  $k_L a_{\text{O}_2}$  exceeds the tap water value by a factor of 2.2. It seems the mechanism that reduces mass transfer at the lower power densities for O<sub>2</sub> exerts the same influence on the VOC's. Because of the importance of gas side resistance, an increase in power density above 700 W/m<sup>3</sup> does not increase  $K_L a_{\text{VOC}}$  in tap water. Therefore, an increase in  $\alpha$  above one is not expected.

The gas film coefficient,  $k_G a$ , is not changed by the presence of DSS (Figure 45), nor is the function of the ratio of  $k_G a/k_L a$  with power greatly changed. The curve in the presence of DSS deviates somewhat from the curve found for the water/VOC/air system, because of the decrease in  $k_L a$  by DSS in the moderately turbulent region and increase in the highly turbulent region.

The relationship between the mass transfer coefficients,  $\Psi_m$ , seems to be little changed by the surfactant. Figure 46 shows the decrease in  $\Psi_{mDSS}$  compared to



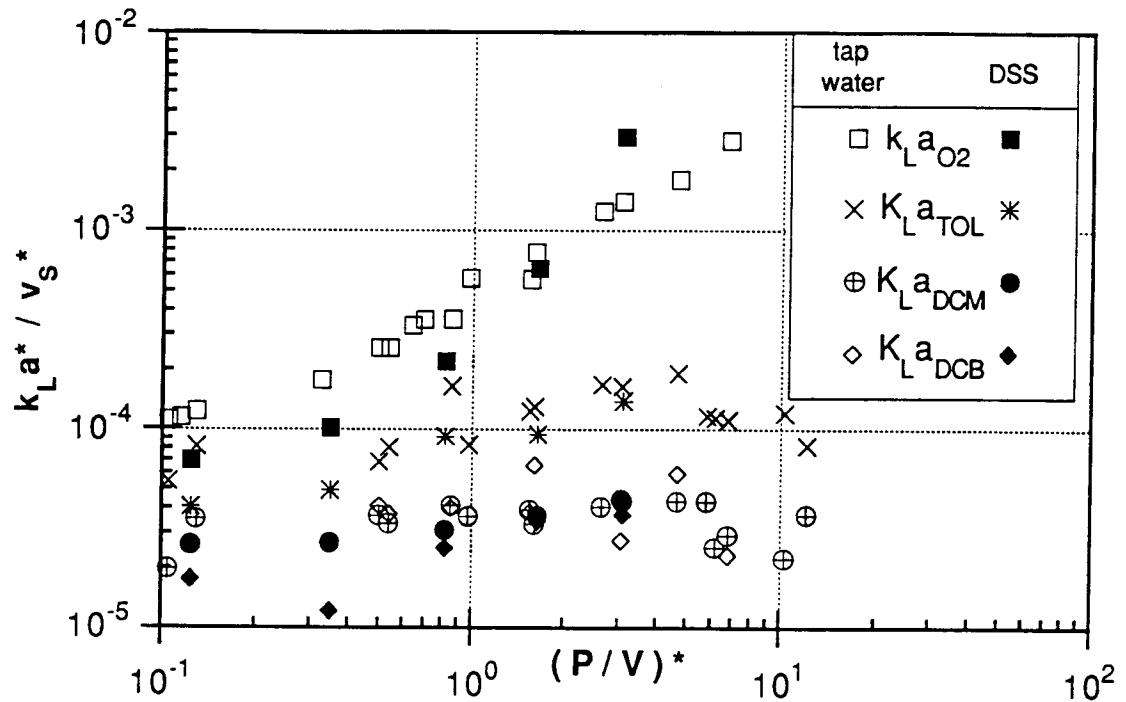


Figure 43. Comparison of  $K_{L,a_{VOC}}$  values measured in tap water and in a DSS solution ( $\sigma = 55$  mN/m).

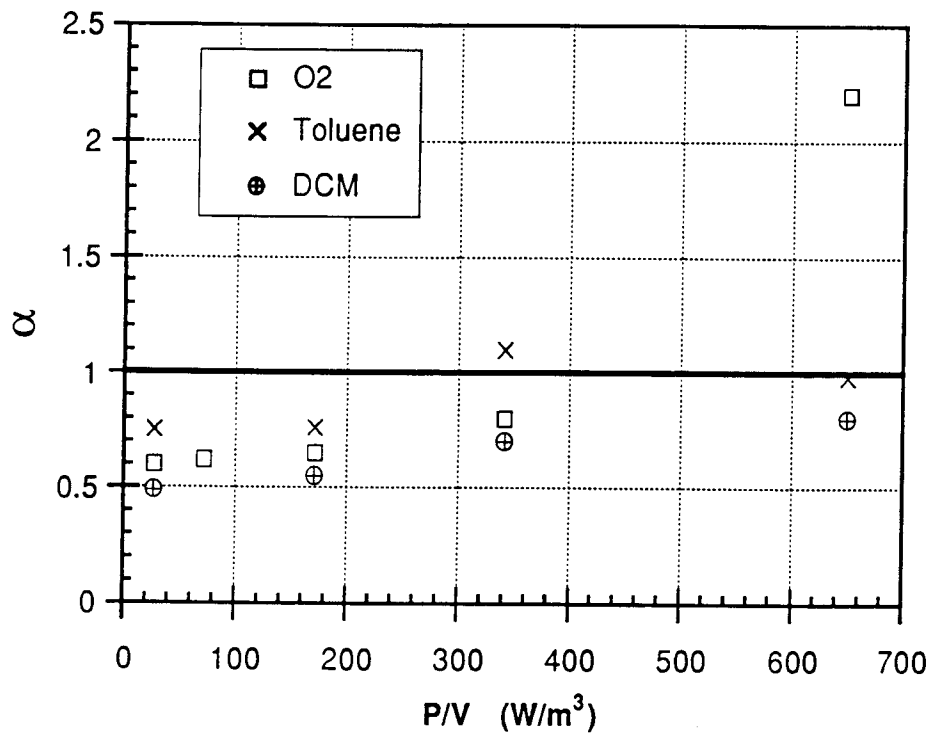


Figure 44. Alpha factors for oxygen and VOC's as a function of power density for the DSS solution ( $\sigma = 55$  mN/m).

$\Psi_{mTP}$  as a function of dimensionless power density. The steeper fall in  $\Psi_{mDSS}$  occurs at the point where the  $k_L a_{O_2}$  values in the presence of DSS become larger than the tap water  $k_L a_{O_2}$ 's. In coalescing systems the fall in  $\Psi_m$  should follow the line. This deviation is similar to the curve in Figure 26 for VOC's in tap water. It is important to remember that the addition of m-cresol hinders coalescence, thus causing an increase in  $k_L a_{O_2}$  similar to the effect of DSS.

As discussed in Section 2.1.5, most studies have found  $\Psi_m$  to be constant, independent of power density, because of the relatively high  $k_G a/k_L a$  ratios used. In studies on the effect of surface active agents on  $\Psi_m$  in diffused aeration, Matter-Müller et al.(1981) found that there was no change in the value of  $\Psi_m$ , although the mass transfer coefficients were reduced by up to 46% in the presence of palmitic acid. This is similar to the results of Rathbun et al.(1978). They studied the effect of phenol, an anionic surfactant, and an oil film on the ratio of the mass transfer coefficients of propane and ethylene, and oxygen under conditions simulating rivers. No significant effects of the additives on  $\Psi_m$  was found.

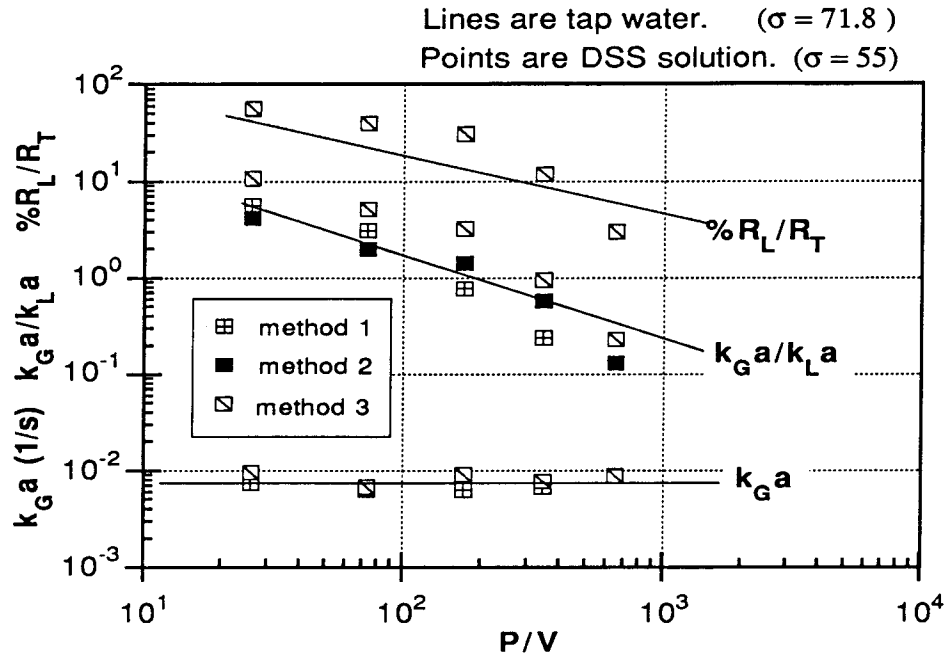


Figure 45. Comparison of the vales of  $k_G a$ ,  $k_G a/k_L a$ , and  $\%R_L/R_T$  measured in tap water and the DSS solution.

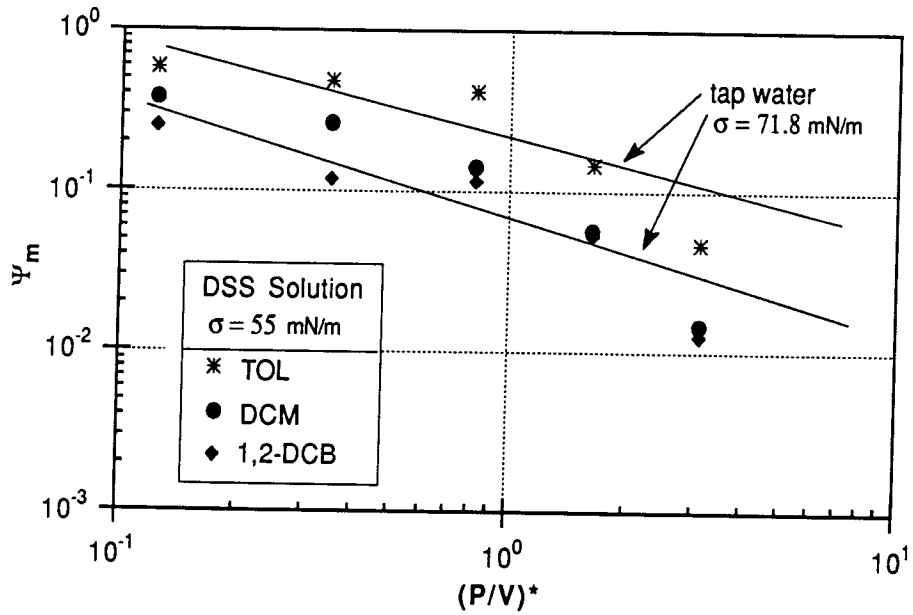


Figure 46. Comparison of  $\Psi_m$  in tap water and in the DSS solution.

### 4.2.3 Application of results

The relationship  $K_L a_{\text{VOC}} = \Psi * k_L a_{\text{O}_2}$  is being used to estimate stripping losses for compounds of medium and low volatility in wastewater treatment processes. As discussed in the previous sections, the mass transfer of semi-volatile compounds is not controlled by liquid side resistance, but is a function of resistance in both phases, so that  $\Psi_m < \Psi$ ; therefore, the predicted VOC emissions using this technique are being overestimated.

When upgrading aeration systems it is important to consider the effects of gas side resistance on VOC emissions. If  $k_G a / k_L a$  is decreased (i.e. the turbulence is increased due to increased power density or increased gas flow)  $\Psi_m$  decreases, and VOC emissions can remain unchanged, even though the oxygen transfer rates are increased. If the method of aeration is changed, each method must be evaluated in terms of  $k_G a / k_L a$  and  $\Psi_m$  in order to compare VOC emissions. Subsurface aeration systems, such as the one used in this study, have lower  $k_G a / k_L a$  ratios than surface aerators for the same oxygen mass transfer coefficients (Hsieh, 1991), so that  $\Psi_m \ll \Psi$  for subsurface aerators, resulting in lower VOC emissions. Care should be exercised with free surfaces, weirs, and other high  $k_G a / k_L a$  aeration devices.

VOC emissions from a reactor are also very dependent on the hydraulic retention time. The use of a process with a shorter hydraulic retention time and higher oxygen mass transfer coefficient is preferable to a process with a longer hydraulic retention time and lower oxygen mass transfer coefficient.

## 5 Conclusions

Volatilization, the mass transfer of chemicals from water to air, is an important phenomenon to be considered when assessing the effectiveness of an activated sludge process in treating wastewater high in volatile organic compounds (VOC's). The aeration process can remove volatile compounds and less volatile but not easily biodegraded compounds by the stripping effect. Volatilization can also occur in other activated sludge unit processes, though theoretically the major source of VOC emissions is the aeration process. This study investigated the quantification of the simultaneous mass transfer of oxygen and volatile organic compounds in an aerated stirred tank reactor.

The mass transfer coefficients of oxygen and three VOC's, toluene, dichloromethane, and 1,2-dichlorobenzene, were determined in three water systems: tap water, tap water with an anionic surfactant, dodecyl sodium sulfate (DSS), and tap water with biomass (oxygen only). A steady state method was chosen as the appropriate method for studying the simultaneous mass transfer of oxygen and VOC's in a stirred tank reactor. Experiments were made to span the range of mass transfer coefficients found in both municipal and industrial wastewater treatment processes.

### Water/Air

The experimental  $k_L a_{O_2}$  values were compared to published correlations, which describe the relationship between power input, superficial gas velocity and  $k_L a$ . Comparison of this study's results to correlations made from data measured with methods designed to avoid errors associated with gas phase depletion shows good agreement.

Analysis of the results using dimensional analysis,  $k_L a^*$  as a function of  $(P/V)^{*a}$  and  $v_s^{*b}$ , showed that the results can be separated into two power regions, with  $a=0.64$  for 20-200 W/m<sup>3</sup>, and  $a=1.0$  for >200 W/m<sup>3</sup>;  $b=1.0$  for both regions. The mass transfer process in the low power range (20-200 W/m<sup>3</sup>) in the stirred tank reactor is not well described by the superficial velocity. Using bubble velocities and bubble retention time could possibly improve the correlation.

### Water/VOC/Air

The addition of the three VOC's studied, toluene, dichloromethane, and 1,2-dichlorobenzene, to the tap water had no effect on  $k_L a_{O_2}$  at the concentrations used. However, the addition of m-cresol as an internal standard at concentrations >25 mg/L inhibited bubble coalescence, which became important at the higher power densities and increased  $k_L a_{O_2}$  dramatically.

Ratios of  $k_G a/k_L a$  measured in the stirred tank reactor were low, ranging from 0.1 to 5. As power density increased,  $k_G a/k_L a$  decreased. The gas film mass transfer coefficient,  $k_G a$ , was found to be constant over the range of power densities investigated.

$K_L a_{VOC}$  increased initially as power density increased and then became constant ( $\cong H_c k_G a$ ), because both gas and liquid side resistance become important for compounds with lower volatility ( $H_c < 1$ ) under the experimental conditions studied. The increase was a function of the Henry's constant,  $H_c$ . The  $K_L a$  for toluene, the most volatile compound, increased the most.

The stripping losses of the VOC's became independent of power, because  $K_L a_{VOC}$  approached a constant as power increased. Stripping loss becomes controlled by the retention time, not by  $P/V$ . The range of power densities where  $K_L a$  and

stripping loss become independent depended on the  $H_c$  of the compound and the value of  $k_{Ga}$ , i.e. for toluene ( $H_c=0.24$ ), at  $P/V > 400 \text{ W/m}^3$ , and for dichloromethane ( $H_c=0.105$ ), at  $P/V > 100 \text{ W/m}^3$ .

The ratio of the two mass transfer coefficients,  $K_{La_{VOC}}/k_{La_{O_2}} (\Psi_m)$ , decreased over the range of power studied ( $20\text{-}2820 \text{ W/m}^3$ );  $K_{La_{VOC}}$  approached a constant and  $k_{La_{O_2}}$  increased with power.  $\Psi_m$  can be calculated for a system from the Henry's constant and the ratio of  $k_{Ga}/k_{La}$ .

#### **Water/DSS/VOC/Air**

The effect of an anionic surfactant (DSS) on mass transfer varied according to the hydrodynamic conditions in the reactor.

In the moderately turbulent region both mass transfer coefficients were reduced in the presence of DSS due to the dampening of interfacial turbulence by the adsorbed layer of surfactant on the bubble/water interface. As power increased, both mass transfer coefficients recovered to the values found in tap water; the increased turbulence caused increased surface renewal at the bubble/water interface, thereby annulling the effect of the surfactant. Therefore, in this region,

$$\Psi_{mDSS} = \Psi_{mTP} .$$

In the highly turbulent region,  $k_{La_{O_2}}$  increased significantly, following the curve of the Water/VOC/Air experiments in which coalescence was inhibited by m-cresol. The inhibition of coalescence by the surfactant, as in the case of m-cresol, increased the interfacial area. The VOC mass transfer coefficients recovered to

the values found in tap water. No further increase was seen because of the importance of the gas phase resistance, as discussed above. Therefore,  $\Psi_{mDSS} < \Psi_{mTP}$  due to the increase in  $k_L a_{O_2}$ .

#### **Water/Biomass/Air**

The oxygen mass transfer coefficient was measured in the presence of biomass. The  $k_L a_{O_2}$  values were reduced at the lower to medium power densities, recovering only at very high power densities. The mixed liquor was characterized in terms of surface tension, suspended solids, and TOC. A comparison of the effect of surfactant at this surface tension and the effect of the biomass showed that surface tension alone was not enough to describe the changes in  $k_L a_{O_2}$ .



## 6 References

- Addison, C.C. (1944). "The properties of freshly formed surfaces. Part III. The mechanism of adsorption, with particular reference to the octyl alcohol-water system," *J.Chem.Soc.*, 477-480.
- Addison, C.C. (1945). "The properties of freshly formed surfaces. Part IV. The influence of chain length and structure on the static and the dynamic surface tensions of aqueous-alcoholic solutions," *J.Chem.Soc.*, 98-106.
- Allen, C.C., D.A. Green, J.B. White, and J.B. Coburn (1986). "Preliminary assessment of air emissions from aerated waste treatment systems at hazardous waste treatment storage and disposal facilities," US EPA, Hazardous Waste Engineering Research Laboratory, Office of Research and Development, Cincinnati, Ohio.
- Andrews, G.F., R. Fike, and S. Wong (1988). "Bubble hydrodynamics and mass transfer at high Reynolds number and surfactant concentration," *Chemical Engineering Science*, Vol.43, No.7, 1467-1477.
- ASCE, ASCE Standard (1984). "Measurement of oxygen transfer in clean water," ISBN 0-87262-430-7, New York.
- Baillod, C.R., W.L. Paulson, J.J. McKeown, and H.J. Campbell, Jr. (1986). "Accuracy and precision of plant scale and shop clean water oxygen transfer tests," *J. Water Pollut. Control Fed.*, Vol.58, No.4, 290-299.
- Berglund, R.L., G.M. Whipple, J.L. Hansen, G.M. Alsop, T.W. Siegrist, B.E. Wilker, and C.R. Dempsey (1985). "Fate of low solubility chemicals in a petroleum chemical wastewater treatment facility," Presented at the National Meeting of the AIChE.
- Bird, R.B., W.E. Stewart, and E.N. Lightfoot (1960). Transport Phenomena, John Wiley and Sons, Inc., New York.
- Blackburn, J.W., W.L. Troxler, K.N. Truong, R.P. Zink, S.C. Meckstroth, J.R. Florence, A. Groen, G.S. Sayler, R.W. Beck, R.A. Minear, A. Breen, and O. Yagi (1985). "Organic chemical fate prediction in activated sludge processes," EPA-600/2-85/102 US EPA, Cincinnati, Ohio.

- Brown, L.C. and C.R. Bailod (1982). "Modeling and interpreting oxygen transfer data," *J.Env.Eng.Div., ASCE*, Vol.108, No.4, 607-628.
- Campbell, H.J., R.O. Ball, and J.H. O'Brien (1976). "Aeration testing and design - a critical review," 8th Mid-Atlantic Industrial Waste Conference, university of Delaware, January 13, 1976, 1-35.
- Chang, D.P.Y., E.D. Schroeder, and R.L. Corsi (1987). "Emissions of volatile and potentially toxic organic compounds from sewage treatment plants and collection systems," Report California Air Resources Board.
- Chapman, C.M., L.G. Gilibaro, and A.W. Nienow (1982). "A dynamic response technique for the estimation of gas-liquid mass transfer coefficients in a stirred vessel," *Chemical Engineering Science*, Vol.37, No.6, 891-896.
- Corsi, R.L., E.D. Schroeder, and D.P.Y. Chang (1989). "Discussion of estimating volatile organic compound emissions from publicly owned treatment works," *J. Water Pollut. Control Fed.*, Vol.61, No.1, 95-96.
- Danckwerts, P.V. (1951). "Significance of liquid-film coefficient in gas absorption," *Ind.Eng.Chem.*, Vol.43, No.6, 1460-1467.
- Dang, N.D.P., D.A. Karrer, and I.J. Dunn (1977). *Biotechnol.Bioeng.*, Vol.19, 853.
- Dixon, G., and B. Bremen (1984). "Technical background and estimation methods for assessing air releases from sewage treatment plants," Versar, Inc., Memorandum.
- Drogaris, G. and P. Weiland (1983). "Coalescence behavior of gas bubbles in aqueous solutions of n-alcohols and fatty acids," *Chemical Engineering Science*, Vol.38, No.9, 1501-1506.
- Eckenfelder, W.W. and D.L. Ford (1968). "New concepts in oxygen transfer and aeration," Advances in Water Quality Improvements, Ed. by Gloyna, E.F. and W.W. Eckenfelder, Univ. of Texas Press, 215-236.
- Figueiredo, M.M.L. and P.H. Calderbank (1979). "The scale-up of aerated mixing vessels for specified oxygen dissolution rates," *Chemical Engineering Science*, Vol.34, No.11, 1333-1338.

- Gibilaro, L.G., S.N. Davies, M. Cooke, P.M. Lynch, and J.C. Middleton (1985). "Initial response analysis of mass transfer in a gas sparged stirred vessel," *Chemical Engineering Science*, Vol.40, No.10, 1811-1816.
- Gurol, M.D. and S. Nekouinaini (1985). Effect of organic substances on mass transfer in bubble aeration. *J. Water Pollut. Control Fed.*, Vol.57, No.3, 235-240.
- Higbie, R. (1935). "The rate of absorption of a pure gas into a still liquid during short periods of exposure," *Trans. AIChE*, Vol.31, 365-388.
- Hsieh, C.C. (1990). "Estimating volatilization rates and gas/liquid mass transfer coefficients in aeration systems," Ph.D. Prospectus, University of California, Los Angeles.
- Hwang, H.J., and M.K. Stenstrom (1979). "Effects of surface active agents on oxygen transfer," Water Resources Program, Report 79-2, University of California, Los Angeles.
- Hwang, H.J. (1983). "Comprehensive studies of oxygen transfer under nonideal conditions," Dissertation, University of California, Los Angeles.
- Ihme, F. (1975). "Leistungsbedarf und Verformung der Fluessigkeitsoberflaeche beim Ruehren newtonischer Fluessigkeiten mit Turbinenblatt- und Anker-ruehrern," Dissertation, Technical University Berlin.
- Judat, H., (1976). "Zum Dispergieren von Gasen", Dissertation, Universitaet Dortmund.
- Judat, H., (1982). "Gas/liquid mass transfer in stirred vessels-a critical review", *German Chemical Engineering*, Vol.5, 357-363.
- Kapartis, N. (1991). "Einfluss der Biomasse auf die Desorptionsgeschwindigkeit fluechtiger Substrate in beluefteten Ruehrreaktoren," Diplomarbeit, Technische Universitaet Berlin.
- Keitel G. and U. Onken (1982). "Zur Koaleszenzhemmung durch Elektrolyte und organische Verbindungen in waessrigen Gas/Fluessigkeits-Dispersionen," *Chemie Ingenieur Technik*, Vol.54, No.3, 262-263.
- Kincannon, D.F., A. Weinert, R. Padorr, and E.L. Stover (1983). "Predicting treatability of multiple organic priority pollutant wastewaters from single-

- pollutant treatability studies," Proceedings 37th Industrial Waste Conf., May 1982, Purdue University, J. Bell, Ed., Ann Arbor Science, Ann Arbor, Michigan, 640-650.
- Kincannon, D.F. and E.L. Stover (1983). "Determination of activated sludge biokinetic constants for chemical and plastic industrial wastewater," EPA-600/2-83-073A, US EPA, Cincinnati, Ohio.
- Koshy, A., T.R. Das, and R. Kumar (1988). "Effect of surfactants on drop breakage in turbulent liquid dispersions," *Chemical Engineering Science*, Vol.43, No.3, 649-654.
- Khudenko, B.M., and A. Garcia-Pastrana (1987). "Temperature influence on absorption and stripping processes," *Wat.Sci.Tech.*, Vol.19, 877-888.
- Lee, Y.H., G.T. Tsao, and P.C. Wankat (1980). "Hydrodynamic effect of surfactants on gas-liquid oxygen transfer," *AIChE J*, Vol.26 No.6, 1008-1012.
- Lewis, W.K. and W.G. Whitman (1924). "Principles of gas absorption," *Ind.Eng.Chem.*, Vol.16, No.3, 1215-1220.
- Lincoff, A.H. and J.M. Gossett (1984). "The determination of Henry's constant for volatile organics by equilibrium partitioning in closed systems," in Gas Transfer at Water Surfaces, W. Brutsaert and G.H. Jirka (eds.), D. Reidel Publishing Co., 17-25.
- Linek, V., J. Mayrhoferova, and J. Mosnerova (1970). "The influence of diffusivity on liquid phase mass transfer in solutions of electrolytes," *Chemical Engineering Science*, Vol.25, 1033-1045.
- Linek, V., P. Benes, V. Vacek, and F. Hovorka (1982). "Analysis of differences in  $k_L a$  values determined by steady-state and dynamic methods in stirred tanks," *The Chemical Engineering Journal*, 25 (1982) 77-88.
- Linek, V., V. Vacek, and P. Benes, (1987). "A critical review and experimental verification of the correct use of the dynamic method for the determination of oxygen transfer in aerated agitated vessels to water, electrolyte solutions and viscous liquids," *The Chemical Engineering Journal*, Vol.34, 11-34.
- Llorens, J., C. Mans, and J. Costa (1988). "Discrimination of the effects of surfactants in gas absorption," *Chemical Engineering Science*, Vol.43, No.3, 443-450

- Mackay, D. and P.J. Leinonen (1975). "Rate of evaporation of low solubility contaminants from water bodies to atmosphere," *Environmental Science and Technology*, Vol.9, No.13, 1178-?.
- Mackay, D., W.Y. Shiu, and R.P. Sutherland (1979). "Determination of air-water Henry's law constants for hydrophobic pollutants," *Environmental Science and Technology*, Vol.13, No.3, 333-337.
- Mackay, D. and W.Y. Shiu (1981). "A critical review of Henry's law constants for chemicals of environmental interest," *J.Phys.Chem.Ref.Data*, Vol.10, No.4, 1175-1199.
- Mancy, K.H. and D.A. Okun (1960). "Effects of surface active agents on bubble aeration," *J. Water Pollut. Control Fed.*, Vol.32, No.4, 351-364.
- Mancy, K.H. and D.A. Okun (1965). "Effects of surface active agents on bubble aeration," *J. Water Pollut. Control Fed.*, Vol.37, No.2, 212-227.
- Masutani, G.K. (1988). "Dynamic surface tension effects on oxygen transfer in activated sludge," Dissertation, University of California, Los Angeles.
- Masutani, G.K. and M.K. Stenstrom (1991). "Dynamic surface tension effects on oxygen transfer," *J.Env.Eng.Div., ASCE*, Vol.117, No.1, 126-142.
- Matter-Mueller, C., W. Gujer, and W. Giger (1981), "Transfer of volatile substances from water to the atmosphere," *Water Research*, Vol.15, 1271.
- Mueller, J.S. and H.D. Stensel (1990). "Biologically enhanced oxygen transfer in the activated sludge process," *J. Water Pollut. Control Fed.*, Vol.62, No.2, 193-203.
- Munz, C. and P.V. Roberts (1984). "The ratio of gas phase to liquid phase mass transfer coefficients in gas-liquid contacting processes," in Gas Transfer at Water Surfaces, W. Brutsaert and G.H. Jirka (eds.), D. Reidel Publishing Co., 35-45.
- Nagata, S. (1975). Mixing: Principles and applications. Halstead Press, New York.
- Ollenik, R. and W. Nitsch (1981). "Einfluss von Tensiden auf Stroemung und Stoffuebergang in einer Fluessig/fluessig-Kanalstroemung," *Berichte der Bunsengesellschaft fuer Physikalische Chemie*, Vol.85, No.10, 900-904.

- Osorio, C. (1985). "Untersuchung des Einflusses der Fluessigkeitseigenschaften auf den Stoffuebergang Gas/Fluessigkeit mit der Hydrazin-oxidation," Dissertation, Universitaet Dortmund, 1-109.
- Padday, J.F. (1969a). "Surface tension. Part I. The theory of surface tension," *Surface and Colloid Science*, Vol.1, 39-99.
- Padday, J.F. (1969b). "Surface tension. Part II. The measurement of surface tension," *Surface and Colloid Science*, Vol.1, 101-153.
- Philichi, T.L. and M.K. Stenstrom (1989). "The effects of dissolved oxygen probe lag on oxygen transfer parameter estimation," *J. Water Pollut. Control Fed.*, Vol 61, No.1, 83-86.
- Rathbun, R.E., W.S. Doyle, D.J. Shultz, and D.Y. Tai (1978). "Laboratory studies of gas tracers for reaeration," *J.Env.Eng.Div., ASCE*, Vol.104, No.2, 215-229.
- Redmon, D., W.C. Boyle, and L. Ewing (1983). "Oxygen transfer efficiency measurements in mixed liquor using off-gas techniques," *J. Water Pollut. Control Fed.*, Vol.55, No.11, 1338-1347.
- Roberts, P.V., and P.G. Daendilker (1983). "Mass transfer of volatile organic contaminants from aqueous solution to the atmosphere during surface aeration," *Environmental Science and Technology*, Vol.17, No.8, 1983, 484-489.
- Roberts, P.V., C. Munz, and P. Daendliker (1984a). "Modeling volatile organic solute removal by surface and bubble aeration," *J. Water Pollut. Control Fed.*, Vol 56, 157-163.
- Roberts, P.V., C. Munz, P. Daendliker, and C. Matter-Mueller (1984b). "Volatilization of organic pollutants in wastewater treatment- model studies," EPA-600/S2-84-047, US EPA, Cincinnati, Ohio.
- Robinson, C.W., and C.R. Wilke (1973). *Biotechnol.Bioeng.*, Vol 15, 755-782.
- Sherwood, T.K., R.L. Pigford, and C.R. Wilke (1975). Mass Transfer, McGraw-Hill, New York.
- Smith, J.H., D.C. Bomberger, and D.L. Haynes (1981). "Volatilization rates of intermediate and low volatility chemicals from water," *Chemosphere*, Vol.10, No.3, 281-289.

- Smith, J.H., D. Mackay, and C.W.K. Ng (1983a). "Volatilization of pesticides from water." *Residue Reviews*, Vol 85, Springer-Verlag, New York, Inc., 73-88.
- Smith, J.H., D.C. Bomberger, and D.L. Haynes (1983b). "Prediction of the volatilization rates of high volatility chemicals from natural water bodies," *Environmental Science and Technology*, Vol.14, No.11, 1332-1337.
- Spalding, D.B, (1963). Convective Mass Transfer, Edward Arnold Publishers Ltd., London.
- Springer, T.G. and R.L. Pigford (1970). "Influence of surface turbulence and surfactants on gas transport through liquid interfaces," *Ind.Eng.Chem., Fundam.*, Vol.9, No.3, 458-465.
- Stenberg, O. and B. Andersson (1988). "Gas-liquid mass transfer in agitated vessels. II. Modeling of gas-liquid mass transfer." *Chemical Engineering Science*, Vol.43, No.3, 725-730.
- Stenstrom, M.K. and R.G. Gilbert (1981). "Review Paper: Effects of alpha, beta, and theta factor upon the design, specification and operation of aeration systems," *Water Research*, Vol.15, 643-654.
- Stenstrom, M.K. (1990). "Upgrading existing activated sludge treatment plants with fine pore aeration systems," *Wat. Sci. Tech.*, Vol.22, No.7/8, 245-251.
- Treybal, R.E. (1968). Mass Transfer Operations, 2.Ed., McGraw-Hill, New York.
- Truong, K.N. and J.W. Blackburn (1984). "The stripping of organic chemicals in biological treatment processes," *Environ.Prog.*, Vol 3, No 3, 143-152.
- US Environmental Protection Agency (1982). "Fate of priority pollutants in publicly owned treatment works, Vol 1.," EPA-440/1-82/303, US EPA, Office of water regulations and standards, Washington, D.C.
- Van Dierendonck, L.L., J.M.H. Fortuin, and D. Venderbos (1968). "The specific contact area in gas-liquid reactors," *Chem.Reaction Eng.Symp.*, 205-213.
- Verscheuren, K. (1977). Handbook of Environmental Data on Organic Chemicals, Van Nostrand Reinhold Co., New York.

- Versteeg, G.F., P.M.M. Blauwhoff, and W.P.M. van Swaaij (1987). "The effect of diffusivity on gas-liquid mass transfer in stirred vessels. Experiments at atmospheric and elevated pressures," *Chemical Engineering Science*, Vol.42, 1103-1119.
- Wiesmann, U. (1988). Lecture notes, Chemical Engineering Department, Technical University Berlin.
- Yuteri, C., D.F. Ryan, J.J. Callow, and M.D. Gurol (1987). "The effect of chemical composition of water on Henry's law constant," *J. Water Pollut. Control Fed.*, Vol.59, No.11, 950-956.
- Zieminski, S.A., R.L. Hill (1962). "Bubble aeration of water in the presence of some organic compounds," *J.Chem.Eng.Data*, Vol.7, No.1, 51-54.
- Zieminski, S.A., M.M. Caron, and R.B. Blackmore (1967). "Behavior of air bubbles in dilute aqueous solutions," *Ind.Eng.Chem., Fundam.*, Vol.6, No.2, 233-242.
- Zlokarnik, M. (1978). "Sorption characteristics for gas-liquid contacting in mixing vessels," *Advances in Biochemical Engineering*, Vol.8, 133-151.
- Zlokarnik, M. (1980). "Koaleszenzphaenomene im System gasfoermig/fluessig und deren Einfluss auf den O<sub>2</sub>-Eintrag bei der biologischen Abwasserreinigung," *Korrespondenz Abwasser*, Vol.27, No.11, 728-734.



## Appendix

### Power input correlation

The power input into the reactor was calculated using the following correlation from Judat (1976). The correlation is valid for the water/air system with  $Re > 2.6 \cdot 10^4$ .

$$Ne = \frac{4.85A_1B_1 + 1.87 \cdot 10^2 Fr^{-0.32} \cdot \left(\frac{D}{d}\right)^{-1.53} \cdot Q_G^{1.02} - 4.61 Q_G^{1.25}}{1 + 1.36 \cdot 10^2 \left(\frac{D}{d}\right)^{-1.14} Q_G^{1.02}}$$

where:

$$A = 1 + 1/(4.35D/d + 5.11 \cdot 10^{-3}(D/d)^{8.73})$$

$$B = 1 - 1/(3.46 \cdot 10^{-2}(D/d)^{6.5} Fr^{-24(D/d+9.7)} + 7.9 \cdot 10^{-11}(D/d)^{29.87} Fr^{-9.5})$$

and:

$$Fr = \frac{n^2 d}{g}$$

$$Ne = \frac{P}{n^3 d^5}$$

$$Q = \frac{Q_G}{nd^3}$$

Table 13. Experimental data for kLa-O2 evaluation in Water/VOC/Air System.												
Run	Temp	P-Rxr	P-Atm	QG	QI	CI*	CI*adj	cLo	cL	cG	VL	n
	C	bar	bar	L/h	L/h	mg/L	mg/L	mg/L	mg/L	Vol%	L	1/min
1.1	21.0	0.064	0.993	341	76	8.90	9.30	0.2	9.3	0.155	18.5	472
1.2	21.1	0.064	0.993	341	76	8.88	9.28	0.2	9.3	0.160	18.5	472
1.3	21.2	0.064	0.993	341	76	8.87	9.27	0.2	9.2	0.161	18.5	472
1.4	21.3	0.064	0.993	341	76	8.85	9.24	0.2	9.2	0.162	18.5	472
2.1	20.9	0.064	0.993	341	76	8.92	9.32	0.4	8.9	0.150	18.5	250
2.2	20.6	0.064	0.993	341	76	8.97	9.37	0.4	8.9	0.155	18.5	250
2.3	20.8	0.064	0.993	341	76	8.94	9.34	0.4	9.0	0.160	18.5	250
2.4	20.9	0.064	0.993	341	76	8.92	9.32	0.4	8.9	0.155	18.5	241
3.1	20.9	0.058	1.034	130	36	8.92	9.63	0.7	7.7	0.063	18.3	140
3.2	20.5	0.058	1.034	130	36	8.99	9.71	0.7	7.8	0.055	18.3	138
3.3	20.5	0.058	1.034	130	36	8.99	9.71	0.7	7.7	0.058	18.3	138
3.4	20.5	0.058	1.034	130	36	8.99	9.71	0.7	7.7	0.058	18.3	138
4.1	20.9	0.058	1.032	199	36	8.92	9.62	0.2	8.6	0.080	18.5	292
4.2	20.9	0.058	1.031	199	36	8.92	9.61	0.2	8.6	0.078	18.5	292
4.3	20.9	0.058	1.031	199	36	8.92	9.61	0.2	8.6	0.065	18.5	292
4.4	20.8	0.058	1.034	199	36	8.94	9.65	0.2	8.6	0.061	18.5	292
5.1	19.1	0.064	1.039	199	55	9.24	10.08	1.7	7.7	0.120	18.3	107
6.1	19.1	0.064	1.039	199	55	9.24	10.08	1.0	9.0	0.160	18.3	187
6.2	19.0	0.064	1.039	199	55	9.26	10.10	1.0	9.0	0.160	18.3	187
6.3	19.0	0.064	1.039	199	55	9.26	10.10	1.0	9.0	0.160	18.3	187
7.1	19.6	0.064	1.039	199	55	9.15	9.98	0.3	10.3	0.200	18.5	411
7.2	19.8	0.064	1.039	199	55	9.11	9.94	0.3	10.3	0.200	18.5	411
8.1	20.0	0.063	1.023	201	47	9.08	9.75	1.5	7.7	0.080	18.3	105
8.2	20.4	0.064	1.023	201	47	9.01	9.68	1.5	7.7	0.080	18.3	105
9.1	20.6	0.064	1.025	201	40	8.97	9.66	0.7	8.9	0.080	18.3	192
9.2	20.8	0.064	1.025	201	40	8.94	9.63	0.7	8.9	0.080	18.3	192
9.3	21.0	0.064	1.025	201	38	8.90	9.58	0.6	8.9	0.080	18.3	192
9.4	21.1	0.064	1.025	201	35	8.88	9.56	0.6	8.9	0.080	18.3	192
10.1	22.1	0.064	1.025	201	35	8.71	9.38	0.2	9.5	0.110	18.3	410
10.2	22.4	0.064	1.025	201	35	8.66	9.33	0.2	9.4	0.110	18.3	410
11.1	19.1	0.063	1.012	249	76	9.24	9.82	2.4	7.5	0.126	18.5	104
11.2	19.0	0.063	1.014	249	76	9.26	9.86	2.4	7.5	0.126	18.5	104
11.3	19.0	0.063	1.014	249	76	9.26	9.86	2.4	7.5	0.126	18.5	104
12.1	19.2	0.063	1.014	249	76	9.22	9.82	0.9	9.1	0.180	18.5	216
12.2	19.2	0.063	1.016	249	76	9.22	9.83	0.9	9.1	0.180	18.5	218
12.3	19.3	0.063	1.016	249	76	9.20	9.81	0.9	9.1	0.180	18.5	218
13.1	19.4	0.063	1.016	249	76	9.19	9.80	0.5	9.9	0.240	18.8	391
13.2	19.5	0.063	1.016	249	76	9.17	9.78	0.5	9.8	0.240	18.8	391
13.3	19.6	0.063	1.016	249	76	9.15	9.76	0.5	9.7	0.240	18.8	391
13.4	19.7	0.063	1.016	249	76	9.13	9.74	0.5	9.7	0.240	18.8	398

Table 13. (cont) Experimental data for kLa-O2 evaluation in Water/VOC/Air System.												
Run	Temp	P-Rxr	P-Atm	QG	Ql	Cl*	Cl*adj	cLo	cL	cG	VL	n
	C	bar	bar	L/h	L/h	mg/L	mg/L	mg/L	mg/L	Vol%	L	1/min
14.1	19.9	0.063	1.016	249	76	9.09	9.70	0.6	9.8	0.240	19.0	462
14.2	19.9	0.063	1.016	249	76	9.09	9.70	0.6	9.7	0.240	19.0	463
14.3	20.0	0.063	1.018	249	76	9.08	9.70	0.5	9.7	0.240	19.0	464
14.4	20.0	0.063	1.018	249	76	9.08	9.70	0.5	9.7	0.240	19.0	465
15.1	20.5	0.063	1.018	250	77	8.99	9.61	1.3	8.3	0.150	18.5	175
15.2	20.6	0.063	1.018	252	77	8.97	9.59	1.3	8.3	0.156	18.5	175
15.3	20.6	0.063	1.018	252	77	8.97	9.59	1.3	8.2	0.160	18.5	175
15.4	20.6	0.063	1.018	252	77	8.97	9.59	1.3	8.2	0.160	18.5	175
16.1	20.9	0.063	1.019	252	77	8.92	9.54	0.3	9.5	0.222	19.0	382
16.2	21.0	0.063	1.020	252	77	8.90	9.53	0.3	9.5	0.226	19.0	382
16.3	21.1	0.063	1.020	252	77	8.88	9.51	0.3	9.5	0.226	19.0	390
16.4	21.1	0.063	1.020	252	77	8.88	9.51	0.3	9.5	0.226	19.0	390
17.1	21.5	0.063	1.020	252	77	8.82	9.45	0.3	9.5	0.226	19.0	488
18.1	19.8	0.065	1.025	201	59	9.11	9.82	1.7	7.5	0.140	18.3	117
18.2	20.1	0.064	1.025	201	59	9.06	9.76	1.5	7.5	0.170	18.3	117
18.3	20.2	0.064	1.025	201	59	9.04	9.73	1.5	7.5	0.170	18.3	107
18.4	20.2	0.064	1.025	201	59	9.04	9.73	1.5	7.5	0.170	18.3	107
19.1	20.2	0.064	1.024	201	59	9.04	9.73	1.5	8.5	0.200	18.3	177
19.2	20.2	0.064	1.024	201	59	9.04	9.73	1.5	8.5	0.200	18.3	177
19.3	20.2	0.064	1.024	201	59	9.04	9.73	1.5	8.5	0.200	18.3	177
19.4	20.2	0.064	1.024	201	59	9.04	9.73	1.5	8.5	0.200	18.3	177
20.1	20.4	0.064	1.024	201	59	9.01	9.69	0.4	9.4	0.240	18.5	295
20.2	20.5	0.064	1.024	201	59	8.99	9.67	0.4	9.3	0.240	18.5	295
20.3	20.6	0.064	1.024	201	59	8.97	9.65	0.4	9.4	0.240	18.5	298

Table 14. Experimental data for kLa-O2 evaluation in Water/DSS/Air System.												
Run	Temp C	P-Rxr bar	P-Atm bar	QG L/h	QI L/h	CI* mg/L	CI*adj mg/L	cLo mg/L	cL mg/L	cG Vol%	VL L	n 1/min
DSS2	= 39 mN/m			Conc. = 60 mg/L								
2.0	21.6	0.056	1.029	75	63	8.80	9.44	0.2	9.4	0.520	19.0	472
2.1	22.0	0.056	1.029	75	63	8.73	9.37	0.2	9.5	0.800	19.0	472
2.2	20.5	0.056	1.029	75	63	8.99	9.64	0.4	9.1	0.760	19.0	293
2.3	20.9	0.058	1.029	75	63	8.92	9.59	1.7	6.8	0.380	18.5	200
2.4	21.0	0.058	1.029	75	63	8.90	9.57	3.1	5.7	0.240	18.5	150
2.5	20.8	0.058	1.029	75	63	8.94	9.61	0.3	9.1	0.860	19.0	312
2.6	21.1	0.058	1.029	75	63	8.88	9.55	0.3	9.2	0.360	19.0	312
DSS3	= 38 mN/m			Conc.= 83 mg/L								
3.0	19.9	0.056	1.029	75	54	9.09	9.75	0.3	9.5	0.455	18.8	408
3.1	19.9	0.055	1.029	75	65	9.09	9.74	3.3	5.9	0.188	18.5	148
3.2	20.0	0.055	1.029	75	65	9.08	9.73	1.8	7.3	0.320	18.5	198
3.3	19.9	0.055	1.029	75	65	9.09	9.74	0.9	8.4	0.460	18.5	239
3.4	20.0	0.055	1.029	75	65	9.08	9.73	0.6	9.1	0.575	19.0	279
3.5	20.5	0.055	1.029	75	65	8.99	9.64	0.3	9.3	0.830	19.5	325
DSS4	= 47 mN/m			Conc. = 16 mg/L								
4.1	19.7	0.065	1.022	78	63	9.13	9.81	3.2	5.7	0.175	18.5	108
4.2	19.8	0.065	1.023	78	63	9.11	9.80	3.0	6.0	0.185	18.5	131
4.3	19.8	0.065	1.023	78	63	9.11	9.80	2.6	6.3	0.215	18.5	152
4.4	20	0.065	1.023	78.15	62.6	9.08	9.7681	1.3	7.6	0.33	18.5	206
4.5	20.1	0.065	1.023	78.15	62.6	9.06	9.7467	0.68	8.9	0.44	18.5	245
4.6	20.4	0.065	1.023	78.15	62.6	9.01	9.6932	0.35	9.4	0.575	18.5	307
DSS5	= 37 mN/m			Conc.= 116 mg/L								
5	21.6	0.056	1.029	75.04	63.1	8.8	9.4419	0.19	9.4	0.52	19	472
5.1	19.4	0.067	1.023	78.01	64.4	9.19	9.9043	3.8	5.8	0.14	18.3	112
5.2	19.4	0.067	1.023	78.01	63	9.19	9.9043	2.72	5.9	0.2	18.3	152
5.3	19.5	0.067	1.023	78.01	63	9.17	9.8829	1.32	7.5	0.36	18.5	203
5.4	19.7	0.067	1.023	78.01	63	9.13	9.84	0.6	8.9	0.52	18.5	252
5.5	20	0.067	1.023	78.01	60.5	9.08	9.7864	0.27	9.5	0.74	18.5	310

Table 15. Experimental data for comparison of steady /continuous nonsteady state kLa-O2												
	in Water/Air											
Run	Temp	P-Rxr	P-Atm	QG	QI	CI*	CI*adj	cLo	cL	cG	VL	n
	C	bar	bar	L/h	L/h	mg/L	mg/L	mg/L	mg/L	Vol%	L	1/min
ns1	21.1	0.063	1.038	81	55	8.89	9.68	0.20	8.2	0.380	18.5	255
ns2	20.6	0.063	1.039	73	55	8.97	9.78	0.20	8.1	0.410	18.5	254
ns3	20.7	0.063	1.039	73	55	8.95	9.76	0.20	8.2	0.405	18.5	255
ns4	20.8	0.063	1.039	73	55	8.94	9.74	0.10	8.2	0.410	18.5	255
ns5	21.2	0.063	1.039	81	55	8.87	9.67	0.10	8.9	0.430	18.5	345
ns6	21.5	0.063	1.039	81	55	8.82	9.62	0.10	8.9	0.430	18.5	350
ns7	20.1	0.066	1.027	81	62	9.06	9.79	2.00	6.3	0.280	18.3	120
ns7a	20.2	0.066	1.027	81	62	9.04	9.77	1.75	6.3	0.283	18.3	120
ns7b	20.3	0.066	1.027	79	62	9.02	9.75	1.85	6.1	0.280	18.3	120
ns8	20.3	0.066	1.027	79	63	9.02	9.75	1.95	7.8	0.115	18.3	120
ns8a	20.3	0.066	1.027	78	63	9.02	9.75	1.70	6.8	0.263	18.3	152
ns8b	20.5	0.066	1.027	78	63	8.99	9.72	1.70	6.7	0.290	18.3	152
ns8c	20.4	0.066	1.027	78	63	9.01	9.74	1.75	6.8	0.290	18.4	152
ns9a	20.3	0.066	1.027	78	63	9.02	9.75	1.22	7.6	0.352	18.4	206
ns10a	20.5	0.066	1.027	78	63	8.99	9.72	0.85	8.2	0.440	18.5	252
ns10b	20.6	0.066	1.027	78	63	8.97	9.70	0.85	8.2	0.440	18.5	252
ns10c	20.5	0.066	1.027	78	63	8.99	9.72	0.85	8.2	0.440	18.5	252
ns11a	20.5	0.066	1.027	78	63	8.99	9.72	0.55	8.7	0.448	18.5	307
ns12a	20.6	0.066	1.029	78	63	8.97	9.71	0.35	9.2	0.478	18.5	355
ns12b	20.8	0.066	1.029	78	63	8.94	9.68	0.35	9.2	0.500	18.5	370
ns13a	20.5	0.066	1.029	78	63	8.99	9.74	0.25	9.3	0.495	18.5	406
ns13b	21.1	0.066	1.029	78	63	8.88	9.62	0.25	9.3	0.490	18.5	410
ns14a	21.4	0.066	1.029	78	63	8.83	9.56	0.20	9.3	0.495	18.5	460

Table 15b. Experimental data for kLa-O2 evaluation with biomass												
	in Water/Air											
Run	Temp	P-Rxr	P-Atm	QG	QI	CI*	CI*adj	cLo	cL	cG	VL	n
	C	bar	bar	L/h	L/h	mg/L	mg/L	mg/L	mg/L	Vol%	L	1/min
bm2.0	22.4	0.062	1.034	78	65	8.66	9.39	0.05	3.5	0.280	18.5	115
bm2.1	24.0	0.062	1.034	81	65	8.41	9.12	0.74	4.7	0.320	18.5	150
bm2.2	24.7	0.062	1.034	82	66	8.30	9.00	0.90	6.2	0.345	18.5	203
bm2.3	25.3	0.062	1.034	82	66	8.21	8.91	0.66	7.1	0.400	18.5	254
bm2.4	24.8	0.062	1.034	85	62	8.28	8.98	0.30	7.9	0.520	18.5	319
bm2.5	26.2	0.061	1.032	80	60	8.08	8.74	0.02	7.9	0.615	18.5	365
bm2.6	28.3	0.061	1.033	80	62	7.78	8.43	0.20	8.1	0.560	19.0	420
bm2.7	26.8	0.061	1.035	80	60	7.99	8.67	0.10	8.4	0.600	19.0	486

Table 16. Results for kLA-O2 im Water/VOC/Air System.							
Run	P	vS	KLA <sub>g</sub>	KLAI	KLA <sub>g</sub> 20	KLAI 20	diff
	(W)	(m/s)	(s-1)	(s-1)	(s-1)	(s-1)	%
1.1	39.3	1.45E-03					7.5
1.2	39.3	1.45E-03					10.4
1.3	39.3	1.45E-03	0.1809	0.1593	0.1758	0.1548	11.9
1.4	39.3	1.45E-03	0.2676	0.2342	0.2595	0.2271	12.5
2.1	5.3	1.45E-03	0.0263	0.0234	0.0258	0.0229	11.2
2.2	5.3	1.45E-03	0.0242	0.0208	0.0238	0.0205	14.1
2.3	5.3	1.45E-03	0.0346	0.0292	0.0340	0.0286	15.8
2.4	4.7	1.45E-03	0.0272	0.0234	0.0266	0.0229	14.1
3.1	1.1	5.56E-04	0.0009	0.0020	0.0009	0.0019	
3.2	1.0	5.56E-04	0.0008	0.0020	0.0008	0.0020	
3.3	1.0	5.56E-04	0.0008	0.0019	0.0008	0.0019	
3.4	1.0	5.55E-04	0.0008	0.0019	0.0008	0.0019	
4.1	9.6	8.48E-04	0.0034	0.0045	0.0033	0.0044	
4.2	9.6	8.48E-04	0.0033	0.0045	0.0032	0.0044	
4.3	9.6	8.48E-04	0.0026	0.0043	0.0026	0.0042	
4.4	9.6	8.48E-04	0.0024	0.0041	0.0023	0.0040	
5.1	0.4	8.47E-04	0.0022	0.0021	0.0022	0.0021	3.9
6.1	2.4	8.47E-04	0.0064	0.0061	0.0065	0.0063	3.9
6.2	2.4	8.47E-04	0.0063	0.0060	0.0064	0.0062	3.9
6.3	2.4	8.47E-04	0.0063	0.0060	0.0064	0.0062	3.9
7.1	27.9	8.47E-04					3.9
7.2	27.9	8.47E-04					3.9
8.1	0.4	8.57E-04	0.0017	0.0021	0.0017	0.0021	-26.2
8.2	0.4	8.58E-04	0.0018	0.0022	0.0017	0.0022	-26.2
9.1	2.6	8.58E-04	0.0046	0.0066	0.0045	0.0065	-42.6
9.2	2.6	8.58E-04	0.0048	0.0069	0.0047	0.0067	-42.9
9.3	2.6	8.58E-04	0.0051	0.0070	0.0050	0.0068	-36.4
9.4	2.6	8.58E-04	0.0053	0.0066	0.0051	0.0065	-26.0
10.1	27.6	8.58E-04					-2.5
10.2	27.6	8.58E-04					-0.1
11.1	0.4	1.06E-03	0.0029	0.0025	0.0030	0.0026	13.0
11.2	0.4	1.06E-03	0.0029	0.0025	0.0029	0.0025	13.0
11.3	0.4	1.06E-03	0.0029	0.0025	0.0029	0.0025	13.0
12.1	3.6	1.06E-03	0.0134	0.0131	0.0137	0.0134	2.4
12.2	3.7	1.06E-03	0.0131	0.0128	0.0134	0.0130	2.4
12.3	3.7	1.06E-03	0.0135	0.0132	0.0137	0.0134	2.4
13.1	23.0	1.06E-03					16.9
13.2	23.0	1.06E-03					17.5
13.3	23.0	1.06E-03	0.2111	0.1723	0.2131	0.1739	18.4
13.4	24.3	1.06E-03	0.3273	0.2672	0.3296	0.2691	18.4
14.1	38.8	1.06E-03					17.9
14.2	39.0	1.06E-03					18.8
14.3	39.3	1.06E-03					18.4
14.4	39.6	1.06E-03					18.4
15.1	1.9	1.07E-03	0.0062	0.0062	0.0061	0.0062	-1.4
15.2	1.9	1.07E-03	0.0065	0.0064	0.0065	0.0063	3.0
15.3	1.9	1.07E-03	0.0062	0.0058	0.0061	0.0057	7.5
15.4	1.9	1.07E-03	0.0062	0.0058	0.0061	0.0057	7.5

Table 16b. Results for kLA-O2 im Water/VOC/Air System.							
Run	P	vS	KLA <sub>g</sub>	KLAI	KLA <sub>g</sub> 20	KLAI 20	diff
	(W)	(m/s)	(s-1)	(s-1)	(s-1)	(s-1)	%
16.1	21.4	1.07E-03					11.3
16.2	21.4	1.07E-03					12.8
16.3	22.8	1.07E-03					12.8
16.4	22.8	1.07E-03					12.8
17.1	45.9	1.07E-03					12.1
18.1	0.6	8.58E-04	0.0026	0.0022	0.0026	0.0022	15.9
18.2	0.6	8.58E-04	0.0033	0.0024	0.0033	0.0024	27.8
18.3	0.4	8.58E-04	0.0033	0.0024	0.0033	0.0024	27.8
18.4	0.4	8.58E-04	0.0033	0.0024	0.0033	0.0024	27.8
19.1	2.0	8.58E-04	0.0071	0.0051	0.0071	0.0051	28.4
19.2	2.0	8.58E-04	0.0068	0.0049	0.0068	0.0048	28.9
19.3	2.0	8.58E-04	0.0068	0.0049	0.0068	0.0048	28.9
19.4	2.0	8.58E-04	0.0068	0.0049	0.0068	0.0048	28.9
20.1	9.9	8.57E-04	0.0302	0.0231	0.0299	0.0229	23.5
20.2	9.9	8.57E-04	0.0278	0.0211	0.0275	0.0209	24.1
20.3	10.2	8.57E-04	0.0345	0.0262	0.0340	0.0259	23.9

Table 17. Results for kLA-O2 in Water/DSS/Air System.							
Run	P	vS	KLAg	KLAI	KLAg 20	KLAI 20	diff
	(W)	(m/s)	(s-1)	(s-1)	(s-1)	(s-1)	%
DSS2		Conc= 60 mg/L					
2.1	46.6	3.20E-04	0.1946	0.2028	0.1873	0.1952	-4.2
2.2	46.6	3.20E-04					
2.3	10.9	3.20E-04	0.0219	0.0147	0.0216	0.0145	32.8
2.4	3.4	3.20E-04	0.0022	0.0017	0.0021	0.0017	21.4
2.5	1.4	3.20E-04	0.0010	0.0006	0.0010	0.0006	35.1
2.6	13.2	3.20E-04	0.0265	0.0159	0.0260	0.0156	39.9
DSS3		conc.= 83 mg/L					
3.1	1.4	3.22E-04	0.0008	0.0007	0.0008	0.0007	16.1
3.2	3.3	3.22E-04	0.0021	0.0022	0.0021	0.0022	-4.3
3.3	5.8	3.22E-04	0.0055	0.0055	0.0056	0.0055	1.1
3.4	9.4	3.22E-04	0.0143	0.0129	0.0143	0.0129	9.8
3.5	14.9	3.22E-04	0.0380	0.0250	0.0375	0.0247	34.2
DSS4		Conc =16 mg/L					
4.1	0.5	3.33E-04	0.0007	0.0006	0.0007	0.0006	19.9
4.2	0.9	3.33E-04	0.0008	0.0007	0.0008	0.0008	8.4
4.3	1.5	3.33E-04	0.0010	0.0010	0.0010	0.0010	3.5
4.4	3.7	3.33E-04	0.0026	0.0027	0.0026	0.0027	-7.0
4.5	6.3	3.33E-04	0.0087	0.0091	0.0087	0.0091	-4.7
4.6	12.5	3.33E-04	0.0329	0.0290	0.0326	0.0287	11.8
DSS5		Conc. = 116 mg/L					
5.1	0.6	3.33E-04	0.0006	0.0005	0.0006	0.0005	17.4
5.2	1.5	3.33E-04	0.0008	0.0008	0.0009	0.0008	10.1
5.3	3.5	3.33E-04	0.0025	0.0025	0.0026	0.0025	3.0
5.4	6.9	3.33E-04	0.0093	0.0084	0.0093	0.0084	9.8
5.5	12.9	3.33E-04	0.0432	0.0293	0.0432	0.0293	32.3



Table 18. Results for kLA-O2 in Water/Air System.							
Comparison of nonsteady/steady state tests.							
Run	P	vS	KLA <sub>g</sub>	KLAI	KLA <sub>g</sub> 20	KLAI 20	diff
	(W)	(m/s)	(s-1)	(s-1)	(s-1)	(s-1)	%
ns1	7.1	3.4E-04	0.0044	0.0045	0.0043	0.0043	-0.3
ns2	7.1	3.1E-04	0.0038	0.0039	0.0038	0.0039	-3.1
ns3	7.1	3.1E-04	0.0041	0.0043	0.0040	0.0042	-5.6
ns4	7.1	3.1E-04	0.0041	0.0044	0.0041	0.0043	-5.7
ns5	17.8	3.4E-04	0.0097	0.0095	0.0094	0.0093	1.7
ns6	18.6	3.4E-04	0.0104	0.0102	0.0101	0.0099	1.7
ns7	0.7	3.4E-04	0.0014	0.0012	0.0014	0.0011	18.0
ns7a	0.7	3.4E-04	0.0014	0.0012	0.0014	0.0012	14.2
ns7b	0.7	3.4E-04	0.0013	0.0011	0.0013	0.0011	17.6
ns8	0.6	1.1E-03	0.0034	0.0029	0.0034	0.0028	16.7
ns8a	1.5	3.3E-04	0.0015	0.0016	0.0015	0.0016	-9.1
ns8b	1.5	3.3E-04	0.0016	0.0016	0.0016	0.0016	3.0
ns8c	1.5	3.3E-04	0.0017	0.0016	0.0016	0.0016	2.1
ns9a	3.7	3.3E-04	0.0028	0.0028	0.0027	0.0028	-1.9
ns10a	6.9	3.3E-04	0.0049	0.0046	0.0048	0.0045	6.1
ns10b	6.9	3.3E-04	0.0049	0.0046	0.0049	0.0046	6.1
ns10c	6.9	3.3E-04	0.0049	0.0046	0.0048	0.0045	6.1
ns11a	12.5	3.3E-04	0.0074	0.0075	0.0073	0.0074	-2.3
ns12a	19.5	3.3E-04	0.0156	0.0164	0.0153	0.0162	-5.3
ns12b	22.1	3.3E-04	0.0174	0.0175	0.0170	0.0172	-0.7
ns13a	29.4	3.3E-04	0.0190	0.0198	0.0188	0.0195	-4.0
ns13b	30.3	3.3E-04	0.0258	0.0272	0.0252	0.0265	-5.1
ns14a	43.0	3.3E-04	0.0314	0.0329	0.0304	0.0318	-4.6

